Doctoral Dissertations   Graduate School

Spring 2006

Development of self-assembled monolayer-based cell culture platform towards fabrication of a three-dimensional bioreactor

Rajendra Kandoor Aithal

DEVELOPMENT OF SELF-ASSEMBLED MONOLAYER-BASED

CELL CULTURE PLATFORM TOWARDS FABRICATION OF

A THREE-DIMENSIONAL BIOREACTOR

by

Rajendra Kandoor Aithal, M.S.

A Dissertation Presented in Partial Fulfillment
of the Requirements for the Degree of
Doctor of Philosophy

COLLEGE OF ENGINEERING AND SCIENCE
LOUISIANA TECH UNIVERSITY

May 2006

UMI Number: 3218987

INFORMATION TO USERS

The quality of this reproduction is dependent upon the quality of the copy submitted. Broken or indistinct print, colored or poor quality illustrations and photographs, print bleed-through, substandard margins, and improper alignment can adversely affect reproduction.

In the unlikely event that the author did not send a complete manuscript and there are missing pages, these will be noted. Also, if unauthorized copyright material had to be removed, a note will indicate the deletion.

UMI®

UMI Microform 3218987

Copyright 2006 by ProQuest Information and Learning Company.

All rights reserved. This microform edition is protected against unauthorized copying under Title 17, United States Code.

LOUISIANA TECH UNIVERSITY

THE GRADUATE SCHOOL

04/20/2006
<div align="right">Date</div>

We hereby recommend that the dissertation prepared under our supervision

by_____RAJENDRA KANDOOR AITHAL_____

entitled DEVELOPMENT OF SELF-ASSEMBLED MONOLAYER-BASED CELL CULTURE

PLATFORM TOWARDS FABRICATION OF A THREE-DIMENSIONAL BIOREACTOR

be accepted in partial fulfillment of the requirements for the Degree of

Doctor of Philosophy

<div align="right">

Debasish Kuila
Supervisor of Dissertation Research

Ray J. Wheeler
Head of Department

Engineering
Department

</div>

Recommendation concurred in:

Micah J. McShane

David K. Mills

<div align="center">Advisory Committee</div>

Y. Lvov (Debasish Kuila)

P. Bhushan

Approved:

Pula Ramachandran
Director of Graduate Studies

Stan Napper
Dean of the College

Approved:

Jenny McConnothy
Dean of the Graduate School

<div align="right">

GS Form 13
(5/03)

</div>

ABSTRACT

The extracellular matrix (ECM) plays an important role in regulating a number of cellular properties and functions like cell differentiation, cell synthesis and degradation, cell viability and proliferation, cell function, and cell aging. Surface modification of planar substrates with self-assembled monolayers (SAMs) is a promising technique to achieve stable ECMs.

In this work, substrates such as silicon (Si), gallium arsenide (GaAs) and indium tin oxide (ITO) substrates were modified with SAMS containing amino ($-NH_2$), methyl ($-CH_3$), thiol ($-SH$) and carboxylic ($-COOH$) end groups and characterized using contact angle measurements, surface infrared (IR) spectroscopy and atomic force microscopy (AFM). Different cell types such as human dermal fibroblasts (HDFs), mouse stromal mesenchymal stem cells (MSCs), rat brain neurons (RBN), and rat hepatocytes were cultured on these surfaces to develop stable and standard cell culture platforms (CCPs).

Contact angle measurements showed that surfaces modified with SAMs containing amino and carboxylic end groups are hydrophilic, methyl terminal group is hydrophobic, and SAM containing thiol end group has an intermediate property. Reflection absorption infrared spectroscopy (RAIRS) and attenuated total reflectance IR (ATR/IR) confirmed the presence of respective SAMs on surfaces. AFM data show that SAMs with methyl and carboxylic group modified surfaces present an average

roughness of 1.51 and 2.67 nm, which are higher than 1.01 and 1.1 nm obtained for SAMs containing amino and thiol end groups.

For cell culture studies on SAM-modified surfaces, viability was assessed using the LIVE/DEAD® assay, proliferation by the MTT assay, while phenotypic maintenance was monitored by immuohistochemical detection of Type I collagen. Morphological responses of the cells were studied using phase contrast and fluorescence imaging to document changes in cell shape and properties. Based on their viability, proliferation and phenotype, HDF cells preferred the substrates in the following order: ITO-ODT > Si-APTES > ITO > Si > GaAs-ODT > GaAs. MSCs grew well on all SAM-modified surfaces with highest proliferation observed on thiol (–SH) terminated ITO substrates. For neuronal cells, addition of 1% serum initially to the cell suspension maintained their viability on methyl and amino modified ITO substrates by neutralizing the effects of dimethyl sulfoxide (DMSO). Neurons preferred amino over methyl terminated SAMs on ITO. For hepatocytes cultured on SAM-modified substrates, cellular responses revealed that charge on the amino group enhanced hepatocyte attachment, while addition of L-Glutamine caused the proliferation. Lower lactate dehydrogenase (LDH) activity and higher protein synthesis are consistent with better cell growth of hepatocytes on SAMs with positively charged amino ($-NH^{3+}$) groups under physiological conditions.

The results obtained from these 2D modified surfaces were incorporated to develop a SAM-modified silicon-based 3D cell-based bioreactor. Physiologically based pharmacokinetic (PBPK) model was used to design the reactor and CoventorWare™ was used to simulate the fluid flow. The reactor was fabricated using photolithography and packaged for cell culture studies. The reactor consisted of fluidic network of channels (50

μm width and 100 μm depth) to mimic the circulatory system and a chamber containing

HDF cells. The LDH analysis showed that the SAM-modified-3D system enhanced the

performance of the cells and could be used for other cell types, such as hepatocytes for

drug toxicity screening.

APPROVAL FOR SCHOLARLY DISSEMINATION

The author grants to the Prescott Memorial Library of Louisiana Tech University the right to reproduce, by appropriate methods, upon request, any or all portions of this Dissertation. It is understood that "proper request" consists of the agreement, on the part of the requesting party, that said reproduction is for his personal use and that subsequent reproduction will not occur without written approval of the author of this Dissertation. Further, any portions of the Dissertation used in books, papers, and other works must be appropriately referenced to this Dissertation.

Finally, the author of this Dissertation reserves the right to publish freely, in the literature, at any time, any or all portions of this Dissertation.

Author _K. Rajendra Arthra_

Date _05/03/2006_

GS Form 14
(5/03)

DEDICATION

This dissertation is dedicated to my parents, Ananthakrishna Aithal and Malathi Aithal, my brother, Ramprasad Aithal, and sister-in-law, Vani Aithal.

TABLE OF CONTENTS

LIST OF TABLES

LIST OF FIGURES

xiii

ACKNOWLEDGMENTS

I would like to express my sincere gratitude to my advisor Dr. Debasish Kuila for his gracious support and encouragement throughout my doctoral study. I would like to thank Dr. David Mills, my co-advisor, for his constant help and guidance in carrying out the research on cell biology. I also thank the other members of my committee, Drs. Michael McShane, Yuri Lvov and Sidney Sit for being on my committee and providing valuable comments and suggestions on my dissertation. I am also very grateful to Dr. Ramu Ramachandran for the financial support through the graduate school throughout my doctoral study. Dr. Harihara Mehendale and his students Dr. Sachin Devi and Vishaka Bhave at University of Louisiana, Monroe, are acknowledged for their help in supplying hepatocytes and valuable discussions.

I would like to thank Mr. Philip Coane and other staff members, Jeanette Futrell, Marie Pipes, Scott Williams, Dee Tatum, Karen Xu, John McDonald, and Deborah Wood at IfM for providing a good working and friendly environment. I would like to thank our research group members, Asma Anjum Parveen, Deepak Kumaraswamy, Varun Shanigaram, and Amber Doss for their help throughout this project. I also like to thank Dr. Kuila's present group members, Priyank Sukul, Krithi Sridhara Shetty, Shirish Mehta, Dr. Shihua Zhao and also past group members, Saurabh Singh, Shailender Kolipaka, Avinash Potluri, Satish Nagineni, Sridevi Bala, Himabindu Indukuri, and Devendra Patel for providing a friendly environment in the lab.

I would like to thank my roommates- Karunakar Cheruku, Krishna Kishore Chirumamilla, Sankarsh Reddy and Naveen Pochiraju- for their support and encouragement. I would like to express my wholehearted gratitude to my friends- Mangilal Agarwal, Rajneek Khillan, Rohit Dikshit, Aravind Chamarti, Anirban Chakraborty, Jeevan Vemagiri, Anand Paka, Suryakanth Murthy, Jayaram Sermadevi, Partha Dubasi, Ravikanth Gonela, Balasubramanyam, Mohammed Rafi, Ponnam Bhavani Srikanth and Sudhindra Purohit- for their support and encouragement throughout my studies at Louisiana Tech University.

Finally, I would like to thank my parents Ananthakrishna and Malathi Aithal and my brother Ramprasad Aithal, and my sister-in-law Vani Aithal, without whose support this dissertation would hardly have been possible.

CHAPTER 1

INTRODUCTION

1.1 Cell Culture Platforms (CCPs)

Cells play a major role in building tissues and maintaining tissue function in their own unique microenvironments. However, after cells are removed from their microenvironment and placed within an *in vitro* environment, they typically lose some or all of their normal *in vivo* behavior.[1] Cellular microenvironments play a crucial role in stem cell differentiation, cell synthesis and degradation, cell function, and cell aging. A principal objective of cell and tissue engineering, therefore, is to reach a fundamental understanding of the factors in the cellular microenvironment that control and regulate cell behavior and function. Efforts to understand the interaction of cells in culture with their environment could benefit from a more detailed understanding of the molecular structure of the surface to which the cells are attached.[2,3] Thus, the development of cell culture platforms (CCPs), using an *in vitro* animal or human surrogate based on micro/nanofabrication technologies, is a promising area of research. CCPs should be extremely useful in the fields of toxicology and drug testing because they can increase the accuracy of *in vitro* predictions, simplify testing procedures, and reduce the costs of such tests.

1

The extracellular matrix (ECM) plays an important role in the development of CCPs as they regulate a number of cellular properties and functions like cell viability, proliferation and differentiation.[4] The ECM is made up of a complex mixture of structural proteins (collagen, elastin), specialized proteins (fibrin, laminin) and proteoglycans. Each of these components has its own specialized function contributing to the entirety of the ECM.[4] Significant advances in cell and tissue engineering have been made to the successful recreation of this cellular microenvironment *in vitro*.

Development of *in vitro* models of the ECM or CCPs is challenging because they require several characteristics pertinent in cell biology. These models ought to present a homogenous environment of ligands on the surface for the attachment of proteins and subsequently the cells, and also be able to resist nonspecific adsorption of proteins, which could render the ligand surface inactive.[2] Also, the surface should be compatible with conditions of the attached cell culture.[5] Several studies have been carried out to study cell-cell, cell-ECM and cell-substrate interactions.[3] They have provided inputs for the development of microscale and nanoscale technologies, which define and control the *in vitro* cellular microenvironment. Extensive research is directed towards developing biomimetic surfaces, which exert control over spatial properties, defining the microenvironment for different cell types.[6]

CCPs have been developed to study cell interactions within their *in vitro* microenvironment. CCPs provide opportunities to obtain a thorough understanding of the properties of the surface to which the cells are attached and also offer a valuable area of research for engineering biomedical devices.[7] CCPs find their applications in many areas of tissue engineering like developing scaffolds for cell growth, construction of cell-based

biosensors, biocompatible implants and in the fields of toxicology and drug testing because they can reduce costs and simplify testing procedures.[7,8] Conventional biomaterial surfaces such as those formed by different biomedical polymers may have a large degree of surface heterogeneity with regard to the type and distribution of functional groups, presence of hydrophilic and hydrophobic domains, surface roughness, etc. Since all these parameters may contribute to cellular response, it is desirable to understand how surfaces should be composed to support attachment, growth and function of the cells. Researchers have studied the use of ECM proteins,[9] biodegradable polymers,[5] hydrogels[10] and nanofilms[11] to develop CCPs. However, most of these methods provide poor control over the presentation of active ligands to a cell thereby limiting prolonged cell viability and functionality.

A promising technique which could overcome some of the above problems in surface modification is the use of self-assembled monolayers (SAMs) for thin film deposition. SAMs are ordered molecular assemblies formed by the adsorption of an active surfactant onto a solid surface. SAMs are attractive because they are well packed, are homogeneous across the assembly, and can be reproducibly assembled and patterned.[12] SAM patterned substrates provide a means to more precisely define and regulate surface chemistry and identify ideal surface properties that enhance or inhibit cell adhesion, cell migration and gene expression. Futhermore, SAMs provide a well-defined and synthetically flexible system which controls the properties of surfaces that can be modified on demand.[13,14] As the surface properties of a SAM are different from those of the bulk substrate, surface modification methods permit development of a more

diverse set of surface chemistries through chemically altering reactive terminal groups, thus permitting development of substrates with diverse surface properties.

Growth of cells on SAMs of alkanethiolates on gold (Au) surfaces has been studied extensively for the past decade.[2,13-16] Previous studies of fibroblast cell growth on SAMs modified Au have indicated that carboxylic acid terminated SAMs are most favorable surfaces for cell attachment followed by methyl and hydroxyl groups.[17] In the case of osteoblasts, both carboxylic and hydroxyl terminated SAMs showed similar levels of attachment followed by methyl terminated SAMs.[16] Similarly, the effect of alkyl chain length on cellular attachment has been studied, and it has been demonstrated that increase in chain length decreases the number of cell attachment.[18] Thus, different cell types exhibit different responses to a specific surface.

However, in contrast to the tremendous amount of cell culture studies done on SAM-modified Au surfaces,[12-24] very few studies have been directed on other surfaces of importance such as indium tin oxide (ITO), silicon (Si), and gallium arsenide (GaAs). ITO has been widely used as an electrode for studying electrochemistry of biomolecules[25] due to its transparent and conductive properties. This dual property and stability under physiological conditions[25] make them ideal for tissue engineering. It has also been shown that acids, amine[26] and proteins[27] specifically adsorb on ITO. Interdigitated microelectrodes made of ITO were also used for the synapse formation by neuronal differentiation of rat pheochromocytoma cells (PC12) and blastocyst-derived murine embryonic stem cells (ES-J1).[28]

Silicon is the most commonly used substrate in the semiconductor industry. The properties and fabrication techniques are known and well-established. SAMs of

organosilanes on Si have been successfully used to tailor material surfaces to obtain control over the molecular composition and the resulting integral properties of the surfaces.[29] Recent studies have used SAMs to evaluate the effect of surface charge, wettability and topography on protein adsorption and cell behavior using *in vitro* assay systems.[30] More specifically, the strength of cell adhesion and spreading on SAMs have been investigated. However, most of the studies with SAMs did not provide a detailed characterization of the behavior of cells from connective tissue in terms of specific cellular functions.

Although silicon is widely used in the semiconductor industry, GaAs–also a semiconductor–has several advantages over silicon. In addition to its useful optoelectrical properties, it offers a higher mobility, which results in faster electronic circuits and switching times, as well as a lower energy dissipation at comparable powers and, therefore, a lower noise level.[31] Although GaAs has found practical uses in many applications, chemical instability of its surface and cytotoxicity creates problems for both *in vivo* and *in vitro* applications.[32,33] GaAs therefore needs to be coated with protective layers that provide biocompatible interfaces. Indeed, biocompatibility has recently led to the development of the first GaAs-based biosensor for direct detection of micromolar levels of nitric oxide under physiological conditions.[34] Thus, the self-assembly of alkanethiol monolayers, a process well studied on gold, has become an obvious strategy for the realization of ultra-thin surface coatings on GaAs.

This dissertation will show how SAMs with different end groups (amino-NH_2, methyl-CH_3, carboxylic-COOH, thiol-SH) SAMs influence or condition cellular (Human dermal fibroblasts (HDFs), Mesenchymal stem cells (MSCs), Rat brain cortical neurons'

(RBNs), Hepatocytes') response and how the cells proliferate on the SAM-substrates (ITO, Si, GaAs) and the resultant molecular assemblies and structures produced. Based on the results obtained from the 2D studies, a 3D SAM-based bioreactor containing microfluidic channels was designed using CovnentorWare software and fabricated on Si using photolithography. The design was based on physiologically based pharmacokinetic (PBPK) model and LDH release was determined to assess the effect of SAM, 3D and dynamic flow on HDF response.The ultimate goal is development of bioreactors capable of supporting growth and functional differentiation of other cell types in a well controlled manner and use these bioreactors for drug toxicity screening.

1.2 Organization of the Dissertation

This dissertation comprises 9 chapters including introduction, summary and future work. Chapter 2 presents a literature review of SAMs on different surfaces (Au, Si, GaAs, Ag, Pd, Cu, ITO), their organization and advantages. It also describes different bioengineered surfaces used for cell culture studies leading to the importance of SAMs for such studies. In Chapter 3, experimental details including the materials used, and SAM preparation and their characterization by different methods are discussed. Also the procedures used for cell culture studies are described in detail. Chapter 4 discusses results on human dermal fibroblast (HDF) cell viability and proliferation on different SAM-modified conducting (ITO) and semi-conducting (Si, GaAs) substrates. Chapter 5 focuses on mesenchymal stem cell (MSC) culture on four different SAM-modified ITO substrates. The viability and phenotype of rat cortical neurons on two different SAM-modified ITO surfaces are discussed in Chapter 6. Chapter 7 is the heart of the dissertation, which presents proliferation along with the viability, phenotype and

functionality of primary isolated rat hepatocytes on three different SAM-modified substrates (ITO). Chapter 8 presents simulation and fabrication of a SAM-modified 3D cell-based bioreactor and the analysis of LDH leakage of HDFs cultured in the reactor. Results are presented in each section with detailed discussion presented at the end of each chapter. Finally, Chapter 9 summarizes the entire work along with scope for future studies.

CHAPTER 2

LITERATURE REVIEW

2.1 Self-Assembled Monolayers

2.1.1 Overview

Over past 20 years, the field of self-assembled monolayers (SAMs) has experienced tremendous growth not only in synthetic sophistication but also in depth of characterization.[12,35] This field actually began in 1946 with Zisman and coworkers publishing the formation of a monolayer by adsorption of a surfactant on clean metal surface.[36] This effort was followed by many other works, but the real interest in this field started with Nuzzo and Allara's work, wherein alkanethiolates on gold were prepared by adsorption of di-n-alkyl disulfides from dilute solutions.[37]

It is imperative to know the procedure involved in the formation of SAMs at this point. Figure 2.1 depicts the steps involved in the formation of SAMs on a planar solid surface. The simple process involved in the preparation makes SAMs inherently manufacturable and thus technologically attractive for building superlattices and for surface engineering. SAMs also help in understanding the fundamentals of self-organization, structure-property relationships, and interfacial phenomena. The ability to tailor both head and tail groups of the molecules makes SAMs an excellent system in understanding intermolecular, molecule-substrate and molecule-solvent interactions.

8

Some of the properties like ordering, growth, wetting, adhesion, lubrication and corrosion have been studied previously. In addition, SAMs also provide necessary flexibility both at the molecular and at material level on the structure and stability of two-dimensional assemblies which can be later applied to three-dimensional structures.
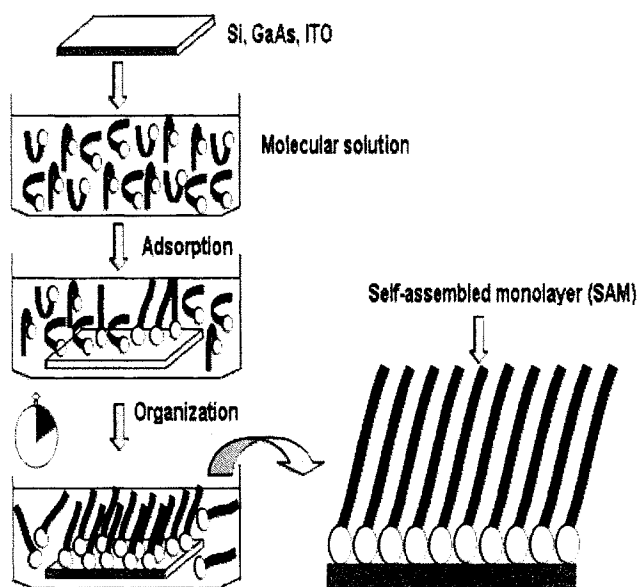
Figure 2.1 Procedure for the formation of SAMs (Adapted from[38]).

Furthermore, SAMs are also well-suited for studies in nanoscience and technology because (1) they are easy to prepare and do not require ultrahigh vacuum (UHV) or other specialized equipment (e.g., Langmuir-Blodgett (LB) troughs) in their preparation, (2) they form on surfaces of all sizes and shapes and are critical components for stabilizing and adding function to nanometer-scale objects such as thin films, nanowires, colloids, and other nanostructures, (3) they can couple the external environment to the electronic (current-voltage responses, electrochemistry) and optical (local refractive index, surface plasmon frequency) properties of metallic structures, and

(4) they link molecular-level structures to macroscopic interfacial phenomena, such as wetting, adhesion, and friction.

2.1.2 Monolayers of Organosilicon Derivatives

Organosilicon derivatives include alkylchlorosilanes, alkylalkoxysilanes, and alkylaminosilanes, are usually formed on hydroxylated surfaces of Si. The *in-situ* formation of polysiloxane, which is connected to surface silanol groups (–SiOH) via Si-O -Si bonds is considered to be the driving force for this self-assembly. The monolayers of these derivatives have been successfully formed on silicon oxide,[39-43] aluminum oxide,[44,45] indium tin oxide,[46,47] mica,[48] quartz,[49] zinc selenide,[50] and germanium oxide.[50]

SAMs of alkyltrichlorosilane derivatives are hard to prepare because they depend on the amount of water present in the solution, the temperature at which the monolayer is formed and the time of deposition. While incomplete layers are formed in the absence of water,[40] excess water results in polymerization in water and siloxane deposition on the surface.[51] The threshold temperature below which an ordered monolayer is formed was found to be a function of chain length (higher for octadecyl: 18 °C and lower for tetradecyl chain: 10 °C).[52] Silberzan et al. also reported that 3 min is enough for the formation of the monolayer; while Wasserman et al. suggested over 24 h for completion.[53] Biernbaum et al. showed that the adsorption mechanisms of trichlorosilane and trimethoxysilane are different with higher tilt angle of chains in methoxysilanes. Also, the presence of amino group at the chain terminal causes more disordered layer because of acid-base interactions.[54]

2.1.3 Monolayers of Organosulfur
on Metal and Semiconductors

Sulfur and selenium compounds have a strong affinity to transition metal surfaces[55,56] because of the possibility to form multiple bonds with surface metal clusters.[57] Many kinds of SAMs have been formed on gold (Au (111))[58-61] but the most studied and understood SAM is that of alkanethiolates.

Kinetic studies of alkanethiol adsorption onto Au (111) surfaces have shown that, at relatively dilute solutions (1 mM), two distinct adsorption kinetics can be observed: [62] A very fast step which can be described as diffusion-controlled Langmuir adsorption. This step takes a few minutes, by the end of which the contact angles are close to their limiting values and the thickness about 80-90% of its maximum. The second step is a slow process described as the surface crystallization process, which lasts several h, at the end of which the thickness and contact angles reach their final values. These have been confirmed by XPS measurements,[63] as well as near edge X-ray absorption fine structure (NEXAFS) studies.[64]

The adsorption or reaction of alkanethiolates on gold is considered as an oxidative addition of the S-H bond to the gold surface, followed by a reductive elimination of the hydrogen. When a clean gold surface is used, the proton probably ends as a H_2 molecule. To be more precise, the fate of H_2 is still not understood.

$$R - S - H + Au_n^0 \rightarrow R - S^- Au^{+\bullet} Au_n^0 + \frac{1}{2} H_2 \qquad (2.1)$$
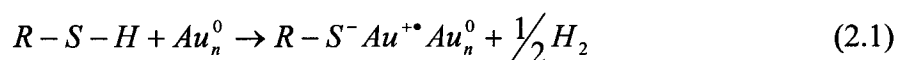
The release of H_2 is an important exothermic reaction in the overall chemisorption kinetics. It has been shown by XPS,[65] Fourier transform infrared (FTIR) spectroscopy,[66]

electrochemistry,[67] and Raman spectroscopy[68] that the adsorbing species is the thiolate (RS⁻).

Early electron diffraction studies[69,70] of monolayers of alkanethiolates on Au(111) surfaces show that the symmetry of sulfur atoms is hexagonal with an S-S spacing of 4.97 Å, and calculated area per molecule is 21.4 Å². Helium diffraction[71] and atomic force microscopy (AFM)[72] studies confirmed that the structure formed by docosanethiol on Au(111) is proportionate with the underlying gold lattice and is a simple $\sqrt{3} \times \sqrt{3}R$ 30° overlayer (Figure 2.2). FTIR studies also revealed that the alkyl chains in SAMs of thiolates on Au(111) usually are tilted ~26-28° from the surface normal, and display ~52-55° rotation about the molecular axis. This tilt is a result of the chains reestablishing vanderwall contact in an assembly with ~5 Å S-S distance, larger than the distance of ~4.6 Å, usually quoted for perpendicular alkyl chains in a close packed layer.
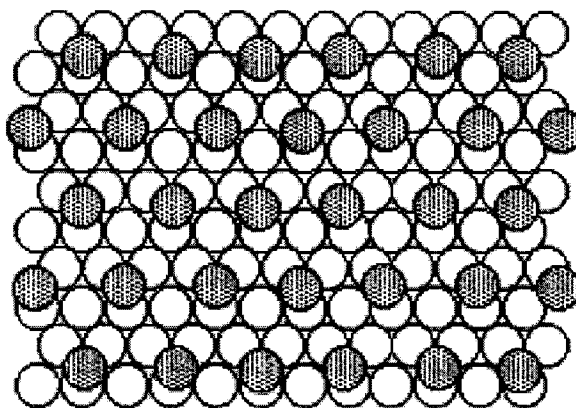
Figure 2.2 Hexagonal coverage scheme for alkanethiolates on Au(111). The open circles are gold atoms and the shaded circles are sulfur atoms.[35]

Although alkanethiolate SAMs have been investigated on gold and other surfaces such as copper and silver (See Section 2.1.5), studies on the construction of SAMs on GaAs surfaces are still limited. GaAs surface is known to have high densities of interface

states compared to Si, mainly due to its stoichiometric deficits and surface defects such as oxides.[73] Allara et al. succeeded in constructing SAMs on GaAs by using molten alkanethiol at higher temperatures.[74] Ohno et al. prepared SAMs on GaAs surface in dilute thiol solution (1 mM) under mild conditions by cleaving the oxide on the surface.[75] However, all these preparation conditions are harsh and are not practical.

Baum et al. demonstrated a novel simple method for formation of alkanethiol SAMs on the GaAs surface.[76] The chemical inertness of the oxide-covered GaAs was overcome by using a small amount of ammonium hydroxide (NH_4OH) in the thiol solution for providing fresh and oxide free GaAs during the modification process. X-ray photoelectron spectroscopy (XPS) characterization of SAM of octadecanethiol (ODT) on GaAs by Ye et al. revealed the formation of S-As bond with the length of molecule estimated to be 1.55 nm.[77] This study gave a tilt angle of 56° which is similar to that obtained from previous works for ODT SAMs on GaAs.[74,78]

2.1.4 Alkyl Monolayers on Silicon

Linford and Chidsey demonstrated first that robust monolayers can be prepared where the alkyl chains are covalently bound to a silicon substrate mainly by C-Si bonds.[79] They used hydrogen-terminated silicon (H-Si(111) and H-Si(100)), and diacetyl peroxide for the SAM deposition.[79] The adsorption of alkyl chains was attributed to a series of free-radical reactions. Either the acyloxy or the alkyl radical abstracts hydrogen from the H-terminated silicon surface to yield a dangling bond:

$$R^{\bullet} + H - Si(111/100) \rightarrow RH + {}^{\bullet}Si(111/100) \tag{2.2}$$
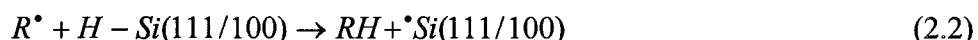
Finally, this surface radical combines either with the alkyl or with the acyloxy radical to give the Si-R or Si-O(O)CR species, respectively.

2.1.5 SAMs on Other Substrates

Gold is the most preferred substrate because it forms good SAMs and has been extensively studied. Other materials offer similar properties, but the SAMs formed on these materials have been studied less than those on gold.

Silver is the most studied substrate for SAMs of alkanethiolates next to gold, but it oxidizes readily in air and is toxic to cells.[80] It does, however, give high-quality SAMs with a simpler structure than gold and bonding of the monolayer in the form of a thiolate.[81] Copper is interesting from a technological perspective because it is a common material for interconnects and seed layers for electroless deposits, but it is even more susceptible to oxidation than silver.[81] The adsorption of an organosulfur adlayer can overcome the tendencies of copper to oxidize and strongly prevent adsorption of contaminants. The chemistry involved or the structures formed on this metal remain incompletely understood.[81]

Palladium has a number of useful characteristics and seems to be a practical alternative to gold for some applications and is superior to gold for others. Some of the properties such as: (1) smaller grain size in thin films compared with gold; this property is important for fabricating micro- and nanostructures with low density of defects and low edge roughness.[82] (2) compatible with complementary metal oxide semiconductor (CMOS) processing compared with gold[83]. Studies of SAMs on palladium as supports for adherent cells indicate that the long-term stabilities of these cell cultures are greater than those on gold.[84] But the cost of palladium make them less useful compared with gold.

ITO is of considerable interest in SAM studies because monolayer formation on ITO has been relatively less investigated. ITO is a mixture of indium (III) oxide [In_2O_3]

and Tin (IV) Oxide [SnO$_2$], typically 9:1 ratio by weight. The common applications of ITO are coatings for electronic displays, gas sensors, and anti-static windows. ITO is also used as an electrode for biochemical studies, due to its transparent and conductive nature.[85] Further investigations have shown specific adsorption of amines and proteins on ITO coated surfaces.[86,87] The transparency of ITO makes it easier to observe and image cell attachment. The surface chemistry of ITO is similar to that of silicon; therefore, alkyloxysilanes are used for monolayer formation. Also, aliphatic and aromatic thiols with –COOH and –CH$_3$ end groups have been reported to form monolayers on ITO.[88]

2.2 Bioengineered Surfaces

Mammalian cells are anchorage dependent, requiring an underlying matrix to attach and carry out their regular metabolic, proliferative and differentiation functions.[89] The attachment of these cells on substrates forms an important prerequisite for the development of bio-implants, CCPs and cell colonization on tissue engineering scaffolds.[90] Cellular attachment is a consequence of protein adsorption on substrates, but how the cell receives information about the nature of the substrate is still under investigation. It has been reported that the cellular microenvironment, i.e., the ECM plays a major role in controlling cell behavior *in vivo*, ensuring proper tissue function.[90,91]

Extensive research in the areas of drug discovery and toxicity studies has led to the development of CCPs which facilitate a thorough understanding of cell-substrate interactions.[92] Cell culture platforms control cellular attachment and growth as a function of space and time. They are incorporated in developing cell based biosensors, which monitor physiological change due to exposure to different antigens.[92]

2.2.1 ECM Modified Surfaces

The ECM is made up of three classes of macromolecules: glycosaminogens, polysaccharide chains covalently linked to proteins forming proteoglycans, and fibrous proteins. There are two functional types of fibrous proteins: structural (collagen, elastin) and adhesive (laminin, fibronectin).[4] The glycosaminoglycans intermesh and form a hydrated gel-like substance, in which the fibrous proteins are embedded.[4] The collagen fiber provides strength to the matrix while the elastin fibers provide resilience. The adhesive proteins help the cells attach to the ECM. These proteins provide specific receptor surfaces and ligands, which are identified by the cell surface receptors. Without adhesion, cells enter into apoptosis, eventually causing cell death.

The need to recreate a suitable microenvironment for cell viability, growth and proliferation has resulted in the development of a large number of bioengineered substrates. Almost all these surfaces have certain common properties like the ability to adsorb protein, uniformity, consistency in surface topography and minimal cytotoxic effect on cells. Cell attachment occurs due to the interaction of cells with the ECM through specific interaction sites called focal adhesion sites. Cell surface receptors identify specific protein domains containing peptide sequences like RGD (arginine-glycine-aspartic acid) and bind to them.[93] To mimic the ECM properties *in-vitro*, bioengineered surfaces coated with ECM components like collagen, fibronectin, vitronectin and fibrinogen have been developed to promote cell-surface interactions by spatially directing attachment of specific cell lines to substrates.

Collagens are a significant component of the ECM and collagen-coated surfaces support growth and viability of different mammalian cell lines.[94] Collagen surfaces are

preferred due to their biocompatibility, biodegrability, mechanical integrity and widespread availability.[94,95] Hepatocytes and epithelia cultured on collagen films expressed phenotypes similar to those observed *in vivo*.[96] Osteoblast culture on patterned collagen films to study cellular alignment and viability showed a high degree of phenotypic expression and cellular viability when the surfaces were stabilized using calcium phosphate deposition.[97]

Modification of collagen films by cross-linking and blending with other polymer increase their mechanical stability upon cell culture. Collagen-chitosan matrices have been used to culture hepatocytes towards the development of artificial livers and shown to support hepatocyte adhesion and division over extended periods of time.[98] Collagen is a major component of the hepatocyte basal membrane and promotes hepatocyte adhesion and growth.

2.2.2 Polyelectrolyte Multilayers

Polyelectrolytes are polymers with units containing an electrolyte group. These polymers dissociate in solution to produce charged species.[99] Since polyelectrolytes are soluble in water, they are being investigated for a number of biomedical applications like implant coatings, controlled drug release and biosensor fabrication. They are ideal candidates for biomaterial applications due to their biocompatibility and inert nature, ability to incorporate biological molecules and control film composition and thickness.

The ability of these multilayers to be patterned effectively using microfabrication techniques like soft lithography and micropatterning gives rise to complex 3D surfaces for biomedical applications.[100] Cell interactions are influenced by the nature and charge of the outermost layer, protein adsorption and thickness of layers.[100] Chondrosarcomas

cultured on alternating layers of poly-L-lysine (PLL) and poly-glycolic acid (PGA) showed increased cellular adhesion on PLL ending films when compared with PGA ending films, upon measurement of the adhesive forces.[101]

Primary hepatocytes, selective in their attachment *in vitro*, have been reported to attach, spread and exhibit differentiated functions on polyelectrolyte multilayers.[102] The PEM used were alternating layers of poly (diallyldimethylammonium) chloride (PDDA) and poly (4-styrenesulfonic acid (PSS)). The hepatocytes exhibited characteristic cell patterns upon adhesion on PEM surfaces and showed increased urea and albumin production which are indicators of cellular viability.[102]

2.2.3 Hydrogels

Hydrogels are networks of water soluble polymer chains. They are present in the form of colloidal gels having water as the dispersion medium. Hydrogels have been widely used for cell culture studies due to their high water content, pliability, and biocompatibility and easily controlled mass transfer properties. These properties of hydrogels resemble those of biological tissue.

Polyethylene glycol (PEG) hydrogels have been used to encapsulate mammalian cells like rat osteoblasts,[103,104] rat cortical neurons,[105] and human hepatocytes.[106] These hydrogels can be microfabricated and modified using peptide sequences.[107,108] Rat hepatocytes encapsulated in PEG hydrogels maintained high cell viability indicated by increased protein production over a period of time.[106]

2.2.4 SAMs as Model Biological Surfaces

A primary challenge in developing *in vitro* model surfaces is developing methods that will allow precise control of the composition and structure of the surface while

permitting natural biological interactions to occur. These interactions should be such that the results can be clearly interpreted and related to those *in vivo*.

SAM-modified surfaces are one of the useful systems for studying these biological and biochemical processes because, like the biological surfaces, they are nanostructured and are formed by self-assembly. They also present a wide range of organic functionalities including functionality that can resist the adsorption of proteins. SAM functionalized with the large, delicate ligands needed for biological studies is easy to prepare just by either synthesizing molecules with the ligand attached to form the SAM or, more commonly, attaching the ligands to the surface of a preformed, reactive SAM. These SAMs are also compatible with a number of techniques such as surface plasmon resonance (SPR) spectroscopy,[109,110] optical ellipsometry,[111,112] RAIRS,[112] QCM,[113] and mass spectroscopy[114] for analyzing the composition and mass coverage of surfaces as well as the thermodynamics and kinetics of binding events.

One disadvantage of SAMs is that the structure of the SAM is essentially static. This characteristic differs from that of biological membranes, which are fluid and rearrange dynamically. Langmuir-Blodgett (LB) films[115] and bilayers of lipids on solid supports[116] present two alternative technologies for creating dynamic models of biological surfaces. Instrument complexity and non-reproducibility makes this area of studies limited. Studies have shown the patterning of lipid regions on solid supports but, these are in their beginning stages.[117]

The first method of attaching cells on surfaces is the use of mixed SAMs composed of a ligand-presenting molecule and a second SAM-forming molecule, usually one terminated with functional groups that can resist protein adsorption. This variation in

the type, density, and the accessibility helps in understanding the interactions taking place at the surface and the cell.[20,118] Patterns of SAMs generated by microcontact printing provide a second method for attaching cells on surfaces: hydrophobic SAMs are printed to define regions that allow cells to attach and subsequent immersion of the substrate into a solution containing a second thiol forms a SAM in the surrounding regions that resists the adsorption of proteins (and cells).[20,21] These patterned surfaces make it possible to study the biochemical response of cells to mechanical stimuli.[119] Also electrochemical methods have been used to remove or modify the SAMs to release the cells from the confinement originally imposed by the pattern of the SAM.[24]

The structure and properties of SAMs immersed in solvents is less understood compared with that for SAMs in air or in a vacuum. The use of SAMs as substrates for studies in biology requires extended contact between SAMs and an aqueous environment containing a high concentration of salts and biomolecules (enzymes, extracellular matrix proteins, plasma components, sugars).[12] The structure and dynamics of the exposed surface of a SAM under these conditions have not been characterized completely. Grunze and co-workers have shown that the conformational changes at the exposed surface of SAMs terminated with PEG (45 EG subunits) upon exposure to water.[120] Also the effect of physiological conditions on the long-term stability of SAMs is not understood. Langer and co-workers have shown that SAMs terminated with EG develop substantial defects after immersion in phosphate buffer solution or in calf serum for 4-5 weeks.[121] The presence of cells at the surfaces also accelerates the process and the ability of EG-terminated SAMs to prevent the adhesion of cells is compromised in ~ 7-14 days.[84]

The flexibility in using SAMs along with some of the advantages makes them ideal to be used as model biological surfaces. Still, many factors have to be considered before the full potential of SAMs can be used for tissue engineering.

CHAPTER 3

EXPERMENTAL

3.1 SAMs Used

In all the chapters described hereafter, four different kinds of SAMs have been used on conducting and semi-conducting substrates. Figure 3.1 shows the molecular formulas and structures of the SAMs used:
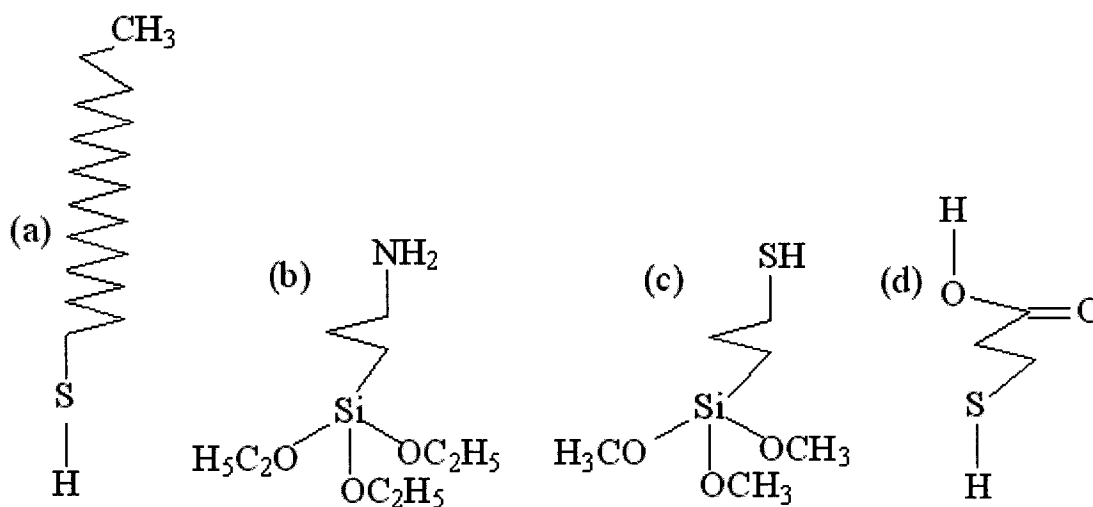
Figure 3.1 Molecular formula and structure of different SAMs used in the research. (a) 1-octadecanethiol (ODT) (b) 3-(aminopropyl)triethoxysilane (APTES) (c) 3-(mercaptopropyl)trimethoxysilane (MPS) and (d) 3-mercaptopropionic acid (MPA).

The molecules vary in their chain length and end groups. Each molecule presents a different moiety and modifies the surface in different ways depending upon the group that binds to the surface.

3.1.1 SAM Formation

3.1.1.1 1-Octadecanethiol (ODT)

The structural formula of 1-octadecanethiol is $CH_3(CH_2)_{17}SH$. This molecule binds to the GaAs and ITO substrate by the formation of sulphide bonds leaving the hydrocarbon end free, forming a hydrophobic surface. GaAs samples were cleaned in acetone followed by ethanol for 5 min by ultrasonic agitation. Just before surface derivatization, the GaAs samples were immersed in 37% HCl for one min to remove oxide present on the surface, rinsed in deionized (DI) water and dried in N_2. SAM deposition on GaAs was performed in 5 mM ODT solutions with the addition of 30% aqueous ammonia solution at 50 °C for 8 h after purging with N_2. Physisorbed ODT was removed by carefully rinsing with ethanol followed by rinsing in DI water and drying in N_2.

ITO substrates were cleaned by sonication in toluene, acetone and ethanol for five minutes each and in DI water for 30 min to remove surface carbon contaminants which interfere with monolayer formation. The substrates were then rinsed, dried in N_2 and used. The substrates were immersed in a solution of neat ODT for one hour at 50 °C followed by rinsing in ethanol, DI water and N_2. The substrates were sterilized in 70% ethanol before use.

3.1.1.2 3-(Aminopropyl)triethoxy Silane (APTES)

APTES (Structural formula NH_2-$(CH_2)_3$-Si $(OC_2H_5)_3$) binds to Si and ITO by the formation of siloxane bonds leaving a free –NH_2 end group. This end group causes the SAM-coated surface to be hydrophilic. Si samples were cleaned by sonication in acetone followed by ethanol for 5 min and finally rinsed in DI water and dried in N_2. The samples

were then immersed in Nanostrip solution at 90 °C for 15 min, rinsed in DI water and dried in N_2. SAMs of 3-APTES were formed by immersing the substrates in 1 mM of the SAM in ethanolic solution for 1-24 h, followed by rinse in ethanol and DI water and finally drying in N_2.

The ITO substrates were cleaned by sonication in toluene, acetone and ethanol for five minutes each and 30 min in DI water. The substrates were dried using dry N_2 gas and then were immersed in a 0.5-5 mM ethanol solution containing 3-APTES for 2-24 h followed by rinsing in ethanol and N_2 drying. The substrates were sterilized in 70% ethanol for a day prior to use.

3.1.1.3 3-(Mercaptopropyl)trimethoxy Silane (MPS)

MPS (Structural formula $SH-(CH_2)_3-Si\ (OCH_3)_3$) binds to ITO by the formation of siloxane bonds leaving a free –SH end group. The cleaned substrates were immersed in a 0.5-5 mM ethanol solution containing MPS for 2-24 h followed by rinsing in ethanol and drying in N_2. The substrates were sterilized in 70% ethanol for a day prior to use.

3.1.1.4 3-Mercaptopropionic Acid (MPA)

MPA (Structural formula: $HSCH_2CH_2COOH$) binds to ITO by the formation of sulphide bonds leaving the carboxylic end free. The cleaned substrates were immersed in a solution of neat MPA for one hour followed by rinsing in ethanol, DI water and N_2. The substrates were sterilized in 70% ethanol before use.

3.2 SAMs Characterization

3.2.1 Contact Angle Measurements

It is necessary to characterize the molecule on different surfaces before their use for cell culture studies. The SAM on metal and semiconductor surfaces can be

characterized by different techniques. Contact angles offer an easy-to-measure indication of the modification of the uppermost surface layers of a solid. The measurement determines wettability and adhesion and also allows prediction of coating properties and detection of trace surface contaminants. Contact angle is a physical manifestation of the more fundamental concepts of surface energy and surface tension. This technique is simple to determine the hydrophobic or hydrophilic property of the SAM.

When a tangent line is drawn from the droplet to the touch of the solid surface, the contact angle is the angle between the tangent line and the solid surface as shown in Figure 3.2. Its operation is simple: A droplet of liquid is dispensed onto the substrate surface (manually or automatically), and a CCD camera reveals the profile of the droplet on the computer screen. Software calculates the tangent to the droplet shape and the contact angle. Data and the images are collected, analyzed, and stored in a computer.

Tangent to drop shape at contact point →

Contact angle = angle between tangent and ← surface
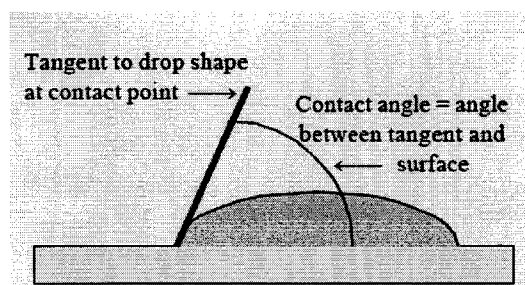
Figure 3.2 Definition of contact angle[122]

Figure 3.3 gives an illustration of two different contact angles formed which determines the nature of the surface. If the angle made by the tangent $\Theta < 90°$, the surface is considered as hydrophilic and for $\Theta > 90°$ the surface is considered as hydrophobic.
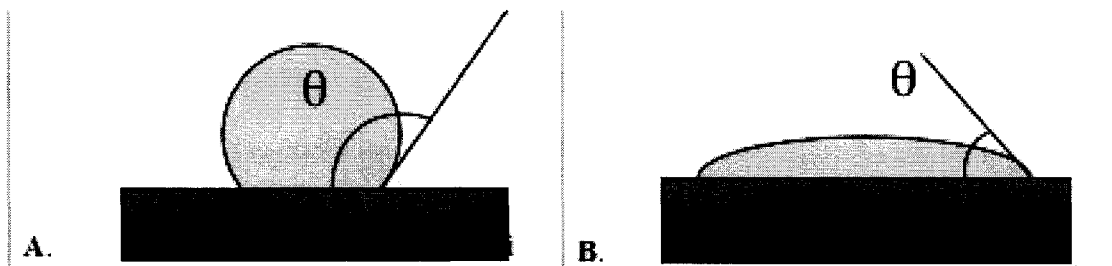
Figure 3.3 Nature of the surface based on contact angle. (a) $\Theta > 90°$: Hydrophobic surface (b) $\Theta < 90°$: Hydrophilic surface.

Contact angle measurements were obtained using the sessile drop method on a Data Physics instrument contact angle goniometer. In this method, a drop of water (0.5 μL) was suspended from a microliter syringe positioned above the sample stage. The syringe was moved towards the sample so that the water droplet makes contact with it. The syringe was then retracted, leaving the sample on the substrate. The image was then recorded using a CCD camera and the contact angle measured using the software provided.

3.2.2 Infrared Spectroscopy

Infrared spectroscopy is a powerful tool for identifying types of chemical bonds (functional groups). The wavelength of IR-light absorbed is characteristic of the chemical bond. By interpreting the infrared absorption spectrum, the chemical bonds in a molecule can be inferred. IR spectra of pure compounds are generally unique in that they behave like a molecular "*fingerprint*" of the molecule. Figure 3.4 shows an illustration of IR absorbance of common organic functional groups.
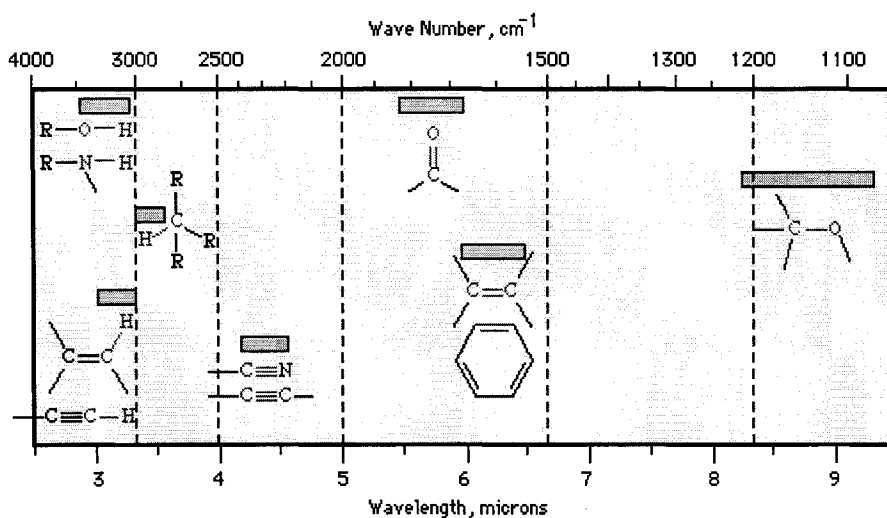
Figure 3.4 IR absorbance of common organic functional groups.

Alcohols and amines display strong broad O-H and N-H stretching bands in the region 3400-3100 cm^{-1} as shown in Figure 3.4. Triple bond stretching absorptions occur in the region 2400-2200 cm^{-1}. Absorptions from nitriles are generally of medium intensity and are clearly defined. Alkynes absorb weakly in this region unless they are highly asymmetric; symmetrical alkynes do not show absorption bands. Carbonyl stretching bands occur in the region 1800-1700 cm^{-1}. The bands are generally very strong and broad. Carbon-carbon double bond stretching occurs in the region around 1650-1600 cm^{-1}. The bands are generally sharp and of medium intensity. Aromatic compounds will typically display a series of sharp bands in this region. Carbon-oxygen single bonds display stretching bands in the region 1200-1100 cm^{-1}. The bands are generally strong and broad.

3.2.2.1 RAIRS

RAIRS is an acronym of Reflection-Absorption Infrared Spectroscopy. It is also known as IRRAS: IR Reflection Absorption Spectroscopy. It is widely used to identify

molecular adsorbates that form on metals and semiconductors in the course of surface chemical reactions. As a molecule sits on a surface, it will vibrate. Such vibrations can be studied by directing infrared light on to the surface. If the molecule has a dipole moment (that is, one end of the molecule has a positive charge and the other end a negative charge), then the molecule can absorb infrared light, but only at certain fixed frequencies. Hence, an infrared spectrum of light reflected from the surface will show absorption peaks which are characteristic of the molecule on the surface. Figure 3.5 shows the reflection geometry of the incident IR on a plane. The amplitude and phase changes experienced on reflection depend upon the direction of the electric field vector of the wavefronts. The direction of the electric field vector of the wavefronts is resolved into components in the incident plane (P polarized) and normal to the incident plane (S polarized).
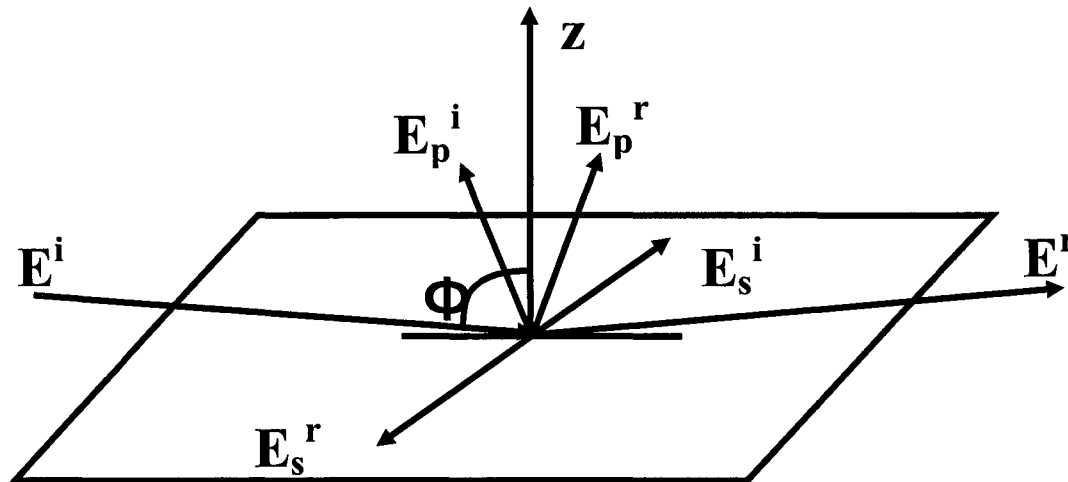
Figure 3.5 The reflection geometry showing the s and p components of the electric fields of incident (E^i) and reflected (E^r) radiation.

Here it should be noted that certain selection rules apply in contribution of absorption peaks, making it different from the regular IR technique. For a grazing angle

of incidence, only the component of the electric field vector perpendicular to the surface, $E^{\perp}$, can interact with the adsorbate oscillating dipole, and it is exclusively the p component of the incident radiation which contributes to $E^{\perp}$, this being optimum at high angles of incidence. Further, the most highly reflecting metal surface will yield the highest absorbance.

3.2.2.2 ATR

Attenuated total reflectance infrared (ATR/IR) spectroscopy also known as Internal reflection spectrometry works on the principle that by pressing small pieces of membrane against an internal reflection element (IRE), e.g., zinc selenide (ZnSe) or germanium (Ge) mid-infrared spectra can be obtained. IR radiation is focused onto the end of the IRE. Light enters the IRE and reflects down the length of the crystal. At each internal reflection, the IR radiation actually penetrates a short distance (~1 mm) from the surface of the IRE into the polymer membrane. It is this unique physical phenomenon that enables one to obtain infrared spectra of samples placed in contact with the IRE.

3.2.2.3 Methodology

RAIRS for SAMs on GaAs, ITO and Si were obtained from a Thermo Nicolet 470 FT-IR spectrometer equipped with a Smart Saga accessory containing a MCT (mercury-cadmium-telluride) detector. The chamber of the instrument was purged with N_2 and the detector was kept cold using liquid N_2. The spectra were recorded at a resolution of 4 cm^{-1}(512 scans) and the base-line corrected. The observed peaks were assigned to vibrations according to published FTIR studies on these or similar compounds using the Smart Saga software. ATR spectra was obtained by using the Smart

Miracle accessory, which is just plugged into the equipment. The spectra were recorded at a resolution of 4 cm^{-1} (512 scans) and compared with the published data.

3.2.3 Atomic Force Microscopy

Atomic force microscope (AFM) was used to measure the roughness of the SAM-modified ITO surfaces. The QUESANT AFM used for all experiments has a profiler unit, an electronics interface, computer to run the software and store the data, and a heating unit for the substrate. The probe has a silicon cantilever at its end, and the stylus tip is at the bottom of the cantilever. The profiler unit has a stepper motor for downward and upward movements. A feedback signal stops the unit from crashing onto the substrate at a minimum distance. The stylus moves from left to right laterally during scanning of the sample. A laser in the profiler unit hits the cantilever and is reflected back. The profiler unit and the sample stage are placed in a vibration-free chamber.

For all samples the scan head of imaging was initiated at the lowest magnification. The imaging was performed in the non-contact mode (or WaveMode) with a NSC16 silicon cantilever. Initially, the scan head was brought down towards the sample and the region of interest was brought into the camera view. Then the scan parameters were set using the SPM configuration menu. An integral gain of 250 and a proportional gain of 300 were used throughout the imaging process. For the initial scans, a scan size of 5μm x 5μm, a scan rate of 3 Hz and a scan resolution of 500 lines/scan were used. Also, in the WaveMode setting, a minimum damping of 50% was selected. Once these large area scans were complete and the images stored, a smaller region of interest was chosen with the previously scanned region using the hard zoom option. For the smaller region

scans, lower scan frequencies of 1 or 1.5 Hz and higher scan resolution of 1000 lines/scan were used.

The roughness of the samples were measured (using already stored image) using the Histogram Analysis Window in AFM. The height histogram shows the statistical distribution of the Z-heights of all the points in the image and, in addition, calculates several measures of surface roughness and displays them in the surface characterization panel. We are concerned with the average roughness (R_a): average deviation from the mean surface plane.

$$R_a = \frac{1}{N}\sum_{n=1}^{n=N}\left|Z_n - \overline{Z}\right|; \quad \overline{Z} = \textit{Average Roughness}; \tag{3.3}$$

3.3 Cell Culture Studies

3.3.1 Cell Morphology

Morphological observations of cell culture were performed using the phase contrast mode of Nikon® inverted fluorescent microscope. The cells were observed periodically for any changes in morphology and visual indications of cellular damage. Observations were recorded using the connected digital camera. The camera was turned on, and the objective was focused to obtain a clear image of specimen being viewed. Both 10X and 40X was used in the experiments. Magnification was changed by rotating the lens. The images were later transferred to a computer attached to the microscope for image analysis.

3.3.2 Cell Viability

Cell viability was measured using the 3-[4, 5-dimethylthiazol-2-yl]-2,5-diphenyl-tetrazolium bromide (MTT) and LIVE\DEAD® assay. The MTT assay is based on the

calorimetric conversion of MTT into formazan by viable cells, while the LIVE\DEAD® assay simultaneously identifies live and dead cells in a population.

3.3.2.1 LIVE/DEAD® Assay

The LIVE/DEAD® (Molecular probes, kit no: L-3224) test is a fluorescence assay which serves an indicator of cellular viability. This test uses two molecular probes which identify live and dead cells based on characteristic fluorescence emission, due to two specific indicators of cellular viability–intracellular esterase activity and cell membrane integration. The dyes used for this reaction are calcein AM and ethidium homodimer. Live cells exhibit intracellular esterase activity which converts the nonfluorescent Calcein AM to the fluorescent Calcein. This dye is contained in the cytoplasm and produces uniform green fluorescence (excitation\emission=495 nm\515 nm). Dead cells, on the other hand, are identified by a bright red fluorescence (excitation\emission =495 nm\635 nm) emitted by the binding of ethidium homodimer with the nucleic acids. This dye enters the dead cells through the broken cell membranes and undergoes a 40-fold magnification of fluorescence upon binding to the DNA.

The experiment starts with the removal of media from the well dishes and rinsing the substrates with phosphate buffer saline (PBS) or Hanks Balanced Salt Solution (HBSS) (without phenol red) twice and once with media. The working solution of the reagent was prepared by adding 4 μL of 2 mM ethidium bromide and 1 μL of 4 mM calcein AM to 2 mL of D-PBS and vortexed vigorously to ensure complete mixing of the reagent. 50 μL of this working solution is added to the substrates, and they are incubated for 45 min at room temperature. After incubation, the substrates are viewed using the fluorescent microscope using optical filter excitations of 485±10 nm (fluorescein optical

filter) for calcein and 530 ± 12.5 nm (Rhodamine optical filter) for ethidium bromide. Images of live and dead cells are taken using the CCD camera attached to the Nikon® inverting microscope. All the experiments were done in triplicate.

3.3.2.2 MTT Assay

The MTT based cell growth determination kit (Sigma, St. Louis, MO, Stock no: GCD1) was used to quantify the cellular viability and growth as a function of the mitochondrial activity. The mitochondrial dehydrogenase enzymes of viable cells cleave the tetrazolium ring of MTT to form purple MTT formazan crystals which are soluble in 1N HCl. The resulting purple solution can be spectrophotometrically analyzed. An increase in absorbance is directly proportional to the amount of formazan production and hence, the number of viable cells.

In this method, the cultured cells are rinsed with buffer and incubated with MTT working solution for four hours. The formazan crystals formed on the surface are then dissolved in 1N HCl in isopropanol and their absorbance monitored at 595 nm using the TECAN® plate reader with the reference set at 690 nm.

3.3.3 Cell Functionality

3.3.3.1 Measurement of Lactate Dehydrogenase (LDH) Release

LDH is a stable cytoplasmic enzyme present in most cell types. When cells are damaged, there is rapid release of LDH into the cell culture media through damaged cell membranes. The LDH cytotoxicity kit (Thermo Electron Corporation, CO) was used to measure LDH activity in the cell culture supernatant, which provides quantification of cell death and cytotoxicity. LDH activity was measured in an enzymatic reaction wherein

LDH oxidizes lactate to pyruvate, reducing nicotinamide adenine dinucleotide (NAD) to NADH.

$$L - Lactate + NAD \xrightarrow{\quad LDH \quad} Pyruvate + NADH \qquad (3.4)$$

The LDH reagent is prepared by adding 10 mL of DI water to the lyophilized powder of LDH-L reagent kit. 25 μL of media is added to 1.5 mL of the reagent in a cuvette and mixed well. The experiment is carried out at 37 °C with the help of a water bath connected to the UV-vis spectrophotometer. UV-Vis spectrophotometer is set in the kinetics mode with the time set at 180 sec and wavelength set at λ = 340 nm. The slope of the curve is then calculated and substituted in the equation below to obtain the LDH quantity:

$$Activity\ in\ U/L = \Delta Abs/\min \times Factor, \qquad (3.5)$$
$$Factor = \frac{TV \times 1000}{6.3 \times SV \times P},$$

where

TV = Total reaction volume in mL (1.525 mL)

SV = Sample volume in mL (0.025 mL)

6.3 = mM absorption coefficient of NADH at 340 nm

P = Cuvette pathlength in cm

3.3.3.2. Measurement of Total Protein Content

The measurement of total protein content is performed using the Bio-Rad protein assay. The assay, based on the method of Bradford, is a simple and accurate procedure for determining concentration of solubilized protein. It involves the addition of an acidic dye to protein solution, and subsequent measurement at 595 nm with a spectrophotometer

or microplate reader. Comparison with a standard curve provides a relative measurement of protein concentration.

The Bio-Rad Protein Assay is a dye-binding assay in which a differential color change of a dye occurs in response to various concentrations of protein. The absorbance maximum for an acidic solution of Coomassie® Brilliant Blue G-250 dye shifts from 465 nm to 595 nm when binding to protein occurs.[123] Beer's law is applied for accurate quantitation of protein by selecting an appropriate ratio of dye volume to sample concentration.

Bovine serum albumin (BSA) (Kit II, catalog number 500-0002) is used as the standard and is reconstituted by adding 20 mL DI water and mixed until it is dissolved. Protein Assay Dye Reagent Concentrate (catalog number 500-0006) contains 450 mL of solution containing dye, phosphoric acid, and methanol. Five dilutions of BSA protein standard were prepared, and the linear range of the assay for BSA which is 1.2 to 10.0 µg/mL is determined. 800 µL of each standard and sample solution is pippeted into a clean, dry cuvette. Protein solutions are assayed in triplicate. Then, 200 µL of dye reagent concentrate is added to each tube and vortexed. The mixture is then incubated at room temperature for at least five minutes. Absorbance increases over time and the absorbance is measured at 595 nm using UV-Vis spectrophotometer in the spectrum mode. The protein content is then calculated using:

$$O.D\ 595\ corrected\ for\ blank.\ 1.25 - 10\,\mu g/mL \times 0.8\,mL = 1 - 8\,\mu g\ protein \qquad (3.6)$$

3.3.4 Immunohistochemical Studies

Detection of Type I collagen was performed using the Vectastain ABC kit (Vector Laboratories, Burlingame, CA) and monoclonal antibodies raised against type I collagen

(Chemicon, Temicula, USA). The cells on the substrates were fixed by placing them in a series of gradient alcohol. 100% ethanol for three minutes, followed by 95% ethanol for three minutes, then in 75% ethanol for three minutes and finally in 50% ethanol for three minutes. Then the substrates were rinsed in PBS. Few drops of DAKO peroxidase blocking reagent was then added for the removal of endogeous peroxide and incubated for 30 minutes. Then the substrates were rinsed with PBS (three times for five minutes each). This rinsing was followed by removing excess PBS and adding non-immune blocking serum on the substrates and incubating for five minutes at room temperature. The blocking serum was then removed and primary antibody (anti collagen 600-401-1-4)1:99 ratio) is added and incubated overnight at 2-8 °C. The excess antibody was removed and stored for further use. Then the substrates were washed in PBS four times for five minutes each and incubated in secondary antibody for one hour. The substrates were then washed in PBS for four times, five minutes each and ABC reagent complex was added and incubated for 30 min. This process was followed by washing the substrates in PBS 4 times 5 minutes each. Finally, diaminobenzidine (DAB) substrate (to make DAB, add one silver and one gold tablet in 1 mL of tap water) was added on the substrates in dark and observed under the microscope for the formation of brown reaction. The reaction was then terminated by washing with PBS.

CHAPTER 4

HUMAN DERMAL FIBROBLAST CELL

CULTURE ON SAM SUBSTRATES

4.1 Human Dermal Fibroblasts

Engineered cell-tissue composites that mimic skin have been developed for use as

an *in vitro* system in sensitivity assays for potential skin-irritant compounds, drug

permeation studies, cytotoxicity tests, and detection of chemical warfare threats.[4,124,125] A

major objective of bioengineered skin mimics is the need to enhance functionality and

responsiveness and to improve the methodology for irritant and toxic reactions, reduce

the costs of testing, and facilitate decision-making.[126] Collagen and fibronectin can

modulate several physiological and pathological processes including tissue repair and

wound healing.[127] In addition, the organization of fibronectin matrix, acting as an

adhesive linker, regulates the composition and stability of the extracellular matrix.

Fibroblasts play a major role in building and maintaining the connective tissues in

the dermis of adult skin. Fibroblasts are anchorage-dependent cells; hence it is very

important that the surface on which they are cultured have properties that support

attachment.[17] Adhesion of cells to solid surfaces plays an integral role in several key

cellular processes.[128] The initial attachment of a cell to a surface is by receptors in the

cell membrane associated with the cytoskeleton, of which integrins are probably the most

37

important. The attachment process depends on the nature and conformation of adhesion proteins, such as fibronectin and vitronectin.[128] Cell attachment is normally followed by reorganization of cytoskeletal actin, resulting in flattening and spreading of the cell and formation of focal contacts, replete with clustered integrins, which participate in cell signaling events and in regulating cell behavior.[128] At each site of membrane-surface attachment, integrin receptors cluster and several intracellular signaling molecules are recruited. The signaling produced by integrin attachment to the ECM helps proteins in cell adhesion.[128] The adhesion of cells to the ECM and a host of subsequent signaling events are mediated by specific interactions between cell-surface receptors and ligands of the matrix.[129]

Matrix made of organic polymers is less attractive for the culture of these cells due to some of the problems such as reorientation of surface on transfer to aqueous media, heterogeneous nature and difficulty in analyzing the morphological characteristics.[130-132] Design of surfaces to elicit specific cell responses has thus been delayed. In this regard, SAMs have the capability to produce well defined surfaces of known structures and properties that may be carefully regulated and manipulated. It has been demonstrated that fibroblast cells attach more extensively to carboxylic acid terminated SAMs than to methyl terminated SAMs, with the cells spreading effectively on carboxylic end group.[16,17,133,134] While long chain methyl terminated SAMs exhibited lowest levels of cell attachment, small chain methyl ones exhibited intermediate levels of attachment and growth.[17] Cell attachment may also be influenced by the increased absorption of fibronectin on these SAMs or binding of the protein in an orientation such that cell binding sites are accessible.[30] Thus, the ability of human fibroblasts to assemble

their ECM is very important for cell growth. In addition, the organization of fibronectin matrix regulates the composition and stability of the ECM. We have used SAMs of methyl and amino end groups on Si, GaAs and ITO surfaces to understand the influence of both the nature of the end group and the chain length on the cellular response. The objective of this work in to identify ideal substrate properties that either enhances or inhibits cell adhesion, cell migration, or gene expression, as well as direct assembly of an ECM or functional tissue.

4.2 Materials and Preparation & Characterization of SAMs

4.2.1 Materials

Boron-doped (100) - oriented silicon wafers were purchased from Montco Silicon Technologies Inc., Semi-Insulating (100) - Undoped GaAs wafers were purchased from American Xtal Inc., ITO coated glass slides (2.5 cm x 2.5 cm x 0.1 cm) were purchased from Delta Technologies Ltd. All the substrates were diced into approx. 1 cm x 1cm samples.

Chemicals used were ODT (98%, Aldrich), APTES (99%, Aldrich) and Nanostrip (stabilized formulation of sulfuric acid and hydrogen peroxide compounds, Cyantek Corp.). All chemicals were used as received. ODT and APTES were stored in inert atmosphere after use.

4.2.2 Methods

Si samples were cleaned by sonication in acetone followed by ethanol for 5 min and finally rinsed in DI water and dried in N_2. The samples were then immersed in Nanostrip solution at 90 $^{\circ}$C for 15 min, rinsed in DI water and dried in N_2. SAMs of

APTES were formed by immersing the substrates in 1 mM of the SAM in ethanolic solution for one hour, followed by rinse in ethanol and DI water and finally drying in N_2. GaAs samples were also cleaned in acetone followed by ethanol for five minutes by ultrasonic agitation. Just before surface derivatization, the GaAs samples were immersed in 37% HCl for one minute to remove oxide present on the surface, rinsed in DI water and dried in N_2. SAM deposition on GaAs was performed in 5 mM ODT solutions with the addition of 30% aqueous ammonia solution at 50 °C for 8 h after purging with N_2. Physisorbed ODT was removed by carefully rinsing with ethanol followed by rinsing in DI water and drying in N_2. The ITO-coated slides were cleaned by sonication in toluene, acetone, ethanol each for five minutes and then in DI water for 30 min. The substrates were then rinsed, N_2-dried, and used. SAMs of ODT were formed on ITO by immersing the samples in the neat liquid for one hour, followed by ultrasonic agitation in ethanol, then a rinse in ethanol, DI water and N_2-dried. All the samples were sterilized in 100% ethanol for one day before culturing cells.

4.2.3 Characterization

4.2.3.1 Contact Angle Measurements

Figure 4.1 shows the contact angle measurements of different SAM-modified surfaces. An advancing contact angle in the range $22°-24°$ was observed for Si before SAM deposition, while an angle in the range $34°-36°$ was observed after SAM formation. This angle indicates the hydrophilic nature of the SAM. Advancing contact angle in the range $75°-77°$ was observed for GaAs and $40°-45°$ for ITO, while contact angle in the range $102°-105°$ was observed after SAM deposition, indicating the hydrophobic nature of the SAMs.
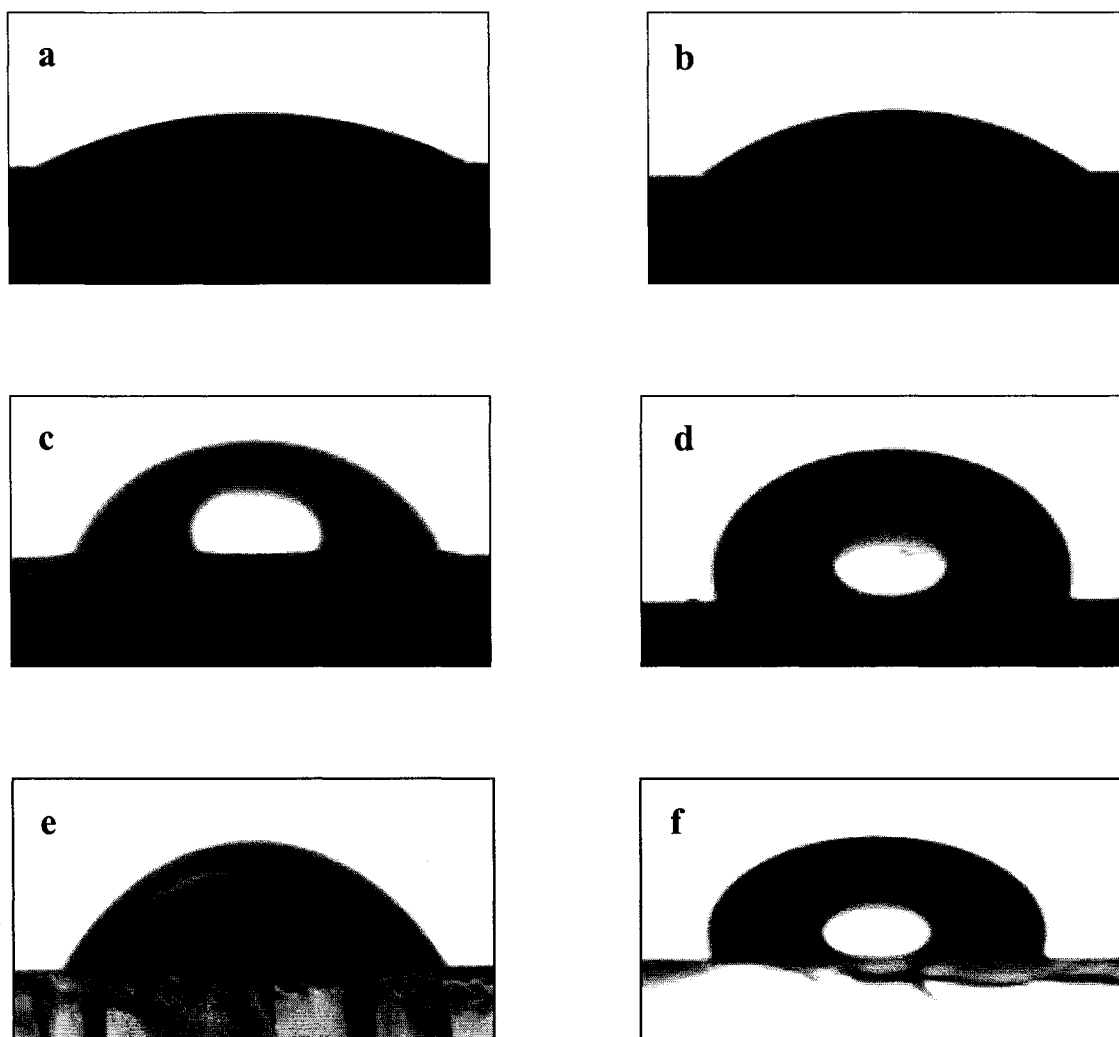
Figure 4.1 Contact angle measurements of (a) Si (22-24°) (b) Si-APTES (34-36°) (c) GaAs (75-77°) (d) GaAs-ODT (102-105°) (e) ITO (40-45°) and (f) ITO-ODT (102-105°).

4.2.3.2 Reflection Absorption Infrared Spectroscopy (RAIRS)

The asymmetric and symmetric bands of methylene (CH_2) stretches are observed at 2917 and 2850 cm^{-1} (Figure 4.2), while the asymmetric C-H stretching mode of CH_3 is observed at 2964 cm^{-1} for GaAs and ITO. These IR (Table 4.1) and contact angle data are remarkably similar to alkanethiol SAMs formed on noble metals[81] and suggest that ODT forms a close packed, crystalline monolayer on ITO and GaAs. For APTES on Si, strong primary amine band is observed at 1575 cm^{-1}.
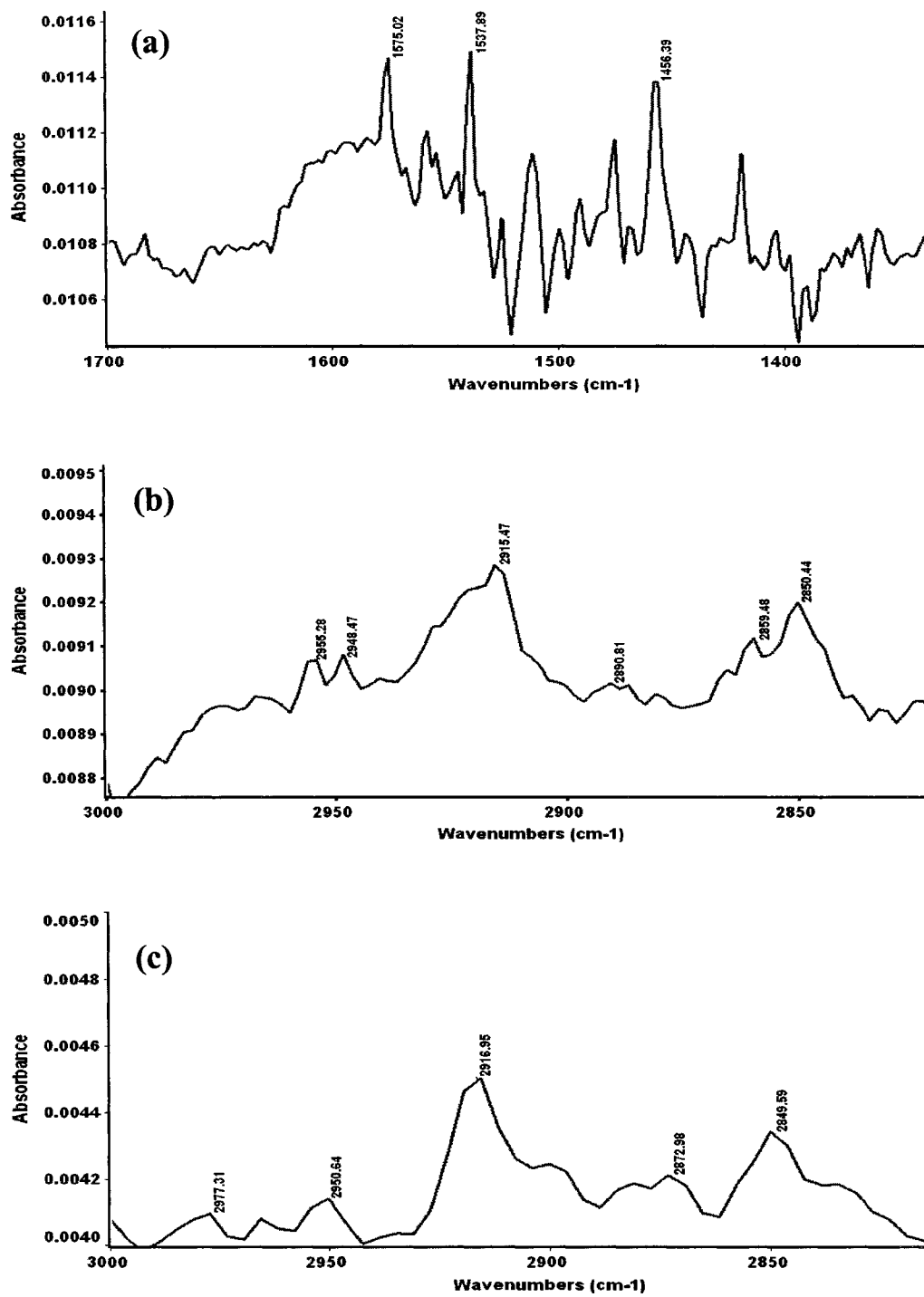
Figure 4.2 RAIRS spectra of (a) APTES (–NH₂) on silicon (Si) (b) ODT (–CH₃) on GaAs and (c) ODT (–CH₃) on ITO

Table 4.1 Comparison of peak positions for ODT stretching modes in crystalline and liquid states at gold to ITO and GaAs.

Structural group	C-H Stretching mode	Peak positions of crystalline and liquid states,[81] cm^{-1}		Peak positions for ODT adsorbed at gold,[81] cm^{-1}	Peak positions for ODT adsorbed at ITO, cm^{-1}	Peak positions for ODT adsorbed at GaAs, cm^{-1}
		Crystalline	Liquid			
-CH$_2$-	ν_a	2918	2924	2917	2917	2915
	ν_s	2851	2855	2850	2849	2850
CH$_3$-	ν_a	-	-	2965	2964	2964

4.3 Cell Seeding and Morphology

4.3.1 Cell Seeding

HDFs were washed twice with HBSS and then trypsinized with 1X trypsin (1 mL of trypsin and 99 mL of HBSS) and allowed to incubate for eight minutes. Once the HDFs detached from the bottom of the dish, the cells were placed in a 15 mL conical tube and centrifuged for seven minutes at 1620 rpm. The supernatant was poured off, and the pellet was washed with complete Dubelco's modified eagle medium (DMEM) to remove any excess trypsin. Then, 400 μL of complete DMEM was added to the pellet and gently pipetted to disrupt the pellet. The substrates were then washed with DMEM three times and then 50 μL of cells (~400 cells: counted by hemacytometer) were added to each substrate. HDFs were allowed to incubate for one hour on the substrates and then two milliliters of complete DMEM was added to each of the dishes.

4.3.2 Cell Morphology

Figures 4.3-4.5 show the HDF morohology on different SAM-modified substrates after 48 h. It can be observed that on ITO and ITO modified with ODT (–CH$_3$) the nuclei, nucleoli, and cytoplasmic processes are very prominent compared with modified and

unmodified Si and GaAs. The cells on Si, Si-APTES and GaAs-ODT appear with the nucleus (enclosing the nucleoli) while very few cells are observed on GaAs indicating cell death. Cellular processes showing cell flattening can be observed predominantly on modified and unmodified ITO substrates indicating the preference of HDF for this substrate.
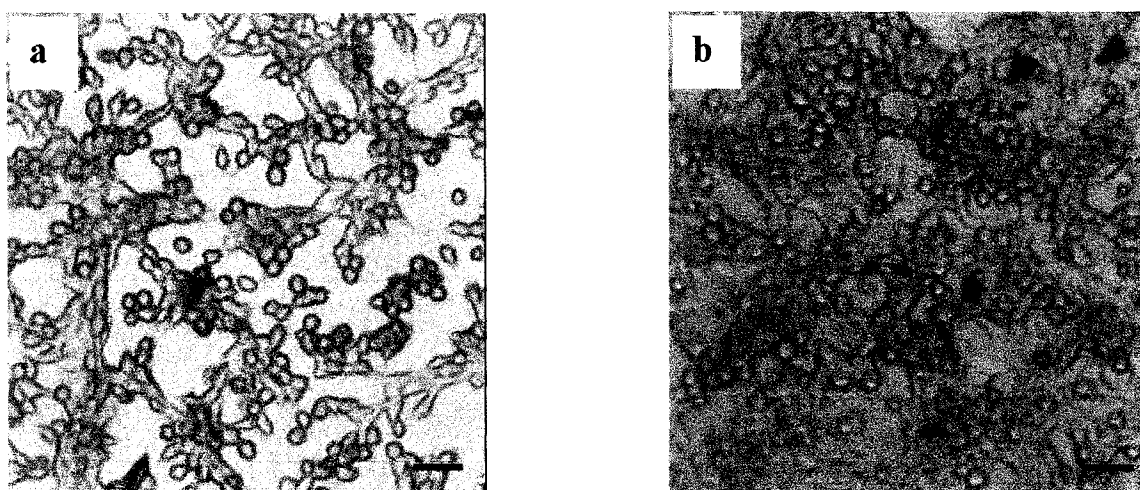
Figure 4.3 Phase contrast images of HDFs on (a) Si and (b) Si-APTES (–NH₂ end group) after 48 h (Bar represents 10 μm).
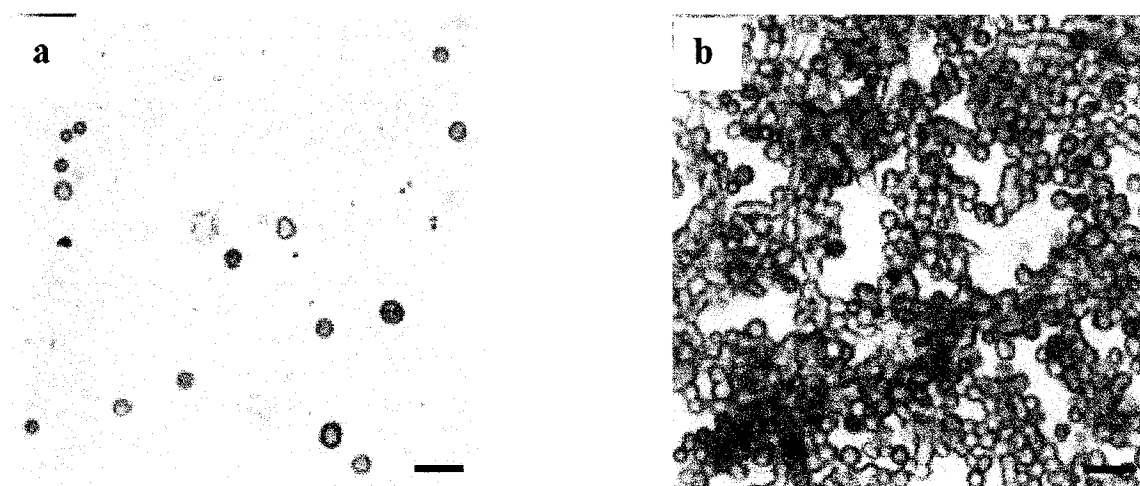
Figure 4.4 Phase contrast images of HDFs on (a) GaAs and (b) GaAs-ODT (–CH₃ end group) after 48 h (Bar represents 10 μm).
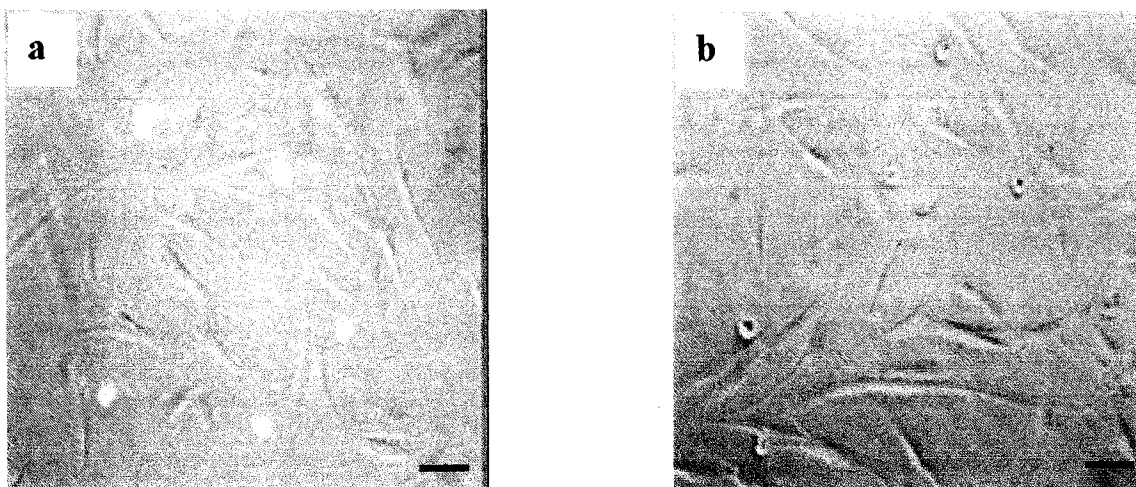
Figure 4.5 Phase contrast images of HDFs on (a) ITO and (b) ITO-ODT (–CH₃ end group) after 48 h (Bar represents 10 µm).

4.4 Cell Viability

The viability of HDFs cultured on SAM-modified substrates was assessed using two color Live/Dead® flouroscence assay following 48 h of seeding. ITO substrates were observed under the Nikon microscope while opaque substrates (Si, GaAs) were viewed using the optical microscope. Qualitative observations of number of viable cells were made by observing the flouroscent response. Live cells flouresce green but dead cells flouresce red as discussed in the experimental section.

Viability analysis performed on HDFs cultured on GaAs and GaAs modified with ODT showed extremely low cellular viability on GaAs (Figure. 4.6a) compared to GaAs-ODT (Figure. 4.6b). The low cellular viability is due to the arsenic leakage in the media during culture, which is toxic, causing cell death.[32,33] The viability notably increased on ITO-ODT due to the presence of ODT monolayer which protects the surface and prevents arsenic leakage.
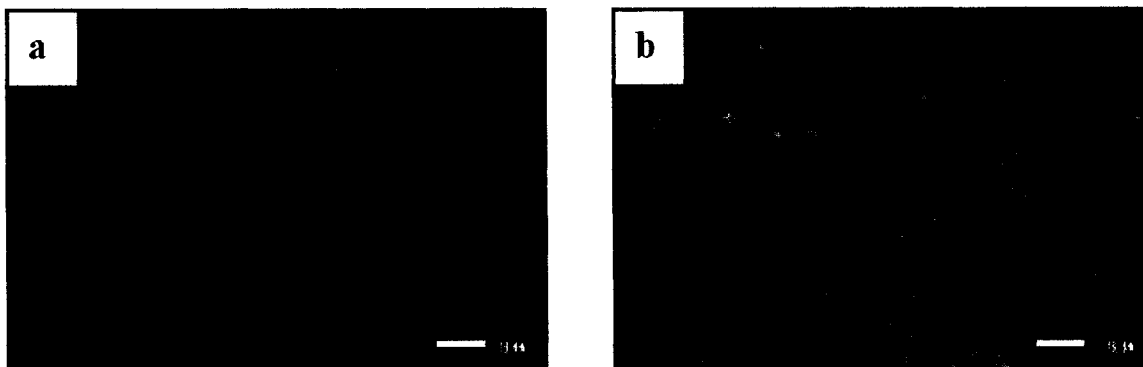
Figure 4.6 Cellular viability observed by LIVE/DEAD® analysis on (a) GaAs and (b) GaAs-ODT (-CH₃) after 48 h (Bar represents 10 μm).

Viability studies on Si and Si-APTES (Figure 4.7 (a,b)) indicate good cellular viability on both the surfaces, with Si-APTES showing a comparatively better response. This result indicates the cell supportive nature of Si. The amino (−NH₂) functionality provides better environment for cell growth.
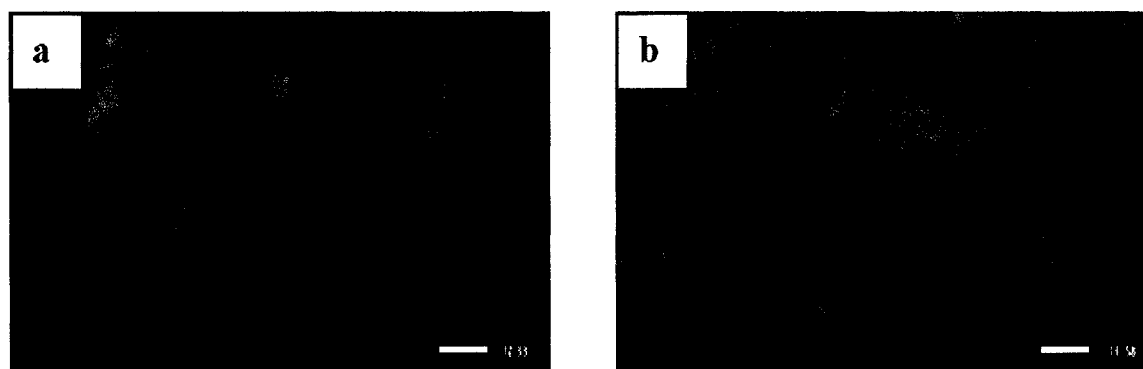
Figure 4.7 Cellular viability observed by LIVE/DEAD® analysis on (a) Si and (b) Si-APTES (-NH₂) after 48 h (Bar represents 10 μm).

Similar results were observed on ITO and ODT-modified ITO (Figures 4.8 and 4.9). Cell spreading was the highest in the case of ITO-ODT compared with all other substrates. Cell viability on all these substrates followed this trend: ITO-ODT>ITO>Si-APTES>Si>GaAs-ODT>GaAs.

Figure 4.8 Cellular viability observed by LIVE/DEAD® analysis.(a) Live cells on ITO and (b) Dead cells on ITO after 48 h (Bar represents 10 μm).

Figure 4.9 Cellular viability observed by LIVE/DEAD® analysis.(a) Live cells on ITO-ODT and (b) Dead cells on ITO-ODT after 48 h (Bar represents 10 μm).

4.5 Cell Proliferation

Proliferation of the cells was determined using MTT assay. Cells were seeded at a density of 2,000 cells/cm^2 and proliferation was determined after 3, 5 and 7 days of culture. Figure 4.10 shows an increased absorbance at 570 nm after 5 DIV compared with 3 DIV indicating the proliferation of the cells. After 3 DIV, no cells were observed on GaAs surface indicating cell death due to arsenic leakage in the media. Proliferation was

highest for SAM-modified surfaces compared to other surfaces after 5 and 7 DIV. High

cell densities were observed on ODT modified ITO (ITO-CH$_3$) followed by APTES

modified Si (Si-NH$_2$). Among the unmodified surfaces, proliferation was observed on

both ITO and Si and there were not significantly different. Cell proliferation was least on

ODT modified GaAs (GaAs-CH$_3$). There was only small increase in cell density from 3

DIV to 7 DIV. But, this result clearly shows that protection of the GaAs surface by a

monolayer of organic molecules does prevent arsenic leakage to a certain extent enabling

the cells to attach and proliferate for a certain period of time (in this case, for seven days).
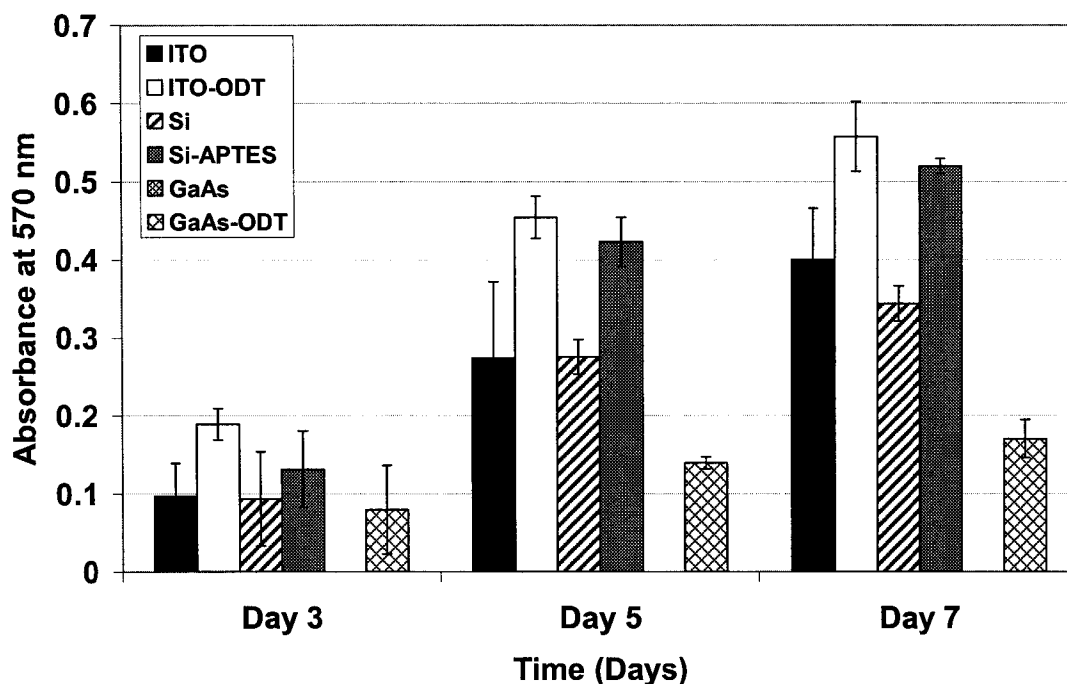
Figure 4.10 Proliferation of HDFs on SAM-modified and unmodified Si, GaAs and ITO surfaces after 3, 5 and 7 DIV. Data represent the mean±S.D, n=3.

4.6 Immunocytochemical Analysis

Immunohistochemistry (IHC) analysis was conducted against Type-I collagen. Figures 4.11-4.13 illustrate HDFs on GaAs, GaAs-ODT, Si, Si-APTES, ITO and ITO-ODT respectively. The brown reaction indicates that an antigen antibody complex has formed a positive immunoreaction. The brown reaction (indicated by arrows) that occurred on all of the substrates as a result of IHC analysis indicated that the HDFs did not lose their *in vivo* behavior in the *in vitro* environment. The cells maintained type-I collagen, which is needed for continuous growth of the cells. The brown reactions around the cytoplasm indicate the antigen-antibody complex.

The results indicate that HDF's cultured on ITO, ITO-ODT, Si, Si-APTES and GaAs-ODT, with the exception of GaAs, tested positive for Type I collagen, maintained their phenotype and were active.
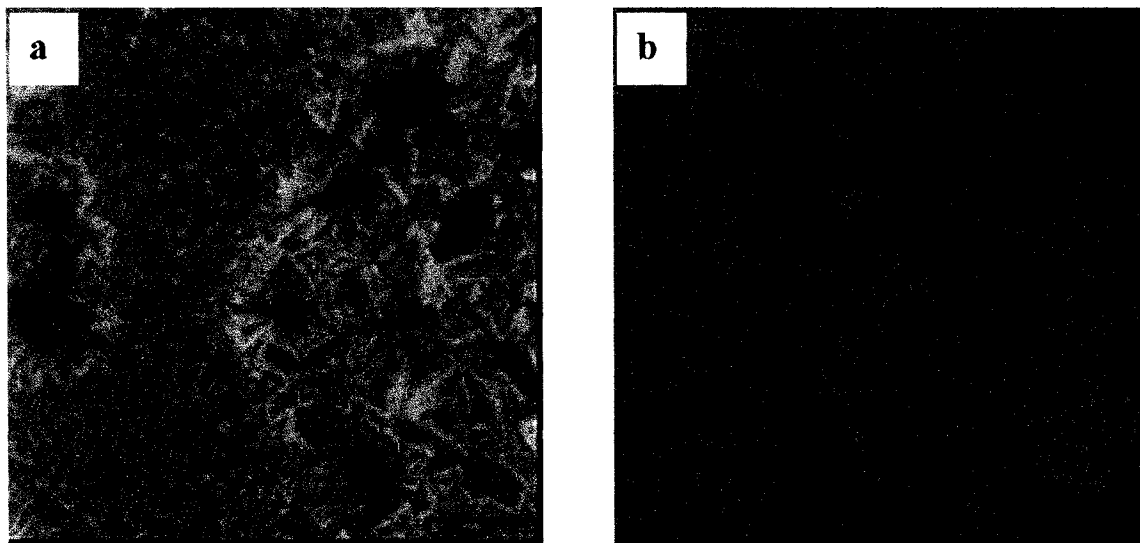
Figure 4.11 Immunohistochemical detection of Type-I Collagen after 48 h in culture. (a) GaAs and (b) GaAs-ODT (Bar represents 40 μm).
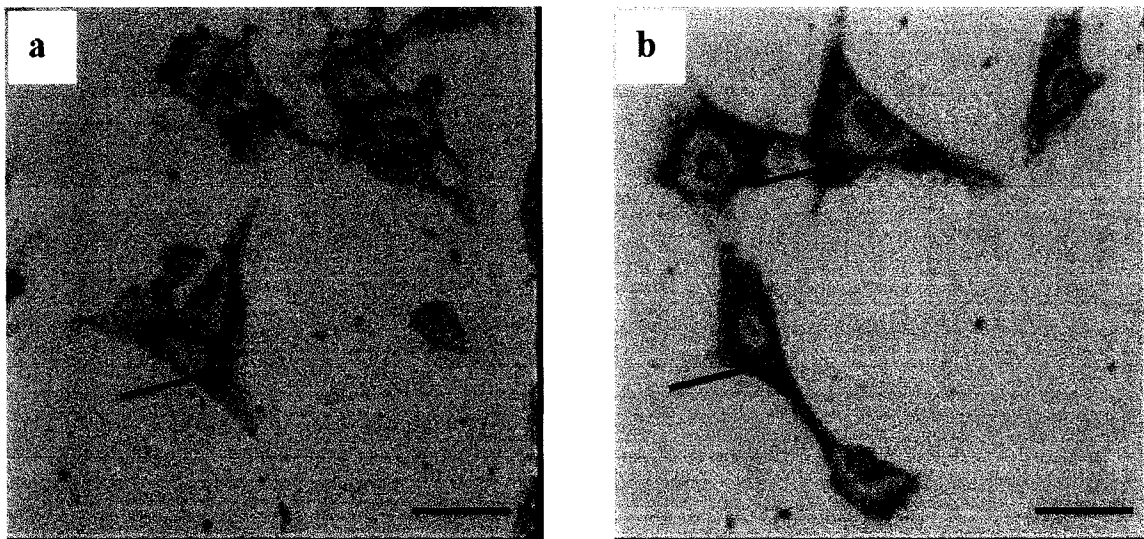
Figure 4.12 Immunohistochemical detection of Type-I Collagen after 48 h in culture. (a) Si and (b) Si-APTES (Bar represents 40 μm).
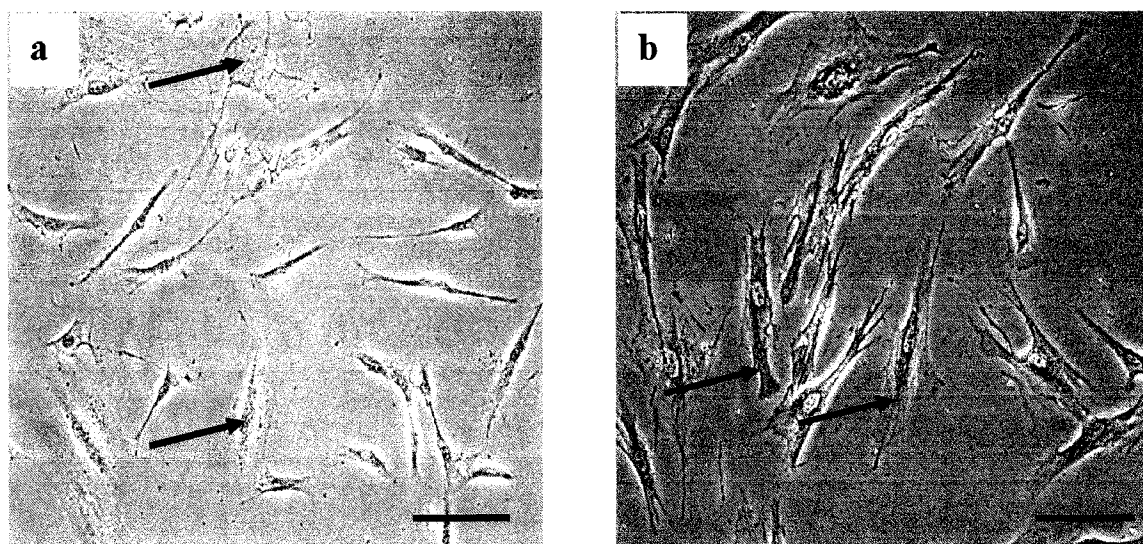
Figure 4.13 Immunohistochemical detection of Type-I Collagen after 48 h in culture. (a) ITO (b) ITO-ODT (Bar represents 40 μm).

4.7 Discussions

Many approaches, such as those done by Mrksich et al., have been investigated to

obtain predictable surface chemistries of biomaterials that either alter or inhibit specific

cell functions.[2,3,13-15,19-22,24] The strength of cell adhesion and spreading on SAMs has been especially studied.[30]

The results from our cytotoxicity, proliferation and functionality studies indicate that HDFs proliferated well on all SAM substrates and exhibited the characteristic long spindle-shaped fibroblast morphology. The HDFs exhibited no visible signs of stress or cytoplasmic vacuolation. HDFs also maintained their phenotype, and were synthetically active. Table 4.2 shows the immunoreactivity of different substrates used in this study based on optical images of 4.11, 4.12 and 4.13. ITO-ODT presents the best surface wherein the HDFs maintain their best phenotype.

Table 4.2 Immunoreactivity of both SAM-modified and unmodified ITO, Si and GaAs substrates

Substrate	Immunoreacivity
Control	+++
GaAs	-
GaAs-ODT	++
Si	+
Si-APTES	+++
ITO	++
ITO-ODT	+++

No immunoreactivity = - ; Weak immunoreactivity = + ; Moderate immunoreactivity = ++; Strong immunoreactivity = +++.

The cell culture substrates used in this research encouraged HDFs to attach, grow, and maintain cell functionality. Initial adhesion of proteins from the media on the SAMs is responsible for the cellular adhesion. In case of ITO-ODT we assume that the hydrophobic end group (–CH₃) couples with the hydrophobic part of the unfolding protein releasing many hydrophobically structured water molecules and leading to the large entropy gain for the system.[135,136] It has been shown that HDFs translocate and

organize their β_1 integrin subunits preferably to –NH$_2$ and –COOH SAMs because of the deposition of fibronectin on these groups.[30,137,138] This forms the basis for the cellular attachment and subsequent proliferation.

The results from our studies also provide strong evidence that cellular attachment to surfaces is influenced by small changes in the substratum chemical composition and molecular structure. It has been demonstrated that HDFs exhibit different responses to specific surface chemistries when cultured under similar conditions and the length of the alkyl chain has a significant influence over the outcome of cellular interactions with SAMs. The number of attached cells decreased significantly with increasing alkyl chain length as shown by Cooper et al.[17] Also the influence of the substrate alone revealed that the HDF cells attached better on indium tin oxide (Figure. 4.5a, 4.8a, 4.13a) substrates compared to all other unmodified substrates.

The significance of this work was to determine right kind of substrate and the SAM that encouraged human dermal fibroblast to attach, grow and preserve the cell functionality. It was determined that on ITO and SAM-modified ITO, the HDF viability, proliferation and functionality were higher compared to other surfaces. Based on these results, ITO has been used as the substrate for SAM modification in our cell culture studies using well-established cell lines such as hepatocytes or stem cells whose differentiation pathway can be directed, leading to the development of biosensors/bioreactors that can be used in cancer research.

CHAPTER 5

MESENCHYMAL STEM CELLS ON SAM-

MODIFIED ITO SUBSTRATES

5.1 Stem Cells

Stem cells are the precursor cells which have the ability to self renew and differentiate into multilineage cells in response to appropriate signals.[139,140] They are classified as either embryonic stem (ES) cells or tissue-specific stem cells. ES cells have varying degree of potential ranging from totipotency (ability to form the embryo and the trophoblast of the placenta of the fertilised oocyte (the zygote)), to the pluripotency (ability to differentiate into almost all cells that arise from the three germ layers) of ES cells.[141-143] Tissue specific stem cells (adult stem cells) are unspecialized cells found in differentiated tissues which can renew for long periods of time and are multipotent (capable of producing a limited range of differentiated cell lineages appropriate to their location). ES cells can be maintained in undifferentiated state indefinitely while adult stem cells can proliferate only for a limited number of generations.

In this decade, isolation and expansion of tissue-specific adult stem cells are concentrated more due to some of the ethical debates surrounding the isolation of ES cells. Adult stem cells (ASC) have been found to reside in a variety of tissues including skin,[144] the central nervous system,[145] muscle,[146] bone marrow,[147] liver,[148] mammary

53

gland,[149] and many others (Figure 5.1). The haematopoietic stem cell (HSC) resident in the bone marrow is the most described ASC because they are relatively easy to isolate. The multipotency and self-renewal capacity of this population has been established by the ability of single murine HSCs to engraft and repopulate both the myeloid and lymphoid blood lineages of a myeloablated host.[150]
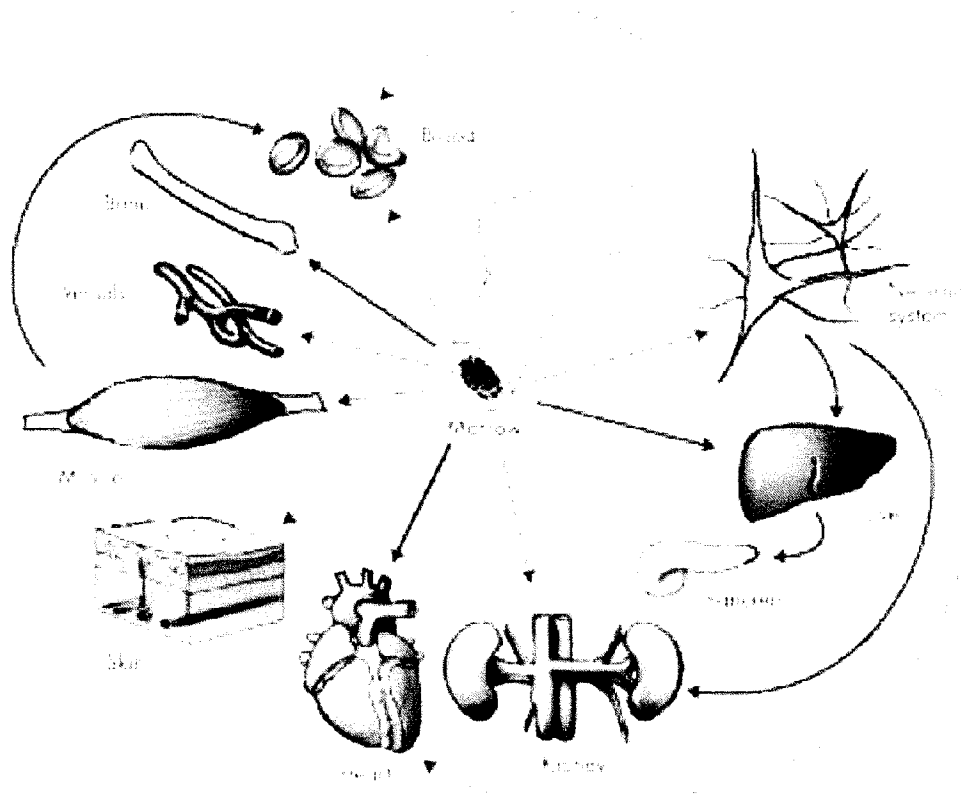
Figure 5.1 Possible pathways of differentiation in adult stem cells.[151]

The recent discovery of neural stem cells (NSCs) in the adult central nervous system (CNS) and their regenerative roles in brain damage opened new approaches for the treatment of neurodegenerative disease and CNS injury.[152] The fact that the neural progenitors are restricted to generate specific types of CNS cells *in vivo*, can differentiate into all the three CNS cell types: neurons, astrocytes, oligodendrocytes, suggest that the

environment (ECM) can influence the fate of these progenitors.[153] Multipotent mesenchymal cells (MSCs) can differentiate into a number of nonhematopoietic cells such as osteoblasts, chondrocytes and adipocytes. It was shown that a mouse mesenchymal progenitor cell line C3H10T1/2 when induced with 3-aza-C, it differentiated into myoblasts, osteoblasts, adipocytes and chondrocytes.[154] Also chemicals like dexamethasone and ascorbic acid can induce osteogenesis or adipogenesis of MSCs under carefully defined conditions.[155,156]

It was a notion in developmental biology that tissue-specific stem cells are restricted to differentiating into cell types of the tissue in which they reside. But recent studies have shown the *in vivo* plasticity of the bone marrow-derived stem cells, which are mainly based on cell fusion events.[157-160] However in some cases, tissue-specific stem cells have overcome their intrinsic lineage-restriction when exposed to a specific set of signals both *in vitro*[161] and *in vivo*.[162] The ability to dedifferentiate to multipotent progenitor cells might overcome many of the obstacles associated with the ES cells and adult stem cells in clinical applications.

Many factors such as cell-cell contact,[157,163] extracellular materials[164] and structural factors[165] have a strong influence on stem cell differentiation. Extracellular matrix such as collagen has been used for the realization of osteogenesis of MSCs derived from human bone marrow cells,[166] and it was observed that formation of mineralized bone was more under dynamic conditions compared with static culture conditions. Sawyer et al. showed that low RGD concentrations combined with pro-adhesive serum proteins stimulated MSCs attachment to the hydroxyapatite surfaces.[167] MSCs on nanofibrous scaffolds made by electrospinning of Poly(ϵ-caprolactone) have

also been shown to produce cartilage.[168] MSCs grown on some of the nanostructured materials such as ion-beam deposited metalloceramic materials have also showed enhanced adhesion and spreading.[169] Many other surfaces such as silk biomaterials[170], alginates[171] have also been used. Howver, no systematic work has been done to fully understand the relation between surface properties and stem cell fate.

SAM-modified surfaces have not been used for MSC studies *in vitro*. The aim of this work was to observe the morphology and proliferation of MSCs on different SAM-modified ITO substrates, each presenting a different terminal group with different wetability and charge.

5.2 Surface Characterization

Four different SAM-modified ITO substrates were used: (1) ITO-APTES ($-NH_2$ end group) (2) ITO-MPA ($-COOH$ end group) (3) MPS ($-SH$ end group) and (4) ITO-ODT ($-CH_3$ end group). The surfaces were characterized for their wettability using contact angle measurements and roughness using AFM.

5.2.1 Contact Angle Measurements

Figure 5.2 indicates that the surfaces modified with amino (APTES) and carboxylic (MPA) end groups are hydrophilic, while surfaces with methyl (ODT) and thiol (MPS) end group are hydrophobic. Among the hydrophilic surfaces, carboxylic end ($-COOH$) group presents the least contact angle while methyl ($-CH_3$) end groups present the highest contact angle among the hydrophobic surfaces. Surface modified with thiol ($-SH$) end group presents wettability intermediate between the hydrophilic and hydrophobic surface.
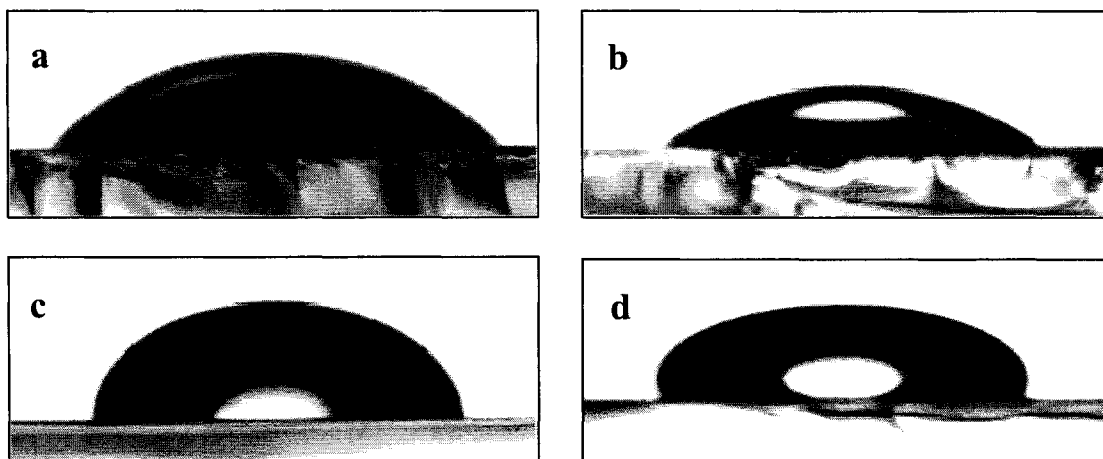
Figure 5.2 Surface wettability of the different SAM-modified substrates determined from contact angle measurements. (a) ITO-APTES (38°) (b) ITO-MPA (33°) (c) ITO-MPS (87-89°) and (d) ITO-ODT (103-105°)

5.2.2 AFM Analysis

A QUESANT Q-Scope 250 AFM was used to analyze the surface roughness. Figure 5.3 shows the 2D images of different SAM-modified ITO surfaces along with unmodified ITO. From the tabulated (Table 5.1) roughness values it can be inferred that bare ITO presents a relatively smooth surface. The cleaning method employed in this research enabled to remove the surface contaminants making the surface smooth. When modified with different end group SAMs, the roughness of surfaces with $-NH_2$ and $-SH$ was ~1nm. The $-CH_3$ group presented a rough surface compared to $-NH_2$ and $-SH$ but comparable with the values obtained by Perrin et al. on Si surfaces.[172] This roughness value indicates that the surface coverage is good with the presence of a densely packed film. High surface roughness of $-COOH$ end group modified ITO surfaces may be attributed to the presence of aggregates. The method of using neat liquids of ODT and MPA for SAM formation also probably leads to the formation of aggregates.
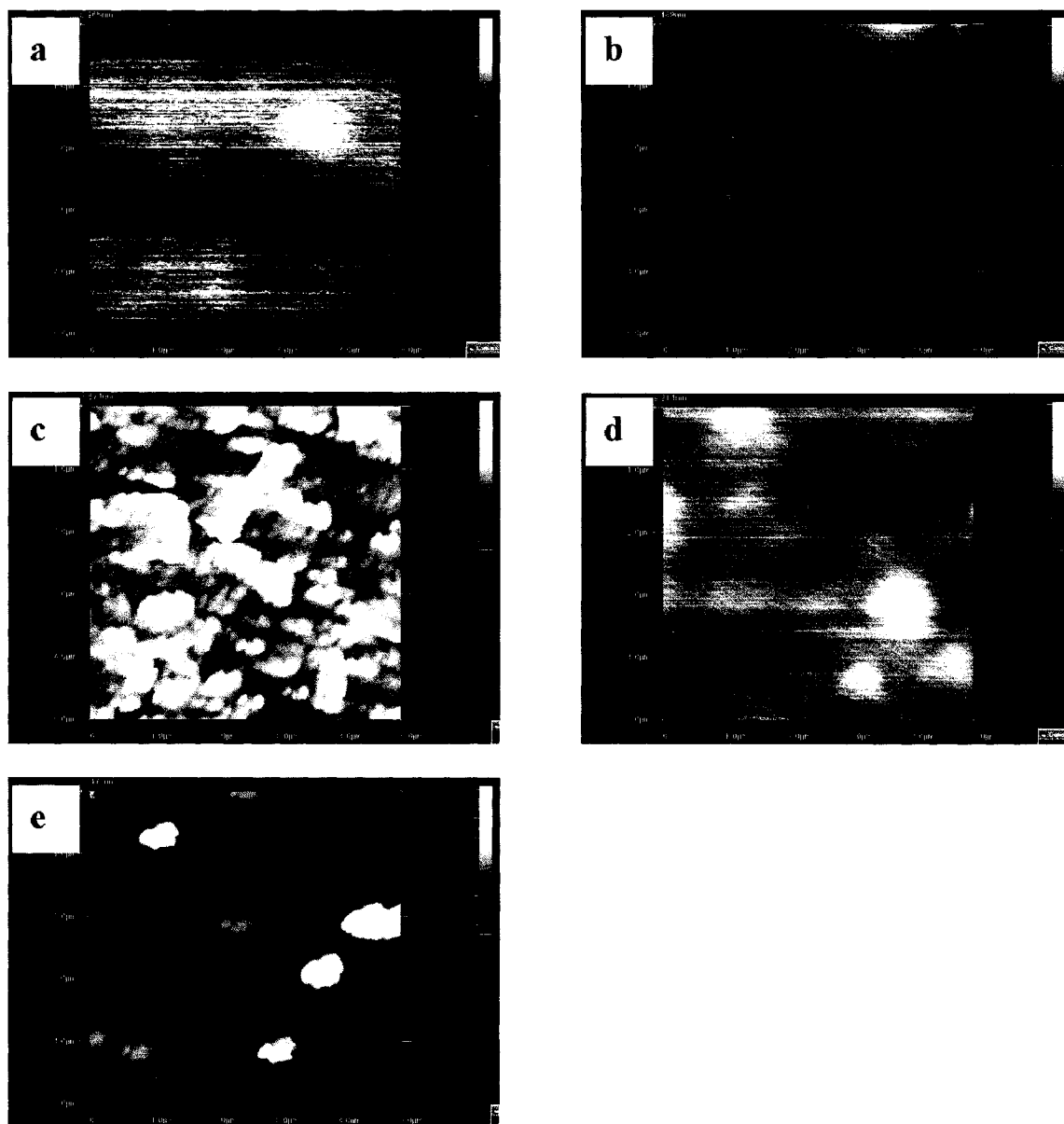
Figure 5.3 Average roughness (Ra) of (a) ITO (b) ITO-APTES (c) ITO-ODT (d) ITO-MPS and (e) ITO-MPA.

Table 5.1 Average roughness of unmodified ITO and SAM-modified ITO surfaces

	Ra (nm)*
ITO	0.93
ITO-NH₂	1.01
ITO-CH₃	1.51
ITO-SH	1.1
ITO-COOH	2.67

*Values are the means of three independent measurements

5.3 Cell Seeding and Morphology

5.3.1 Cell Seeding

MSCs of passage four attached on TCP dish were washed twice with HBSS and then trypsinized with 1X trypsin (1 mL of trypsin and 99 mL of HBSS) and allowed to incubate for eight minutes. Once the MSCs detached from the bottom of the dish, the cells were placed in a 15 mL conical tube and centrifuged for seven minutes at 1600 rpm. The supernatant was drained off and the pellet was washed with complete DMEM to remove any excess trypsin. Then 2 mL of complete DMEM was added to the pellet and gently pipetted to disrupt the pellet. The cell count was then established using a hemacytometer.

Both the bare ITO and TCP dish were used as control. The substrates were washed with HBSS twice and once with DMEM. Cells at a density of 2000 cells/cm^2 (3820 cells per/well (area 1.91cm^2) in a 24 well dish) were seeded on each substrate. 500 µl of media was added to each well containing the cells on substrates and incubated. The cells were observed over a period of seven days for variations in cellular morphology and viability. Triplicate cultures were maintained. For quantification of cell proliferation using MTT assay, substrates were placed in 12 well dishes and 1280 cells/cm^2 (4900 cells per well (area 3.82 cm^2)) were seeded. Triplicate cultures were maintained. A standard curve was determined by seeding known number of cells and observing the absorbance. Cell numbers on substrates were determined using this standard graph.

5.3.2 Cell Morphology

The substrates were observed for a period of seven days to assess cellular attachment and morphology under a Nikon microscope. Optical images were taken every

24 h for seven days at two different magnifications (10X and 40X). Figure 5.4 shows the

attachment and morphology of MSCs on different SAM-modified ITO substrates after 24

hours.
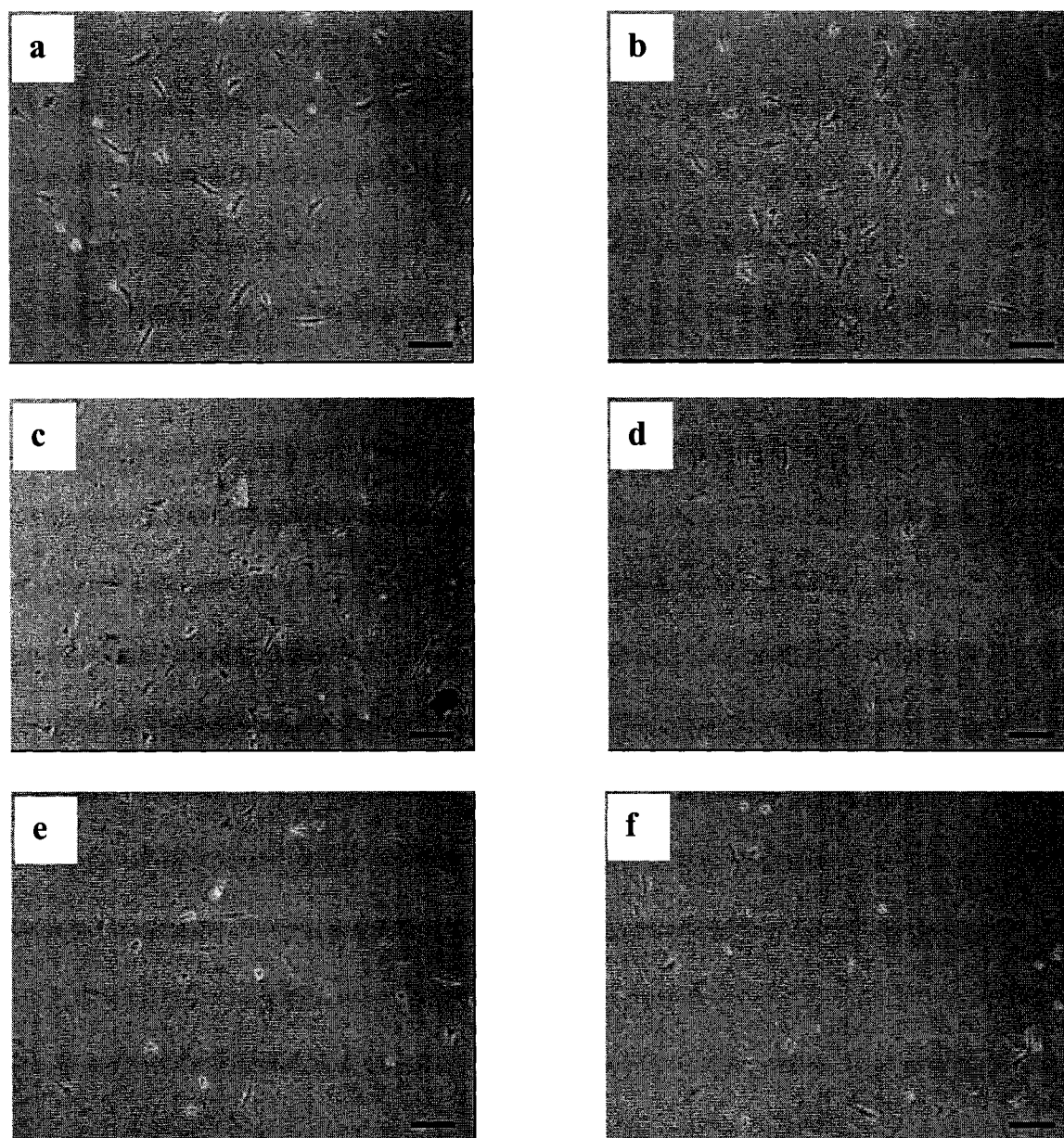
Figure 5.4 Morphology of MSCs on different SAM-modified ITO substrates after 24 h. (a) Control (TCP) (b) ITO (c) ITO-APTES (d) ITO-COOH (e) ITO-ODT and (f) ITO-MPS (Bar represents 10 μm).

It can be observed from Figure 5.4, that most of the adhered cells have already spreaded. There are few cells which are round in nature indicating that these cells can either spread or result in apoptosis. After 72 h, more number of cells started spreading and proliferating (Figure 5.5).
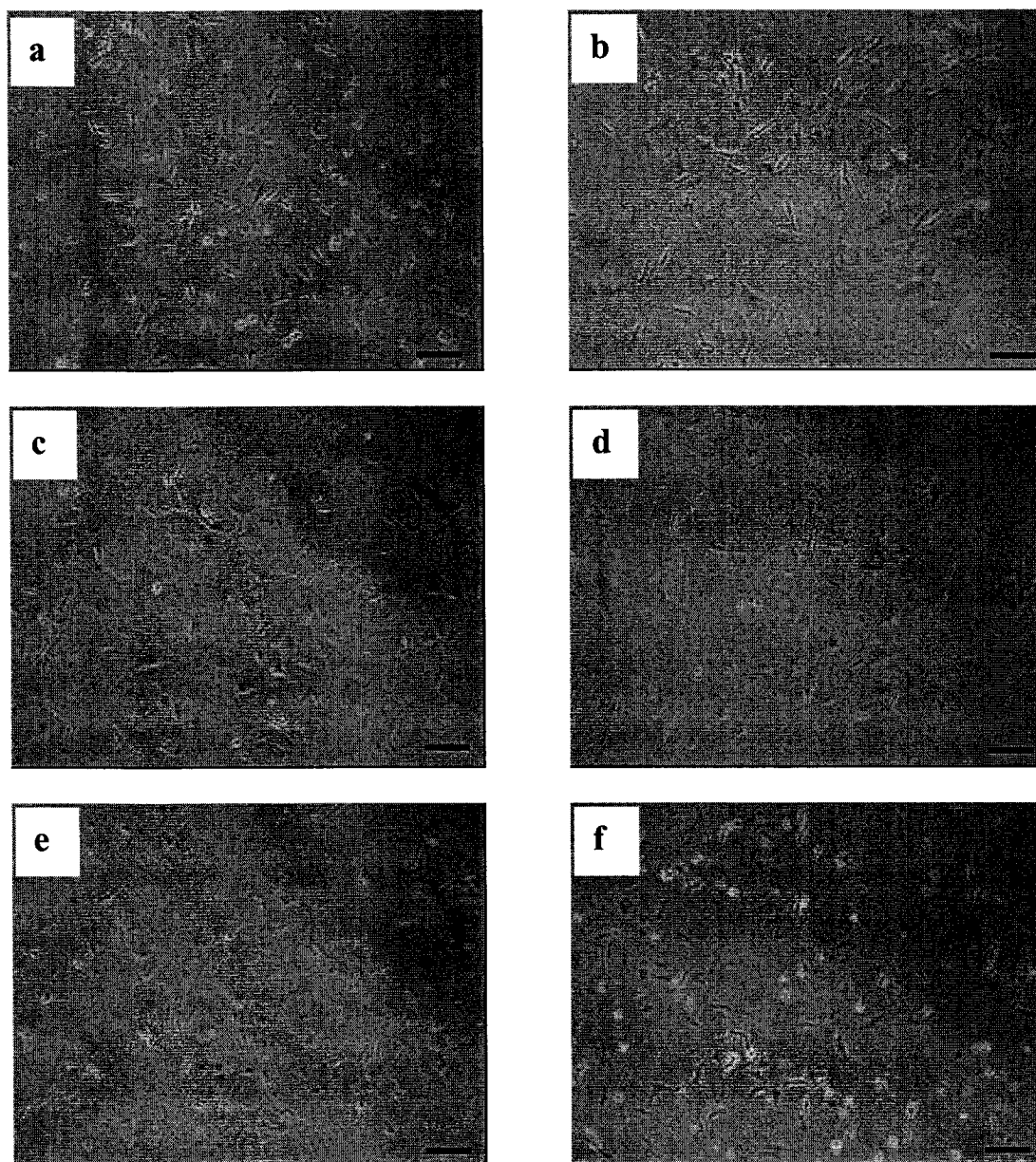
Figure 5.5 Morphology of MSCs on different SAM-modified ITO substrates after 72 h. (a) Control (TCP) (b) ITO (c) ITO-APTES (d) ITO-COOH (e) ITO-ODT and (f) ITO-MPS (Bar represents 10 μm).

The rounded morphology of the cells started disappearing as the cells started spreading. All the substrates exhibited this nature. As the culture time increased, the cell density on all the substrates also started increasing. At the end of seven days (Figure 5.6), all the cells exhibited spread morphology with no rounded cells.
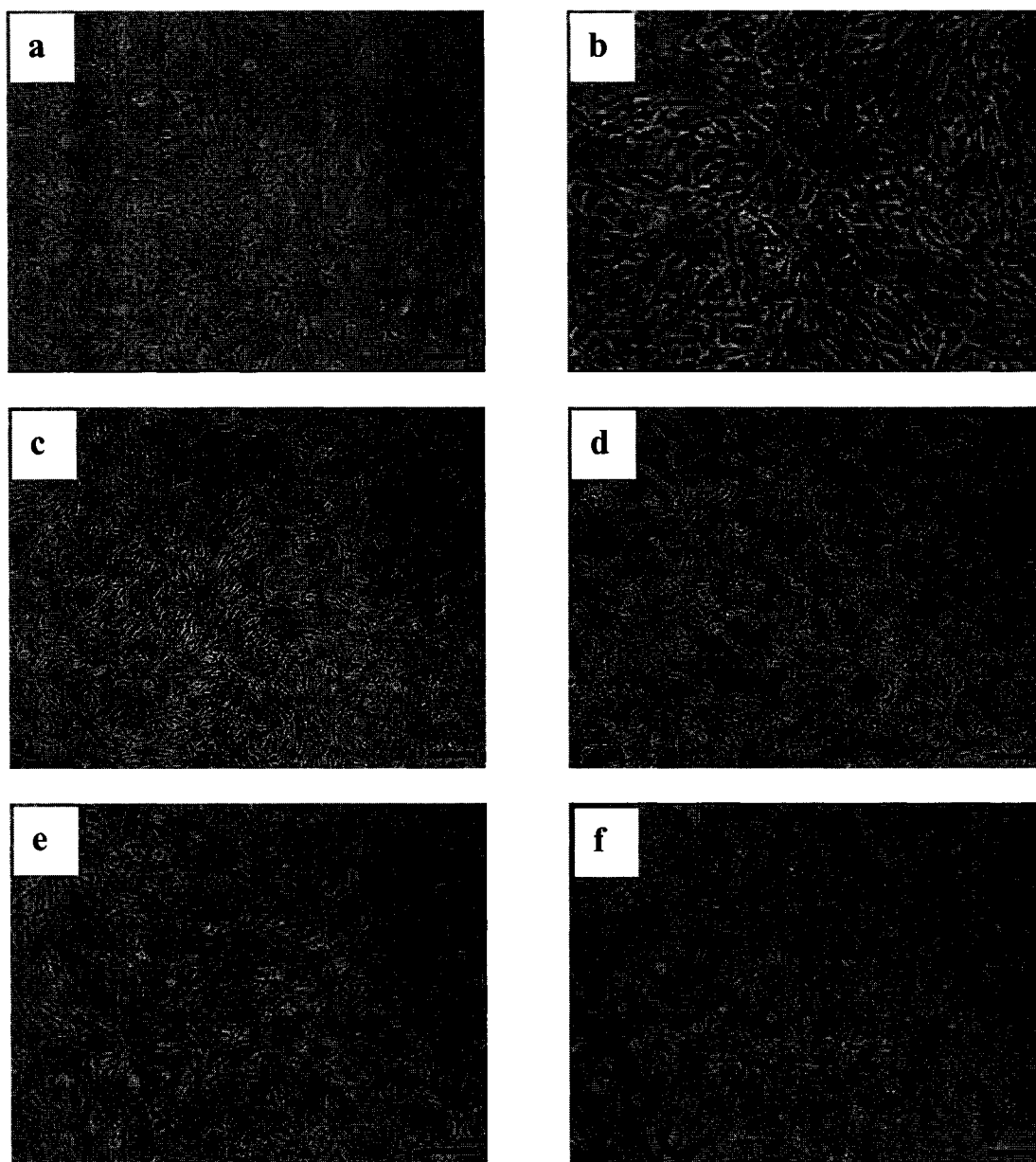
Figure 5.6 Morphology of MSCs on different SAM-modified ITO substrates after 168 h. (a) Control (TCP) (b) ITO (c) ITO-APTES (d) ITO-COOH (e) ITO-ODT and (f) ITO-MPS (Bar represents 10 μm).

The cells on all the substrates looked same without any significant difference in morphology. The cells did not show any preference for particular end group. The cells reached their confluence on all the surfaces. Quantification of the proliferation data is necessary to know the true preference of the cells for the substrates. The morphology results just indicate the shape and spread of the cells.

5.4 Cell Viability and Proliferation

The cytotoxicity of the substrates on MSCs was studied using LIVE/DEAD® Cytotoxicity Kit. After 3 DIV, no or few cell death were observed on all the substrates. Figure 5.7 shows the cytotoxicity test performed on all SAM-modified ITO and the control substrates. More number of live cells (green color) is observed. These results show that all substrates initially support the cell growth and do not produce any toxic effect to the attached cells.

After 7 DIV, it can be observed from Figure 5.8 that some of the cells died (red color). The cell death was pronounced on control (both TCP and ITO) compared to SAM-modified ITO surfaces. More number of dead cells were observed on ITO-MPS substrates. Cell viability was not significantly different on ITO-APTES, ITO-COOH and ITO-ODT surfaces. The results from LIVE/DEAD® assays give us only the qualitative information but more insight into the cell numbers can be obtained only by performing the MTT assay. There is considerable increase in the dead cells after 7 DIV when they are compared with cells after 3 DIV. This result indicates that along with cell proliferation, the process of cell apoptosis is going on simultaneously.
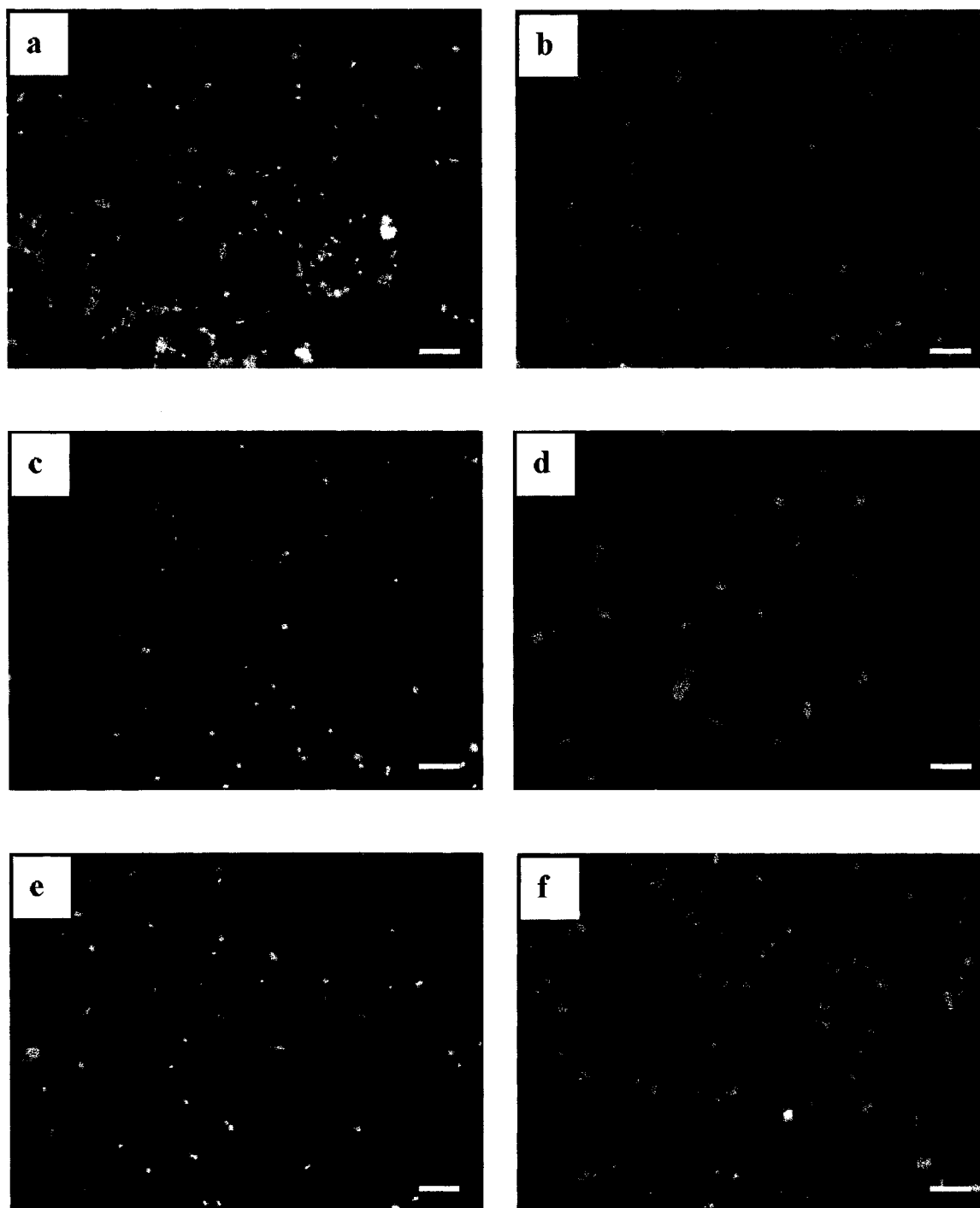
Figure 5.7 Cell viability measured using LIVE/DEAD® assay showing both live and dead MSCs after 3 DIV (10X) (a) Control (TCP) (b) ITO (c) ITO-APTES (d) ITO-COOH (e) ITO-ODT and (f) ITO-MPS (Bar represents 10 μm).
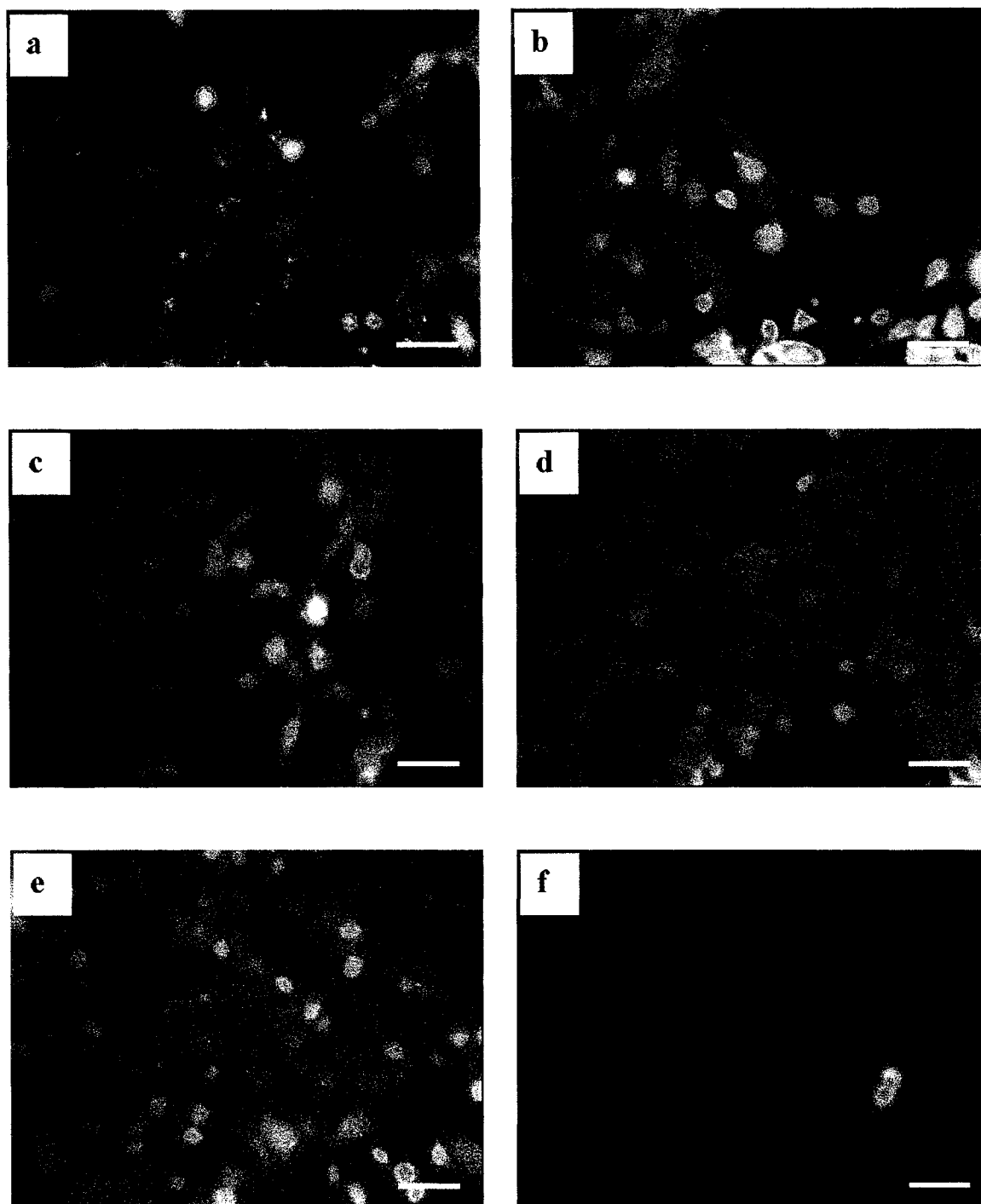
Figure 5.8 Cell viability measured using LIVE/DEAD® assay showing both live and dead MSCs after 7 DIV (40X) (a) Control (TCP) (b) ITO (c) ITO-APTES (d) ITO-COOH (e) ITO-ODT and (f) ITO-MPS (Bar represents 40 μm).

Figure 5.9 shows the plot of proliferation of MSCs on both SAM-modified ITO

and unmodified ITO along with the control (TCP). It can be observed that at Day 1 and

Day 3, the proliferation rate were slower compared with that on Day 7. After Day 1 and

Day 3, there is nothing much to chose among the substrates. Proliferation is not

significantly different. After 7th day, the proliferation rate tremendously increased on all

the substrates, especially with –SH modified ITO substrate producing higher cell

numbers. Cell proliferation was not significantly different on ITO, TCP, ITO-APTES,

ITO-COOH and ITO-ODT surfaces.
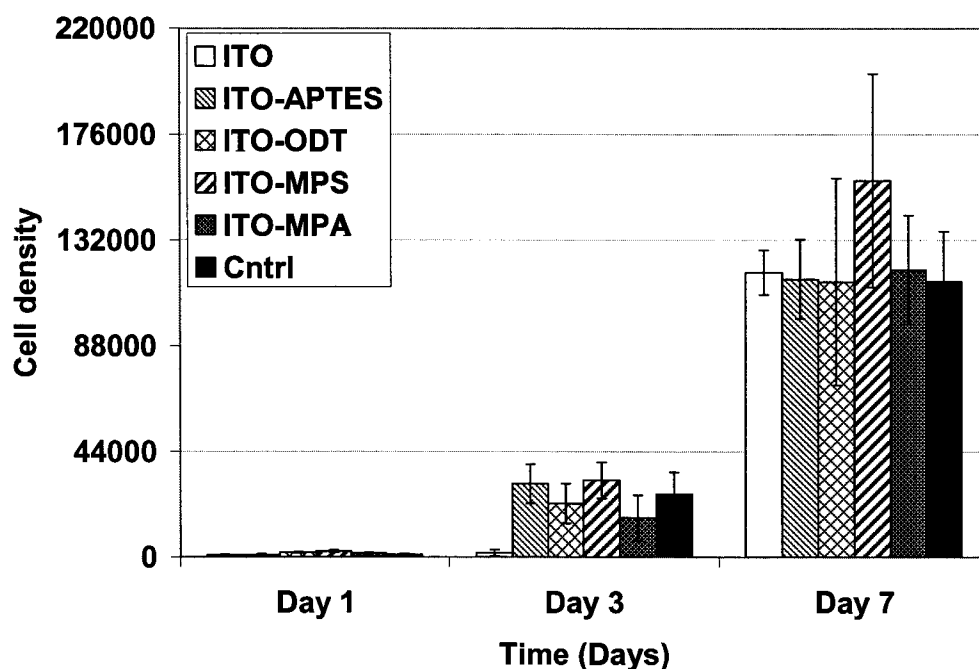
Figure 5.9 MSCs cell proliferation on different SAM-modified ITO surfaces at 1,3 and 7
days. Control: ITO and TCP also included. Data represent the mean±S.D, n=3.

<u>**5.5 Discussions**</u>

To the best of our knowledge, there are very few studies on the culture and

growth of MSCs on SAM-modified surfaces. Based on the results obtained in this study,

some conclusions can be made. The morphology images indicate that the MSCs initially attached to all the surfaces with no specific preference. The viability results also showed that there is no cell death even after 3 DIV. This result indicates that all the surfaces presented an amicable environment for the MSCs to grow. After 7 DIV, the cell proliferation was very high indicating that the substrates used in this study enabled MSC proliferation.

The high cell proliferation observed in the case of –SH modified ITO substrates compared to other substrates can not be rationalized at present as it has been observed that in the case of HDFs (Chapter 4), neurons (Chapter 6) and hepatocytes (Chapter 7), the cells preferred methyl and amino groups. The charge on the surface and the preadsorption of proteins from the media played an important role in the initial cell attachment and the subsequent cell proliferation. But the enhanced MSCs proliferation on –SH modified ITO substrate is difficult to account for. Perhaps stem cells prefer the thiol groups intermediate character in hydrophobicity and hydrophilicity. These surfaces were also used to determine the behavior and response of neurons. The next chapter presents results of our neuronal work.

CHAPTER 6

NEURONAL CELL CULTURE ON SAM-

MODIFIED ITO SUBSTRATES

6.1 Neuronal Cells and Their Culture

The nervous system is classified into the central nervous system (CNS) and the peripheral nervous system (PNS).[173] The CNS, which includes the brain, spinal cord, optic, olfactory and auditory systems, conducts and interprets signals as well as provides excitatory stimuli to the PNS. The PNS consists of cranial nerves arising from the brain, spinal nerves arising from the spinal cord, and sensory nerve cell bodies (dorsal root ganglia) and their processes. The nervous system is composed of two cell types: neurons and neuroglia.[173] Neurons are the major cell type in the nervous system and consist of a cell body (soma) and its extensions (axons and dendrites). Although neurons cannot divide, they can regenerate a severed portion or sprout new processes under certain conditions.

Injury and diseases of the CNS, such as stroke, epilepsy, Parkinson's, Huntington's and Alzheimer's disease, affect a substantial number of people each year and often have long-term consequences for sufferers and their families. CNS diseases often lead to permanent loss of functions (sensory, motor, reflex). These severe

consequences result from the fact that CNS neurons, unlike most other cells in the body, lack the ability to spontaneously regenerate following injury.[174] Recent investigations into the repair of CNS have led to the discovery of neural stem cells and increased understanding of factors that regulate neuron life and death, neurogenesis, neurite outgrowth, and synapse formation.[175] Likewise, organ-specific stem cells (SCs) are responsible for maintenance of tissue homeostasis and tissue regeneration in adult organism by replacement of dying cells by new ones. In the CNS, these functions are performed by neural SCs that can generate precursors of neuronal, astroglial and oligodendroglial cells. Undifferentiated cells with such potential could be used for stem cells therapy to treat CNS diseases resulting from the loss of neuronal or glial cells.[176]

For CNS injury, clinical treatment is less promising, so the challenge has been to find an alternative to the autologous nerve graft, eliminating the need for two surgeries and the removal of tissue from the patient. Also, clinical functional recovery rates typically approach only 80% for nerve injuries treated using autologous nerve grafts. Thus, biomedical science strategies have focused on developing alternative treatments to the nerve graft, including use of synthetic microfabricated substrates to culture neuronal cells.

The ultimate goal of these microfabricated substrates is to mimic the *in vivo* micro-environment present in the body, and to achieve this goal several issues need to be examined, including biocompatibility, cytotoxicity effects, cell phenotype, and cellular response in neurons after culture on microsubstrates. Recent studies have begun to examine these issues using several substrates. These substrates include (a) silicon dioxide[177] (b) silicon dioxide coated with a matrix of PA22-2[178] (c) thin films of titanium

nitride (TiN)[179] (d) a thin layer of silicon dioxide (SiO_2) on Si^{180} and (e) a silicon-based elastomer.[181] The silicon dioxide microsubstrate succeeded in having good growth of axons.[177] However, efforts to date have met with limited success largely because it is still unknown if the geometry proposed is adequate for maintaining the cells in culture.

One of the first examples of neuronal patterning was reported by Kleinfeld et al. in 1988,[182] who used combinations of photolithographic and chemical techniques to prepare biologically active substrates to guide the development of neurons in culture. Later on, a number of photochemical methods,[183,184] such as laser ablation of self-assembled monolayers[185] and microcontact printing,[186,187] were added as tools to create micronscale patterns of adhesive molecules against a nonadhesive background. In one of the recent studies on SAMs, DETA and 13F (tridecafluoro-1, 1, 2, 2-tetrahydroctyl- 1-trichlorosilane) in combination with deep UV photolithography was used to create surface patterns to determine neuronal cell attachment and dendritic/axonal growth. The cultured cells displayed a compliance of more than 50% to the cell-adhesive pattern of DETA at 4-6 days *in vitro*. The neurons survived up to 35 days on the patterns.[188]

Amino groups of SAMs have been implicated in the promotion of cell attachment and growth.[189-191] Examination of adherent cell lines like rat basophilic leukemia cells (RBL) and mouse embryonic carcinoma line (P19) on SAMs terminated with the oligo (ethylene glycol) group (R = (OCH_2–CH_2)$_6$OH, EG_6OH) prevented attachment of cells. The high resistance to adhesion provided by the EG_6OH-terminated SAMs allowed people to study differential attachment in both complex (containing fetal bovine serum) and minimal (protein and serum free) media.[192]

Determination of specific roles of functional groups involved in cell growth is difficult, and contradictory results have been reported. It has been shown that surface hydroxyl and methyl groups do not promote cell attachment or growth.[192,193] In another approach, neurite outgrowths of embryonic chick dorsal root ganglia (DRG) neurons and PC12 cells were investigated using a set of chemically functionalized surfaces prepared by SAMs of alkanethiolates with R = NH_2, COOH, and CH_3 on patterned gold surfaces. Neurons with neurite outgrowths were observed predominantly on a patterned SAM of long-chain alkanethiolates with amino groups.[194,195] Another observation has shown that the substrates patterned with amines had controlled growth of neuroblastoma cells reflecting the underlying growth pattern, whereas random neuronal outgrowth was observed on uniform (unpatterned) substrates.[196]

The discovery of SAMs has essentially transformed surface chemistry and also opened a new area for physically oriented groups. It has brought together the study of well-defined inorganic surfaces and organic species, which from a physics perspective were previously often considered rather undefined. The great flexibility of the concept of SAMs brought about by the wide choice of endgroups which can be anchored to the substrate has led to a broad range of applications of SAMs, including important developments in the area of biotechnology. Also, the use of ITO instead of Au along with the properties mentioned in Chapter 4, allows for high resolution imaging of neuron-to-electrode synapses by confocal fluorescence microscopy.

To develop cell culture platforms for applications such as drug screening, biosensors, neural prosthetic devices and bioreactors, it will be necessary to develop and characterize SAM-based platforms that provide an appropriate environment for cell

attachment, growth and functionality.[197,198] The advantage of SAMs is the ability to make use of the relatively easy and versatile chemistry for modifying the surface and additionally to be able to control the intrinsic and geometric properties of surfaces in contact with cellular systems.[199] In this work, we have used different end groups of SAMs like $-NH_2$, $-CH_3$ and $-SH$ on ITO substrates and assessed the biocompatibility, potential cytotoxic effects, cell longevity, preservation of cell phenotype and cellular response of rat brain cortical neuronal (RBNs).

6.1.1. Cell Culture

Based on the MSCs experimental results presented in Chapter 5, we reduced the number of working substrates to ITO, SAM-coated ITO and PLL substrates. The end groups of the SAMs were selected according to literature review of neurons and SAMs interactions. It is known from the results reported by Yukie et al., that amino, methyl and $-SH$ groups had some success when modified with laminin.[195] Therefore, SAMs of APTES, ODT and 3-mercaptopropyl triethoxysilane (MPS) were selected containing amino, methyl and $-SH$ end groups, respectively.

Standard cell culture techniques were used to culture CNS-derived RBN cells purchased from QBM Cell Science (Pittsburgh, PA). Prior to each experiment, rat CNS neurons were cryopreserved in a liquid nitrogen storage tank. After removal from liquid nitrogen storage, each cryovial was placed in a water bath preheated to 37 °C and disinfected wiping the external surface with 70% ethanol. Cells were then resuspended in serum-free Neurobasal medium containing B27 supplement and 200 mM L-glutamine at 37 °C in 95% humidified air and 5% CO_2. The following protocol was used to culture neuronal cells on substrates.

6.1.1.1 Protocol: 1

(1) Vial of cells from liquid nitrogen were removed and placed in a water bath pre-heated to 37 °C.

(2) After three minutes, the vial was removed and disinfected outside by wiping with 70% ethanol.

(3) Gently, 1 mL cells were transferred (concentration of 1.5 million cells/mL) into a 15 mL centrifuge tube and immediately 3 mL of pre-warmed Neurobasal Medium supplemented with B-27 and L-glutamine was added dropwise onto the cells, while rotating the tube by hand.

(4) 100 µl of cell suspension (containing 37,500 cells) from 15 mL tube were transferred onto each of 12 substrates placed in a 12-well plate and also in control substrates, placed in 35 mm tissue culture dish.

(5) Cells were incubated for four hours in a 37 °C, 5% CO_2 incubator.

(6) A fresh pre-warmed medium of 1.9 mL was added onto all substrates after four hours.

(7) Cells were incubated at 37 °C with 5% CO_2 and media change was done on day 4.

(8) After initial media change on day 4 or 5, 50% of the medium was replaced on the 6th and 7th days.

Further modification to the above experiment protocol was done by performing a quick experiment on collagen-coated 35 mm tissue culture dish by using the above protocol. Morphological observation was documented after 24 h. Immediately after 48 h, the live/dead assay was performed on the above culture. Results showed that almost all the cells were dead within 48 h. Through this experiment, change in experiment protocol

was performed by adding 1% fetal bovine serum (FBS) to the cell suspension containing neurobasal medium. Addition of FBS was done to neutralize the dimethyl sulfoxide (DMSO) present in the thawed cells, because no serum was used in the Neurobasal medium for the RBNs culture.[200] It was assumed that one of the reasons for cell death was the presence of DMSO in cell cultures.

6.1.1.2 Protocol: 2

(1) Vial of cells from liquid nitrogen was removed and placed in a water bath pre-heated to 37 °C.

(2) After three minutes, vial was removed and disinfected outside by wiping with 70% ethanol.

(3) Gently, 1 mL cells were transferred (concentration of 1.5 million cells/mL) into a 15 mL centrifuge tube and immediately 9.8 mL of pre-warmed Neurobasal medium containing 1% FBS was added dropwise onto the cells, while rotating the tube by hand.

(4) 500 μL of cell suspension (containing 70,000 cells) from 15 mL tube were transferred onto each of 24 substrates placed in 35 mm tissue culture dish.

(5) Cells were incubated for four hours in a 37 °C, 5% CO_2 incubator.

(6) Fresh pre-warmed medium of 1 mL was added onto all substrates after four hours.

(7) Cells were incubated at 37 °C with 5% CO_2 and medium change was done on day 2.

(8) After initial media change on day 2, 50% of the medium was replaced on the 3rd, 5th and 7th days. Morphological observations were documented on days 1, 3, 5, and 7.

6.1.2 Cell Preparation for Viability Assay

Neuronal cells were seeded and grown in fresh Neurobasal/B27 media supplemented with 200 mM glutamine as described above in morphological observations. After an observation period of 1, 3, 5, and 7 days, selected cultures were prepared for the cell viability assay as described in earlier protocol for Live/Dead Assay. Observations were monitored using Nikon Eclipse TS100 inverted fluorescent microscope.

6.1.3 Immunofluorescence Studies on Neurons

To confirm morphological identification and to assess phenotypic preservation of RBNs, a molecular neural marker was used. Mouse monoclonal Neuron Specific Enolase (NSE), a monoclonal antibody (mAb) widely used (and recognized) as a marker of the neuronal phenotype, was used.

To identify all neurons on SAM-coated substrates using this anti-NSE mAb, the protocol described below was used. NSE is the cell-specific isoenzyme form of the glycolytic enzyme enolase [2-phospho-D-glycerate hydrolase], which is found only in neurons and neuroendocrine cells. NSE is a useful biochemical marker of neuronal differentiation and their levels determine the neuronal differentiation process occurring in the *in vitro* cultures on the substrates. NSE is present in all neurons and not restricted to a specific subset, it can be useful as a general marker for differentiated neurons. Moreover, it also suggests that neurons maintained *in vitro* do develop in a manner similar to that *in vivo*. NSE containing cells visualized by IHC were fixed in a solution of 4% buffered formaldehyde and stained using mouse-anti-NSE serum, secondary antibody, ABC reagent complex, and DAB substrate. IHC staining for NSE permitted visualization of individual nerve cells on all the substrates.

6.1.3.1 Protocol for IHC on Neurons

(1) After 3, 5, and 7 days of culture on substrates, cells were washed three times with

1x D-PBS and fixed using 4% buffered formalin.

(2) The fixed cells were then rinsed two times for five minutes in PBS buffer.

(3) Non-Immune blocking serum was added onto the substrates and excess was

blotted after 30 min.

(4) Drops of NSE primary antibody were added to cells and were incubated for one

hour at room temperature.

(5) Cells were rinsed four times for five minutes in PBS buffer.

(6) Cells were incubated for 30 min in the secondary antibody.

(7) Cells were rinsed four times for five minutes in buffer.

(8) ABC reagent complex was added to cells and waited for 30 min.

(9) Cells were rinsed four times for five minutes in buffer.

(10) DAB substrate was added to the cells for about 2-10 min.

(11) Cells were washed with DI water.

For negative controls, the primary antibodies are omitted from the first incubation

medium and the samples are incubated with normal serum in PBS.

6.2 Cell Morphology and Viability

6.2.1 Results from Protocol: 1

The effects of specific chemical functionalities on the neurite outgrowths of

RBNs were investigated using a set of chemically functionalized surfaces prepared by

SAMs with end groups of NH_2, CH_3, and SH. RBNs were cultured (37,500 cells/cm^2) on

untreated and SAM-coated ITO for seven days. Figure 6.1 shows the images of RBNs on different SAM-modified ITO substrates after one week in culture.
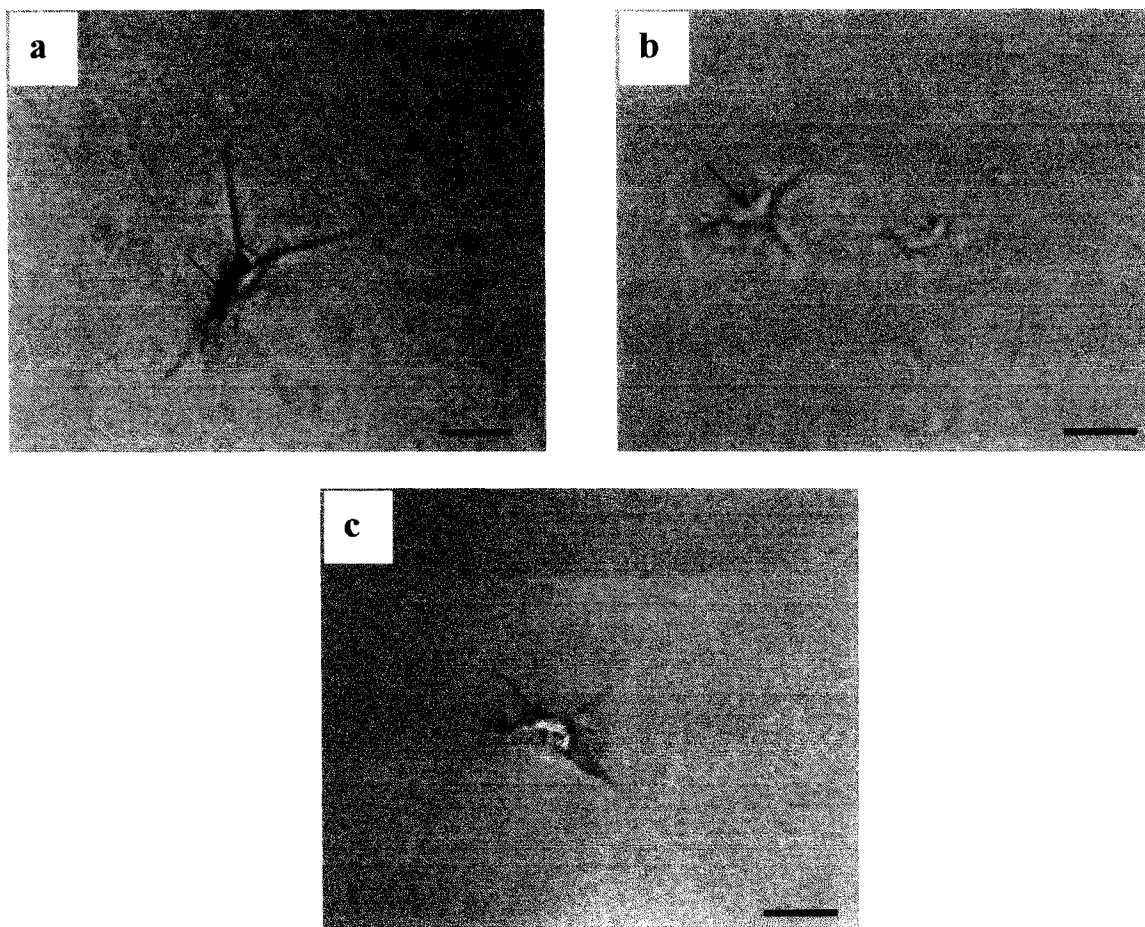
Figure 6.1 Optical images of RBNs with neurite outgrowths on different SAM-coated ITO substrates after one week in culture using protocol 1. (a) ITO (b) ITO-ODT and (c) ITO-APTES (Bar represents 40 μm).

Figure 6.1 shows that neurite outgrowths were predominantly observed on cells cultured on NH_2 (Figure 6.1b) and CH_3 (Figure 6.1c) SAM-coated ITO surfaces. However, the –SH modified ITO substrates did not promote cell attachment and neurite outgrowth. The results shown in Figure 6.1 indicate a need to make some changes in the protocol in order to get sufficient number of cells to attach to the substrate. The arrows

are pointing towards the neuron cells on all substrates. Each arrow in Figure 6.1 points to the nucleus of neurons with extended neurites on the substrates.

6.2.2 Results from Protocol: 2

The experimental protocol was revised by adding 1% FBS to the cell suspension containing neurobasal medium to neutralize the DMSO. It has been assumed that the DMSO present in thawed cells also contributes to the cell death. The cell density was also increased to 140,000 cells/cm^2. After 3 DIV, cells had initial neurite outgrowth activity all around the cell body on all of the substrates which is indicated by the small arrows in Figure 6.2.
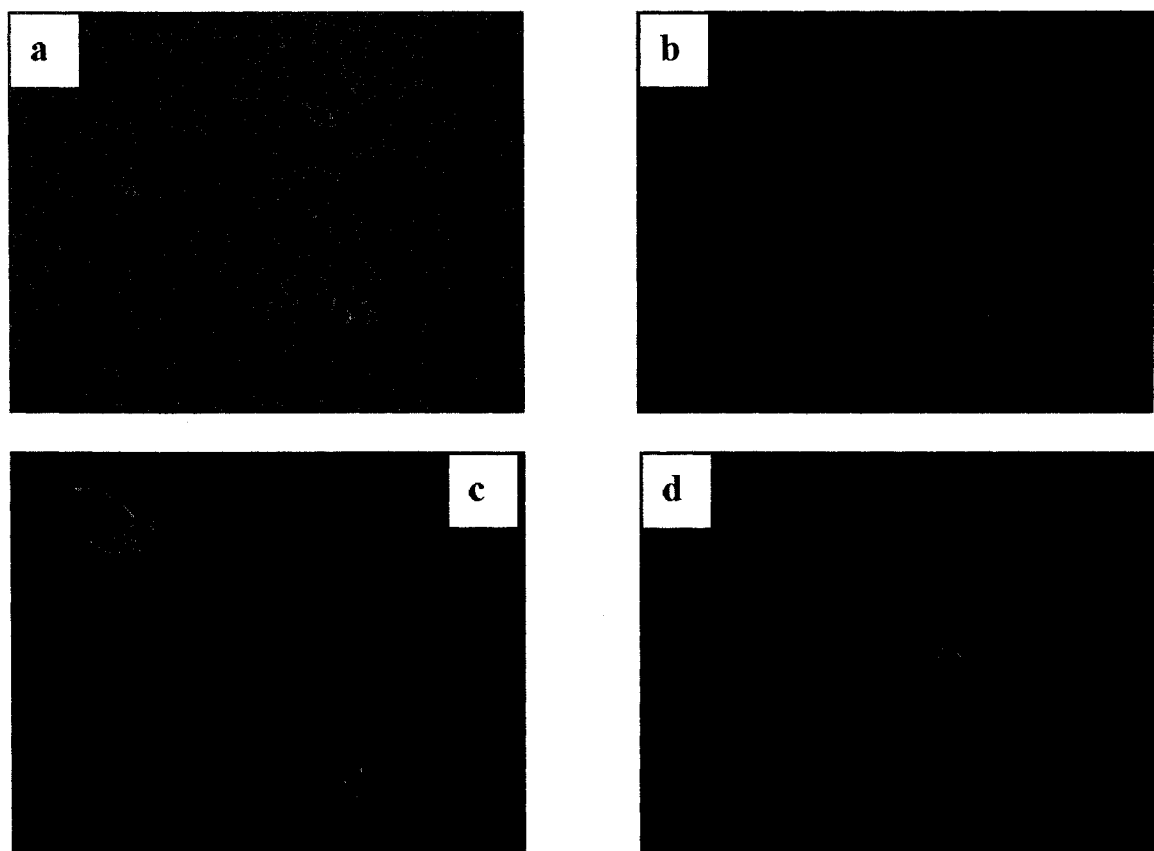
Figure 6.2 Optical images of RBNs after 3 DIV on different SAM-coated ITO substrates using protocol 2. (a) ITO (b) ITO-APTES (c) ITO-ODT and (d) PLL (Bar represents 40 μm).

The cells on SAM-coated substrates remained more active compared to that on the untreated ITO as indicated by the red fluorescent dead cells and green fluorescent live cells in Figure 6.3 (a,b,c).
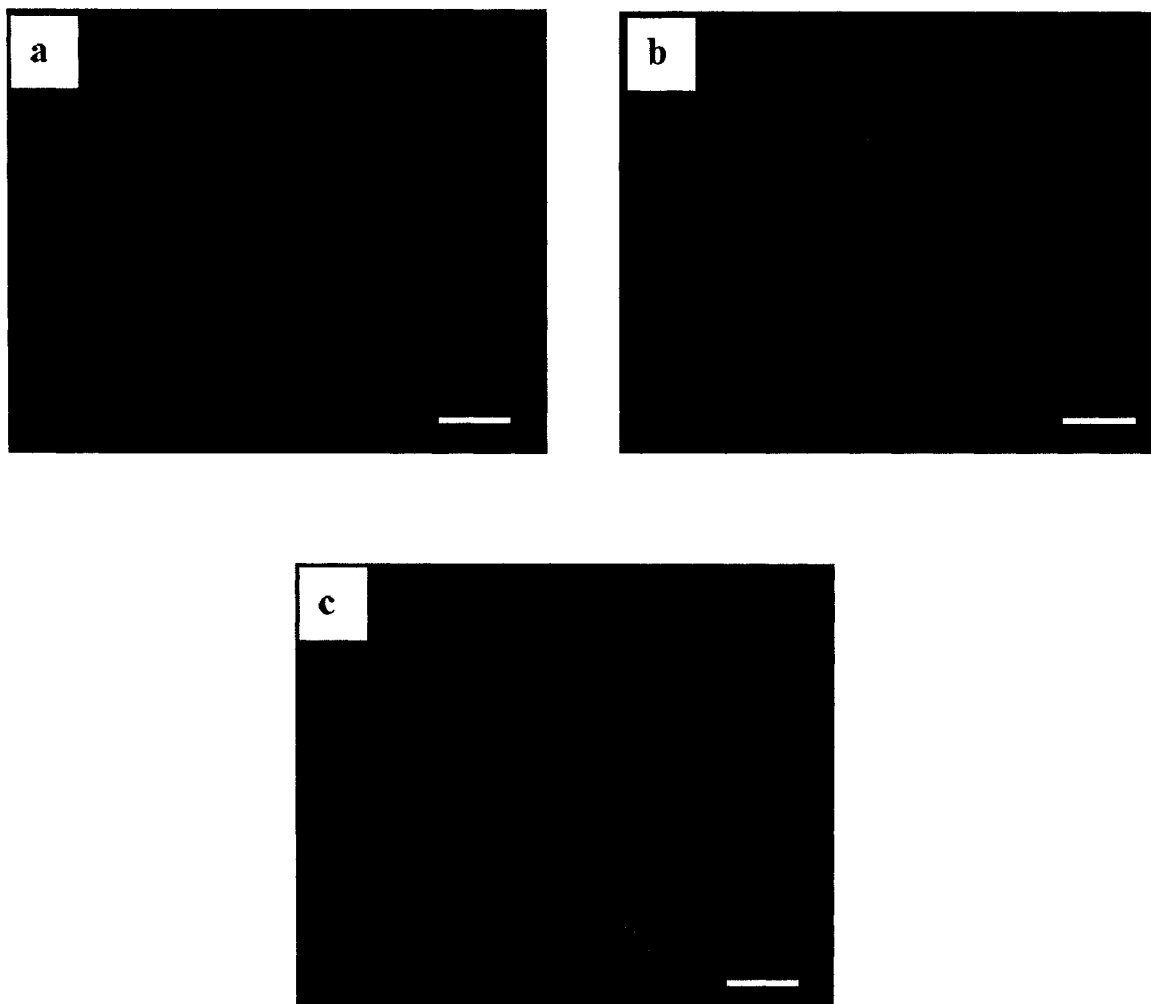
Figure 6.3 Cell viability measured using LIVE/DEAD® assay showing both live and dead RBNs after 3 DIV using protocol 2. (a) ITO (b) ITO-APTES and (c) ITO-ODT (Bar represents 40 μm).

After 5 DIV, cells continued their cytoplasmic extensions on the SAM substrates compared to that on PLL and untreated ITO as indicated in Figure 6.4. Each large arrow in Figure 6.4 points towards the cell cytoplasmic extension. Even though there was

neurite outgrowth activity on ODT (having CH_3 end group) coated substrate, they seem

to be dead by 5 DIV as indicated by small arrow in Figure 6.4c. But, in case of APTES

(having NH_2 end group) the neurite extension as indicated by small arrow on Figure 6.4b

was still alive, emanating the green fluorescent color. After 5 DIV, the cells continued to

remain active and alive on all the SAMs substrates as indicated in Figure 6.5.
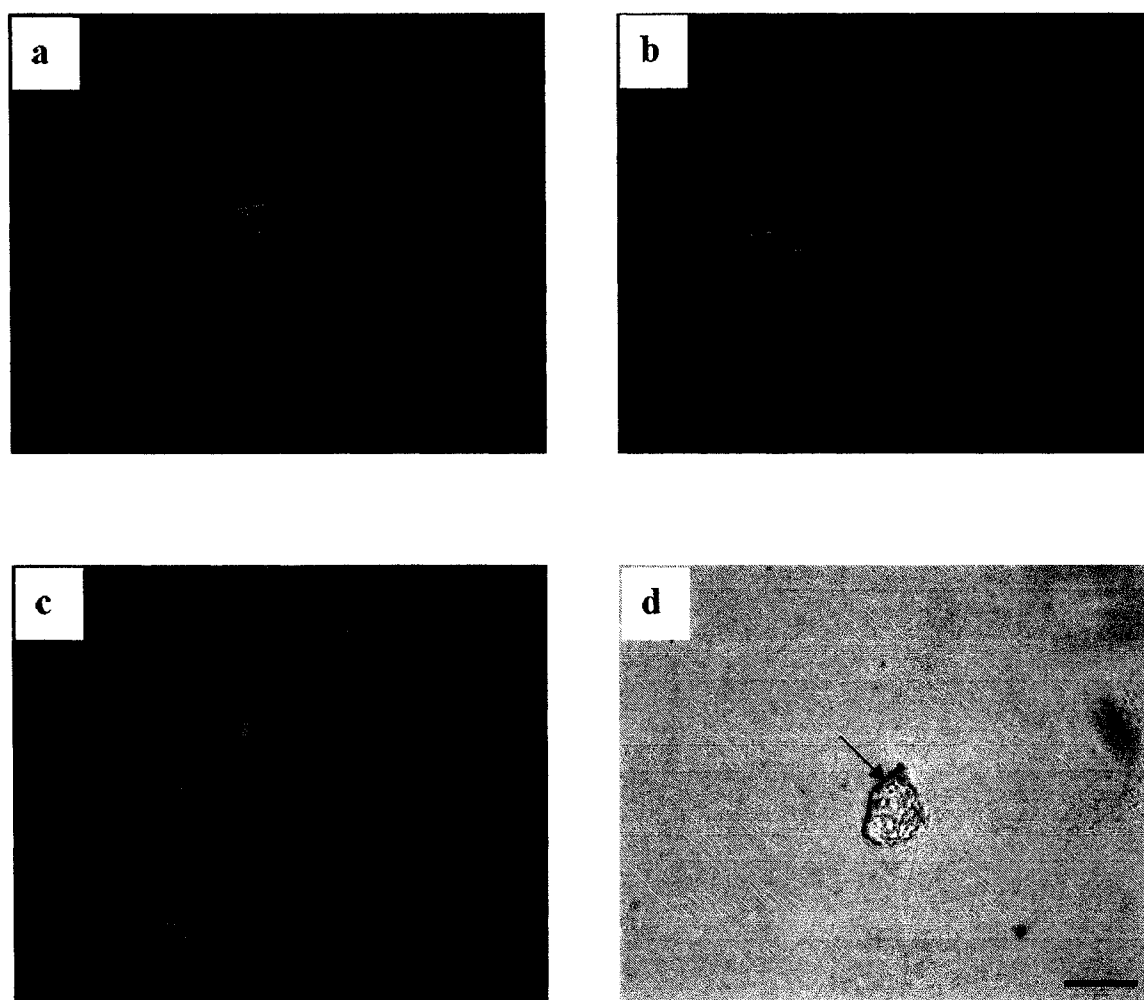
Figure 6.4 Optical images of RBNs after 5 DIV on different SAM-coated ITO substrates using protocol 2. (a) ITO (b) ITO-APTES (c) ITO-ODT and (d) PLL (Bar represents 40 µm).
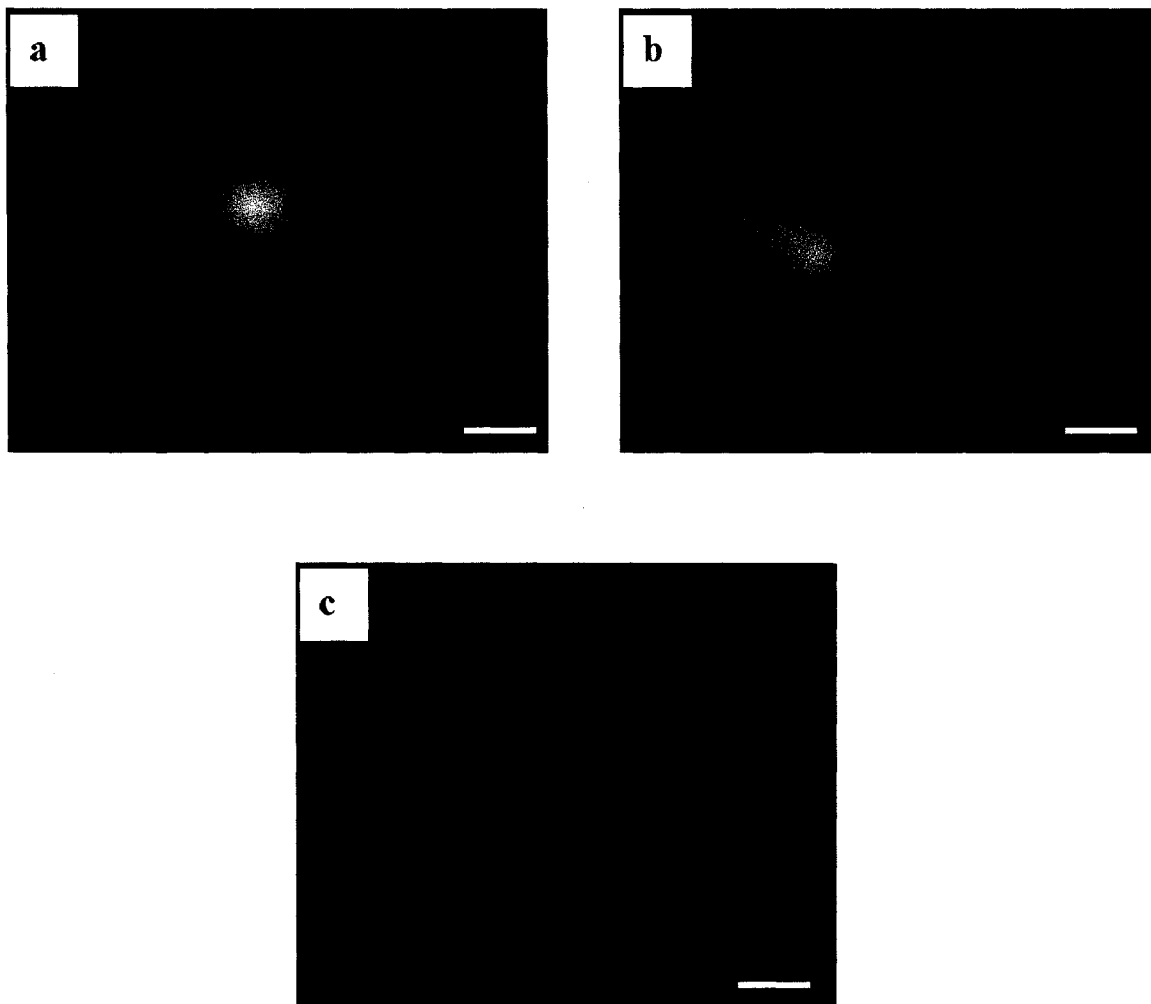
Figure 6.5 Cell viability of RBNs showing live cells after 5 DIV using protocol 2. (a) ITO (b) ITO-APTES and (c) ITO-ODT (Bar represents 40 μm).

After 7 DIV, cells further continued their cytoplasmic extensions on SAM-coated substrates compared to that on PLL and untreated ITO as indicated in Figure 6.6. Each large arrow in Figure 6.6 points towards the cell cytoplasmic extension. Neurite outgrowth activity on ODT seemed to be dead as indicated by the area where the small arrow in Figure 6.6c points. Neurite extension on APTES continued even after 7 DIV. The small arrow on Figure 6b shows the neurite outgrowth on the APTES-coated substrate.
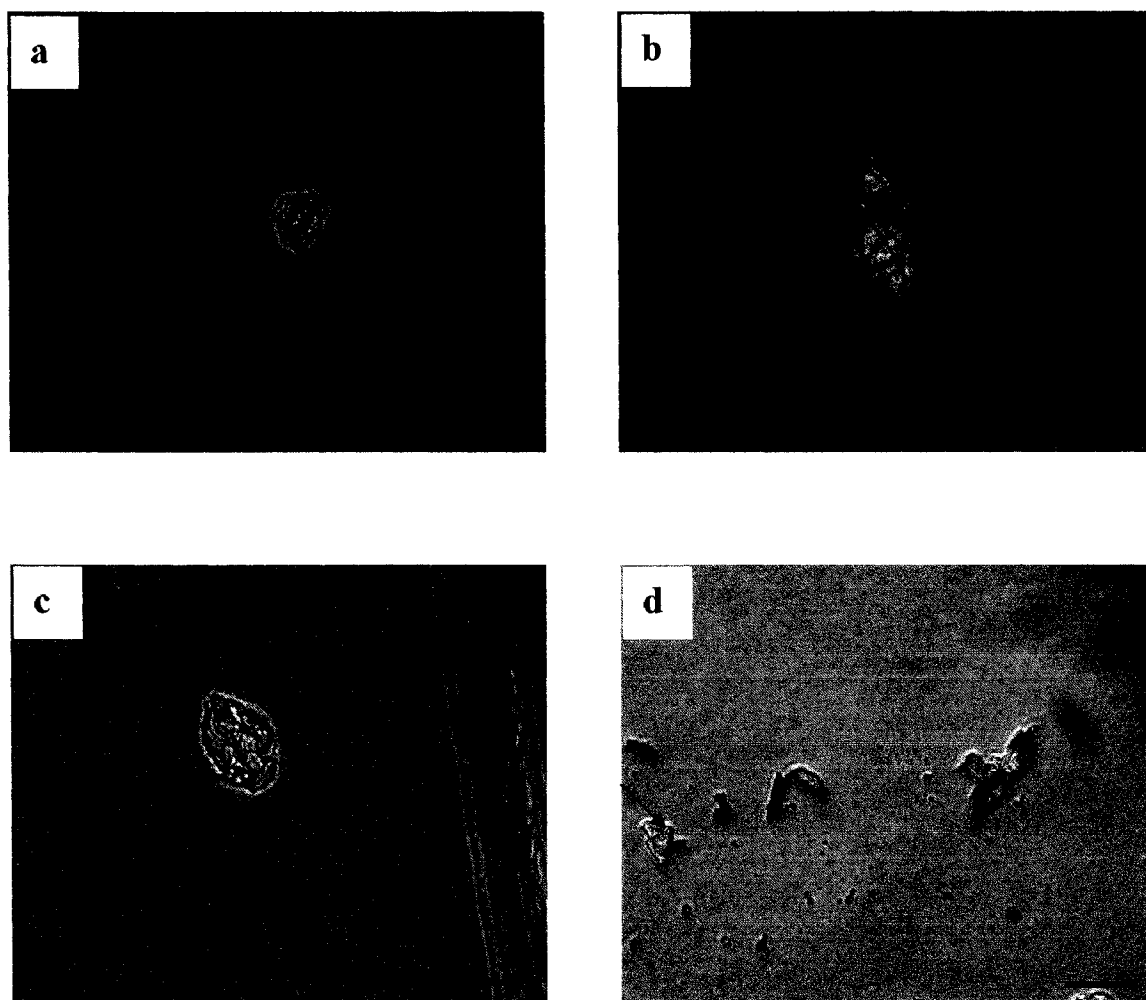
Figure 6.6 Optical images of RBNs after 7 DIV on different SAM-coated ITO substrates using protocol 2. (a) ITO (b) ITO-APTES (c) ITO-ODT and (d) PLL (Bar represents 40 μm).

After 7 DIV, the cells continued to remain active and live only on APTES-coated substrate compared to all other substrates. Figure 6.7b indicates green fluorescent color produced by the live cell on the APTES-coated substrate. Figure 6.7 (a,c,d) represents the dead cells on untreated ITO, ODT-ITO, and PLL respectively.
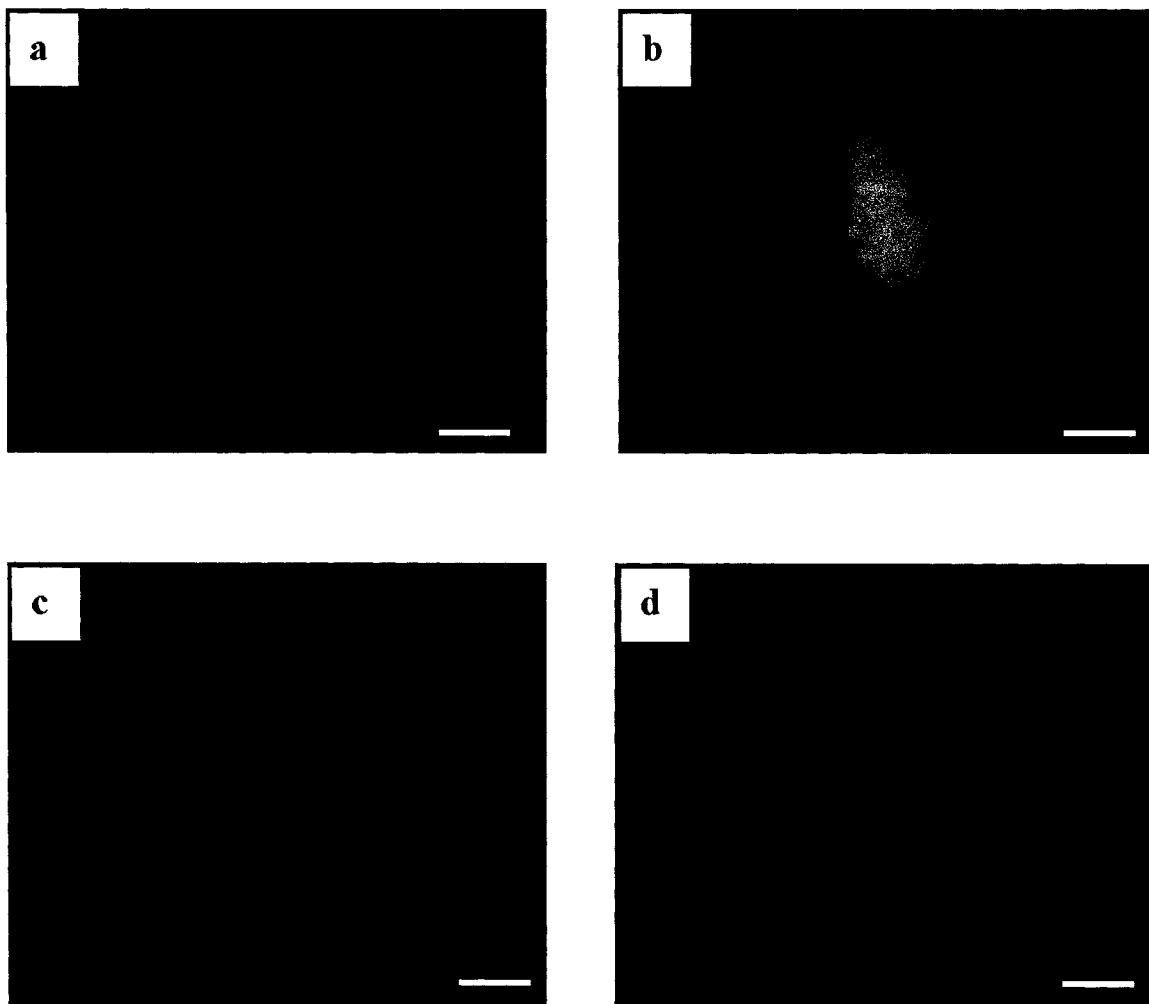
Figure 6.7 Cell viability measured using LIVE/DEAD® assay showing both live and dead RBNs after 7 DIV on (a) ITO (b) ITO-APTES (c) ITO-ODT and (d) PLL using protocol 2 (Bar represents 40 μm).

6.3 Immunohistochemical Study

IHC analysis was conducted against NSE levels on cells cultured on all the substrates. Figure 6.8(a,b,c) illustrates RBNs on APTES coated ITO, ODT coated ITO, and PLL substrates respectively. The brown reaction indicates that an antigen antibody complex has formed a positive immunoreaction and the RBNs did not lose their *in vivo* behavior in this *in vitro* environment. The cells maintained their NSE levels which is

needed for continuous outgrowth of the cells. The arrows point the brown reactions indicating the formation of an antigen-antibody complex.
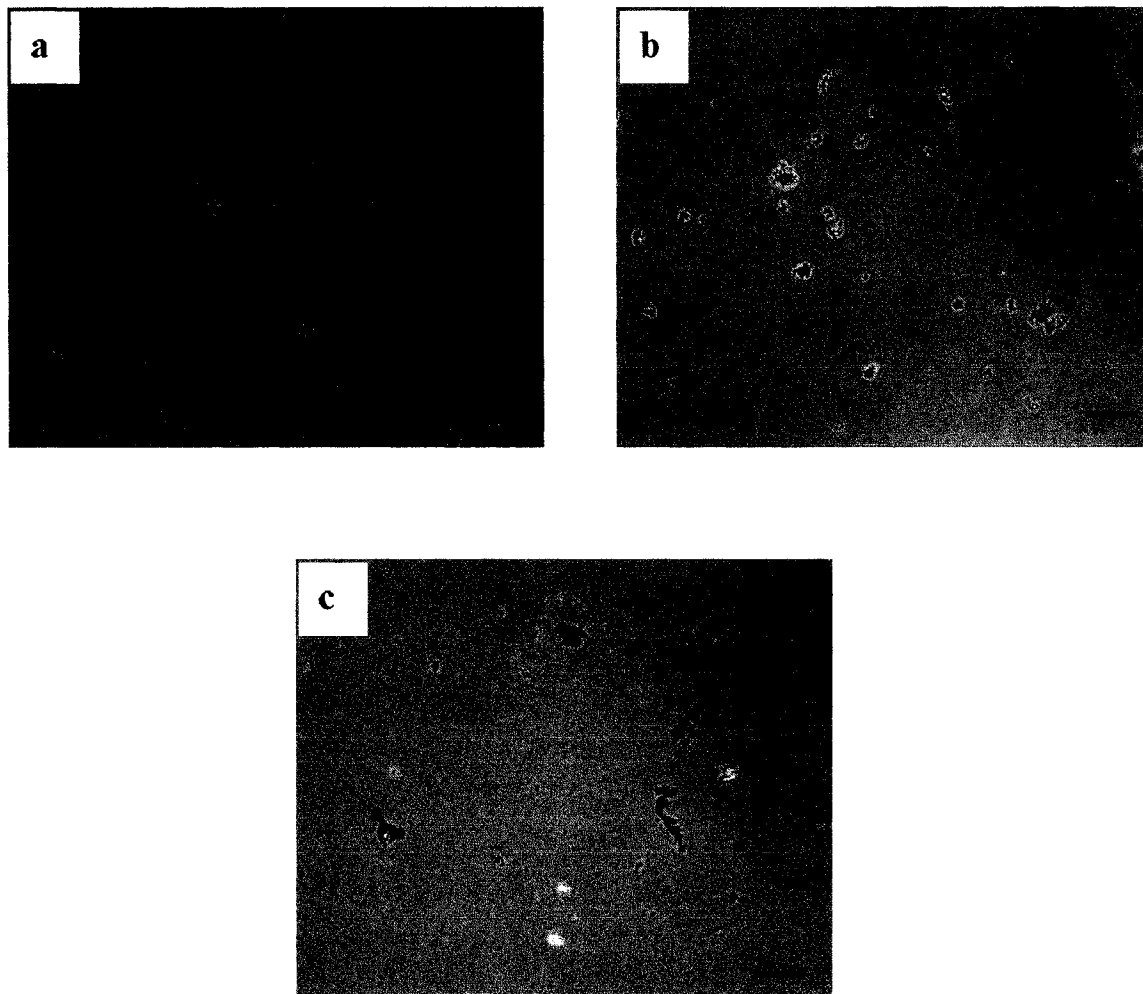
Figure 6.8 Immunohistochemistry observations after 7 DIV on (a) ITO-APTES (b) ITO-ODT and (c) PLL using protocol 2 (Bar represents 10 μm).

6.4 Discussions

The results of this study presented above provide strong evidence that cellular attachment to surfaces is influenced by small changes in the substratum chemical composition and molecular structure. In a study performed by Schaffner et al., hippocampal cells were grown in both serum containing and serum free media.[201] The

results suggested that in the absence of serum, the substrate plays a more dominant role in determining the nature of the cell-surface interactions.

The results from our study performed on SAM-modified ITO substrates suggest that in the absence of serum, cell adhesion is rare. This result was unexpected, as George Whitesides group showed that cells plated from serum-free medium attached on both hydrophobic and hydrophilic areas.[202] Another experiment was performed by our group under the same serum free medium to better understand the underlying mechanism. This time, the cell density was increased by two-fold and the medium was changed much sooner than the earlier experiment. No cells were observed till 5 DIV on substrates. After 5 DIV, neuronal attachment of RBNs was observed predominantly on substrates modified with amino and methyl groups rather than on –SH group and control substrates. Similar results in adhesion were observed by Yukie et al., where nerve cell adhesion on different chemically functionalized surfaces prepared by SAMs of alkanethiolates with NH_2, COOH, and CH_3 end groups on patterned gold surfaces were studied.[195] However, their results still indicated a need for a change in protocol in order to get sufficient number of cells to be attached to the substrate. The experimental protocol was changed by adding 1% FBS to the cell suspension containing Neurobasal medium. Following the protocol modification, a dramatic increase in cell adhesion was observed, with cells remaining viable until one week in culture. Better cell adhesion was observed on SAM-modified ITO surface in comparison to the untreated ITO and PLL surfaces. Similar results in adhesion were observed by Yukie et al.[195] In our work we observed better cell adhesion on amino group compared to methyl group SAM.

LIVE/DEAD® assay performed on the above substrates confirmed that the cells interacted more specifically to the amino end group of SAM substrate. The results also suggest that the viability of cells were found in this order: $NH_2 > CH_3 > PLL > ITO$ when cultured over a period of one week. Nerve cell phenotype was studied by performing IHC using the NSE antibody. A significant amount of immunopositive staining was observed on all SAM-coated ITO substrates followed by ITO and PLL substrates over a week in culture.

Overall, most of the differences in cell-surface interactions on the different substrates were observed in the first 3-5 days of cell culture. While adhesion was greatest on ITO-ODT, viability was found to be more prominent on both SAM-coated substrates. The differences in cell phenotype, between the experimental and the positive control surfaces diminished over time (seven days) in culture as the cell density decreased due to the cell death on all the substrates.

In summary, neurons adhered well to all SAM substrates during the one week observation. Neuronal cell viability analysis indicated that more cells grew well on SAM substrates than on ITO and PLL substrates. Better phenotype maintenance of neurons were observed on the SAM-coated substrates than control substrates, and lastly, a decrease in cell density was noticed on all substrates from day one to day seven.

CHAPTER 7

HEPATOCYTE CELLS ON SAM-MODIFIED

ITO SUBSTRATES

7.1 Hepatocytes and Their Culture

The liver is the primary organ involved in the metabolism of foreign compounds.

It comprises of a complex, metabolic array of vasculature, endothelial cells and

parenchymal cells performing a multitude of functions. Figure 7.1 depicts the cross

section of adult form of the liver.[203,204]
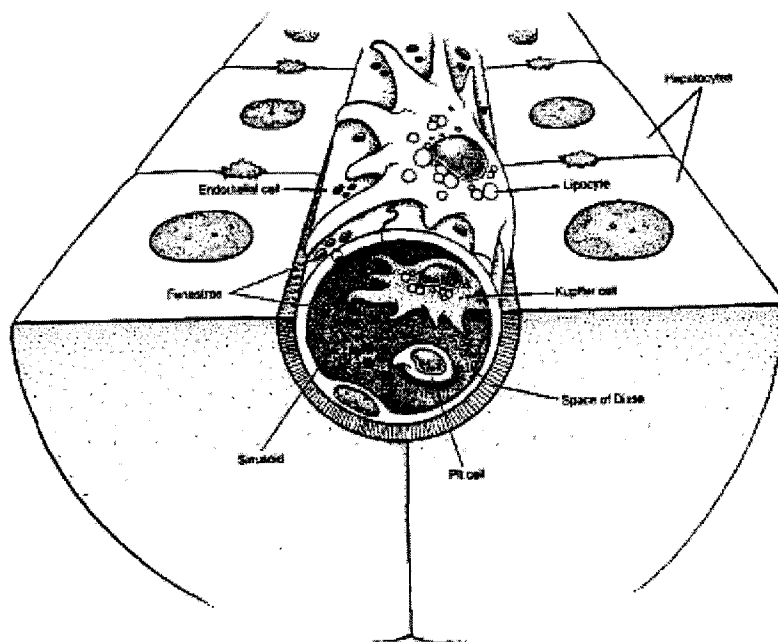
Figure 7.1 Cross-section of the adult liver showing differentiated hepatocytes.[203]

87

It consists of differentiated hepatocytes (H) separated from a fenestrated endothelium (E) by the Space of Disse. Lipocytes (stellate or Ito cells), which encircle the sinusoid are well-positioned for both communication with hepatocytes and have the potential to modify the extracellular space by secretion of extracellular matrix. Biliary ductal cells contact hepatocytes toward the end of the hepatic sinusoid (not depicted) and Kupffer cells (the resident macrophage), and Pit cells (a type of natural killer cell) are free to roam through the blood and tissue compartment. Thus, the adult liver provides a scaffold for many complex cell-cell interactions that allow for effective, coordinated organ function. The primary functions of the liver is detoxification; provide metabolic activity, glycogen storage, urea production, and release of protein, carbohydrates and other metabolic wastes.[205] Hepatocytes comprise about 60% of the liver and function to remove a number of toxins from the body and produce proteins like albumin and transferins.[206]

Hepatocytes rapidly lose their liver specific functions when grown under standard *in vitro* conditions.[207] Immortalized hepatocyte cell lines have been used for *in vitro* testing of drugs, but the lack of phenotypic gene expression makes them useless. Also because of the limitations of liver slices, such as short-term viability and diffusional barriers, primary cultures of hepatocytes have become the "gold standard" for *in vitro* testing of drugs. Isolated hepatocytes have been used as models in various culture systems for studying the toxicological response of drugs, since they closely resemble the liver and provide a metabolic profile of a drug *in vitro*, closest to that found *in vivo*.[208-211] Unlike fibroblasts which can attach to a number of surfaces due to their ability to secrete fibronectin and other ECM proteins, hepatocytes are extremely selective in their

attachment. Further, hepatocytes are anchorage dependent and lose their functionality in suspension within h.

A variety of culture methods have been developed to retain most of the hepatocytic functions such as culture on or in basement membrane gels,[212,213] co-cultures with other liver-derived and nonliver cell types,[203,214,215] culture in collagen gel sandwiches[210,216] and polymers.[217,218] Collagen is an important component of the hepatocyte basal membrane and promotes attachment of hepatocytes *in vitro*. Cells cultured on collagen-coated surfaces showed increased urea production and low LDH release.[210] Collagen was observed to provide the closest alternative to hepatocyte architecture *in vitro*. However, biodegradability and cross-link formation are some of the limitations of using ECM modified surfaces.

High molecular weight polymers like polyethylene glycol (PEG),[219,220] polyglycolic acid (PGA)[221] and polylactic acid (PLA)[219,222] were used to develop scaffolds for hepatocyte culture. However, these polymers lose their strength upon long culture periods. Primary rat hepatocyte culture on porous poly-tetraflouroethylene (PTFE) showed increased protein secretion and polygonal morphology over culture periods varying from 24-48 h. The lack of stability of polymer scaffolds over extended culture periods make them ineffective for cell culture.[223]

Other alternatives used to increase hepatocyte viability include culture on polyelectrolyte multilayers,[224] hydrogels,[106] gold substrates[225] and culture as spheroids.[226] Primary rat hepatocytes cultured on polyelectrolyte multilayer films with poly (4-styrenesulfonic) acid as the topmost layer attached and spread on the PEM surface and liver specific functions like urea and albumin production showed an increase with

duration in culture.[224] Porcine hepatocytes immobilized on gold colloids showed increased protein and albumin production upon culture. The LDH release was minimal which indicated that the cells suffered limited damage upon culture.[225] Murine hepatocytes entrapped within PEG hydrogels were assessed for cell viability and total protein production over a period of seven days. The results indicated that the cellular viability was not affected by the hydrogel concentration, but total protein production decreased with increase in PEG concentration.[10] The use of growth factors and cytokines like hepatocyte growth factor,[227] epidermal growth factor,[228] transforming growth factor (TGF)-alpha and beta[229,230] and norephinephrine[231] have been shown to promote cellular viability, but the cells eventually de-differentiate and lose their functionality.

Co-culturing of hepatocytes with different cell types have been studied extensively within the fields of toxicology as means of maintaining specific hepatocyte functionality. Fibroblasts,[215] stellate cells,[203] liver endothelial cells,[232] liver epithelial cells[233] have been co-cultured with hepatocytes. Co-culture helps retain the polymeric shape of isolated hepatocytes upon adherence. Hepatocyte co-cultures have been shown to express high levels of liver specific proteins like albumin.[203,214] However, the exact mechanism of cell-cell interaction in these co-cultures is not yet understood and is being investigated by a number of research groups. 3T3 fibroblasts were co-cultured with primary rat hepatocytes to study cellular functionality and viability. The co-cultures maintained over a period of two weeks indicated high cell viability, maintenance of liver specific functions like the secretion of albumin and P450 cytochrome activity.[234] Cell culture platforms are incorporated in designing cell-based bioreactors.[235-240] These bioreactors sustain cellular viability without impeding nutrient and metabolite exchange.

A suitable scaffold ensures successful cell culture and permits nutrient perfusion by enabling a homogenous distribution of mass and flow transfer catering to the metabolic requirements of the cells.[235,239] However, most of the methods described above have been limited in controlling prolonged cell viability and functionality.

SAMs of alkanethiolates on noble metals form ordered and uniform monolayers and have been widely used as models for cell culture studies. Mammalian cell lines cultured on SAM-modified surfaces have indicated higher cell viability, maintenance of functionality and expression of cell specific functions.[241,242] In this chapter, we have studied primary hepatocyte culture on different SAM-modified ITO substrates in an attempt to mimic the cellular microenvironment. Liver specific functions such as total protein synthesis and LDH leakage along with cell morphology, viability and proliferation (quantitatively) were determined. These studies would provide valuable resources for studying cell-substrate interactions and arrive at a suitable choice of substrate for the development of stable SAM based cell culture platforms (SCCPs) for *in vitro* drug testing.

7.2 SAM Preparation and Characterization

7.2.1 Substrate and SAM Preparation

ITO-coated glass slides were cleaned by sonication in toluene, acetone, ethanol each for 5 min and then in DI water for 30 min. The substrates were then rinsed, N_2-dried, and used. SAMs of $-CH_3$ and $-COOH$ end group were formed on ITO by immersing the samples in the neat liquid of ODT and MPA for one hour, followed by rinse in ethanol and N_2-dried. SAMs of $-SH$ and $-NH_2$ end group were formed by immersing the substrates in 1 mM ethanolic solution of MPS and APTES for 24 h,

followed by rinse in ethanol and N$_2$-dried. All the samples were sterilized in 70% ethanol for one day before seeding the cells.

7.2.2 Characterization

7.2.2.1 Contact Angle Measurements

After the SAM deposition, the surface is first tested for the presence of the molecule using the contact angle measurements. Figure 7.2 shows the contact angle measurements done on three different SAM substrates and bare ITO.
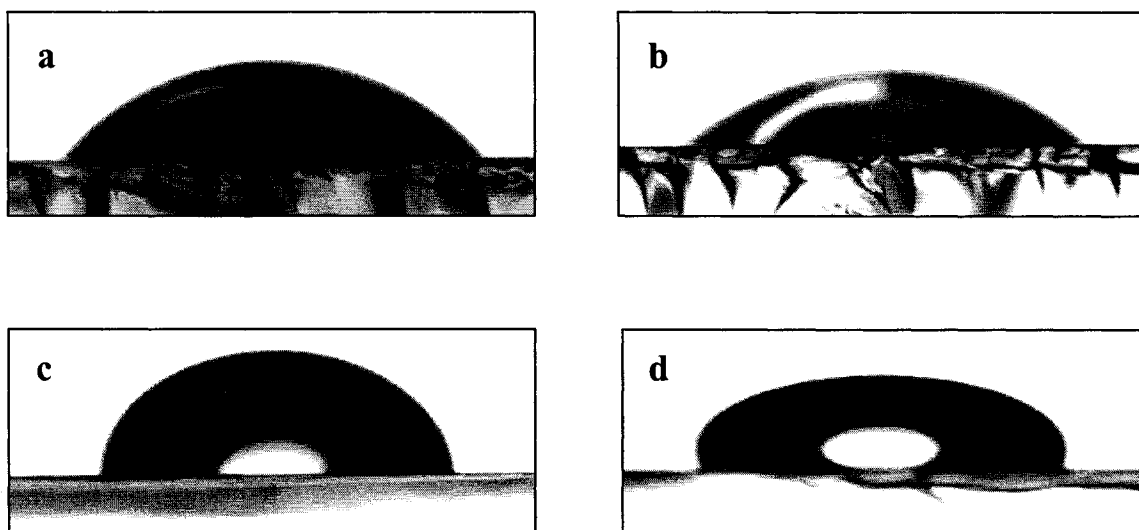
Figure 7.2 Contact angle measurements of (a) ITO (45-48°) (b) ITO-APTES (35-38°) (c) ITO-MPS (89-91°) and (d) ITO-ODT (103-105°).

The contact angle measurements show that ITO modified with APTES presents a highly hydrophilic surface while that of ODT modified substrates are highly hydrophobic. The substrates modified with MPS are intermediate between that of hydrophilic and hydrophobic surfaces.

7.2.2.2 RAIRS and ATR

To further confirm these findings, ATR was carried on all the substrates except on ITO-ODT (RAIRS used). Figure 7.3(a) shows the RAIR spectra of ODT SAM on ITO. By analogy to that of HDT on ITO[243], the asymmetric and symmetric bands of methylene (CH_2) stretches are observed at 2917 and 2850 cm^{-1}, while the asymmetric C-H stretching mode of CH_3 is observed at 2964 cm^{-1} and can infer that ODT forms a close packed, stable monolayer structure on ITO. Figure 7.3 (b) shows the ATR spectra of APTES on ITO in 1500-1800 cm^{-1} range. The strong to medium peaks at 1651 cm^{-1} and 1639 cm^{-1} corresponds to the primary amine N-H bending. While the peak observed at ~3400 cm^{-1} in Figure 7.3 (c) corresponds to the primary amine N-H stretch. Figure 7.3 (d) illustrates the ATR spectra of MPA on ITO. The peaks at 1708 cm^{-1} and 1718 cm^{-1} corresponds to the acyclic carboxylic group while the strong peak at 1653 cm^{-1} corresponds to the carboxylate anion. Figure 7.3 (e) shows the ATR spectra of MPS on ITO. The peak at 2605 cm^{-1} corresponds to the thiol S-H stretching.
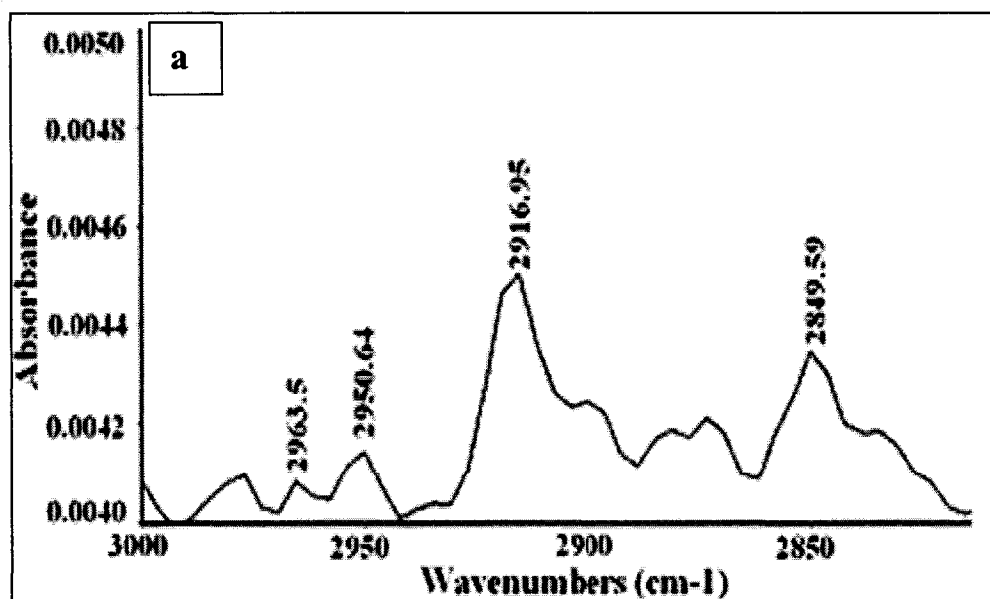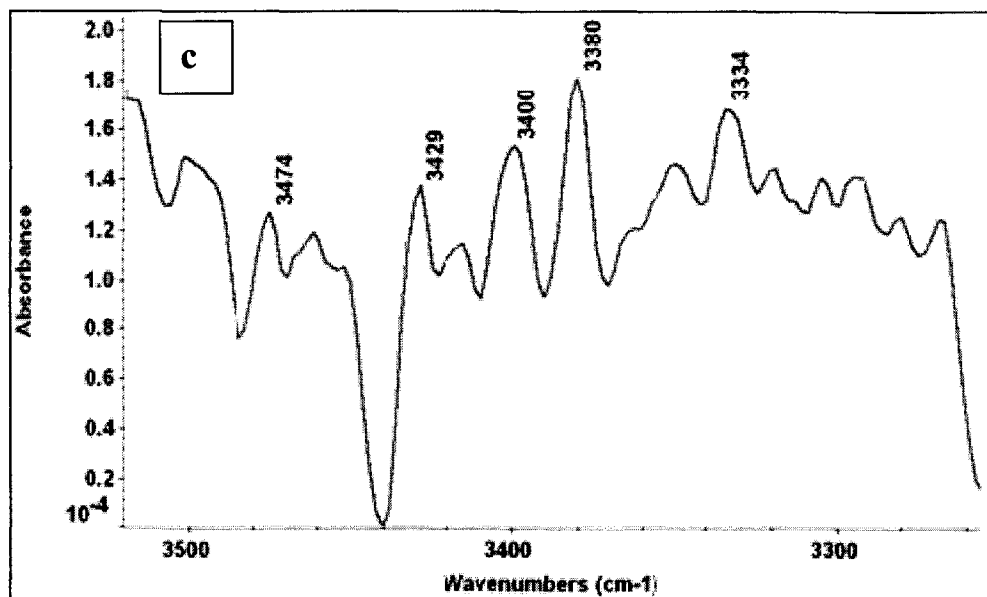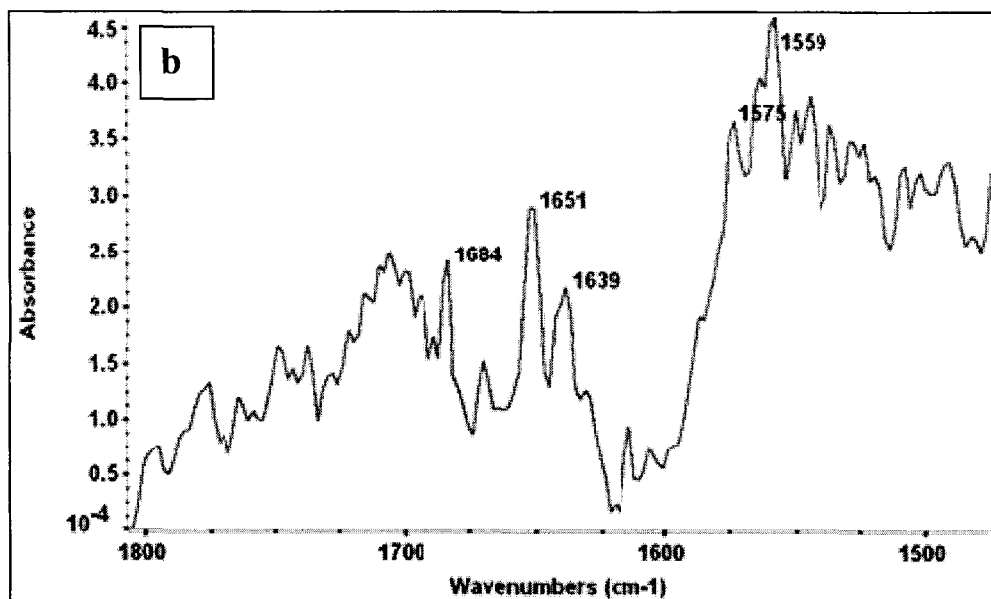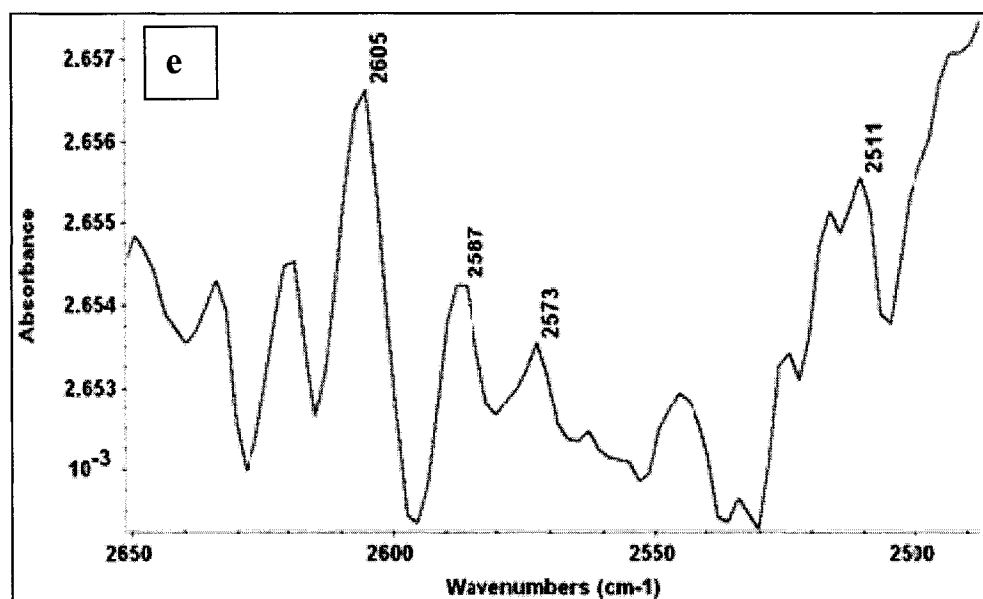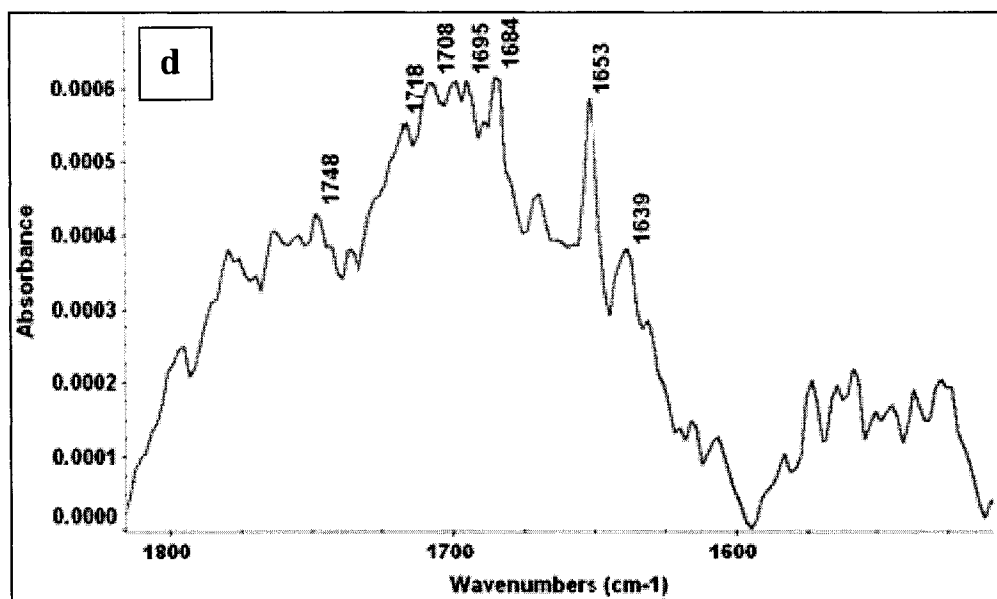
Figure 7.3 RAIR spectra of (a) ODT on ITO and ATR spectra of (b) APTES on ITO in the range 1500-1800 cm^{-1} (c) APTES on ITO in the range 3500-3300 cm^{-1} (d) MPA on ITO and (e) MPS on ITO

7.3 Hepatocyte Isolation and Seeding

Primary cultures are derived directly from excised, normal animal tissue and cultured either as an explant culture or as a single cell suspension. The preparation of primary cultures is labor intensive, and they can be maintained *in vitro* for only a limited period of time. During their relatively limited life span, primary cells usually retain many of the differentiated characteristics of the cell *in vivo*.

Hepatocytes were isolated from adult Sprague-Dawley rats, 6-8 weeks old weighing 250-300 g using the collagen perfusion technique.[244] The animals were maintained in a standard controlled environment and the isolation performed as dictated by the Public Health Service Policy Human Care and Use of Laboratory Animals administered by the Institutional Animal Care and Use Committee at the University of Louisiana at Monroe. The liver was initially perfused with Ca^{2+}-free Hank's buffer and dissociated with collagenase type II (1 mg/mL: Sigma) in Hank's buffer containing 5 mmol/L $CaCl_2$. The isolated hepatocytes were resuspended in Hank's buffer containing 1.2 mmol/L $CaCl_2$ and 0.6 mmol/L $MgSO_4$. The cells were then filtered through 90 μm nylon mesh (per-col gradient) and counted. Their viability was tested using tryphan blue exclusion test. A viability of 95-99% was achieved in most cases. The cells were then suspended in Williams' medium E (Invitrogen corporation) containing 2% L-glutamine, and 1% penicillin and streptomycin.

Cells in the density of 1 x 10^5 cells were seeded on each substrates with 250 μl of media and incubated at 37 °C (5% CO_2) for 4 h. After 4 h, remaining 750 μL media was added and the substrates incubated.

7.4 Cell Morphology

Figure 7.4 shows the morphology of the cells in the absence of L-Glutamine in the media after 24 h. It can be observed that few numbers of cells have attached on the surface with no cell clustering. Much cell debris is observed on the surface of the SAM-modified substrates indicating cell apoptosis. The initial attachment is attributed to the charge, in case of amino ($-NH_2$) group, and hydrophobic nature in case of methyl ($-CH_3$) and thiol ($-SH$) groups. The number of attached cells on ITO and ITO-APTES are more compared to other substrates because of the electrostatic interaction of negatively charged hepatocytes with the positively charged $-NH_2$ groups (pKa of RNH^{3+} is ~ 9) at physiological conditions (pH ~7.4) wherein the other groups are neutral.

Figure 7.5 shows the phase contrast images of hepatocytes on different SAM-modified ITO substrates and also on bare ITO and tissue culture plastic (TCP) in the presence of L-Glutamine in the media. Cells adhered to the surface showed round shapes with part of the cells transformed into polygonal shape after 24 h. It was observed that on ITO modified with $-NH_2$ and $-CH_3$ end groups, the majority of hepatocytes presented polygonal morphology similar to that observed on TCPs. Binuclei cells were observed in the majority of hepatocytes and the boundary between hepatocytes was perfectly clear and bright, illustrating the formation and participation of bile canaliculi. Their morphology changed from spherical to a monolayer flat polygon and was maintained till the end of the culture.
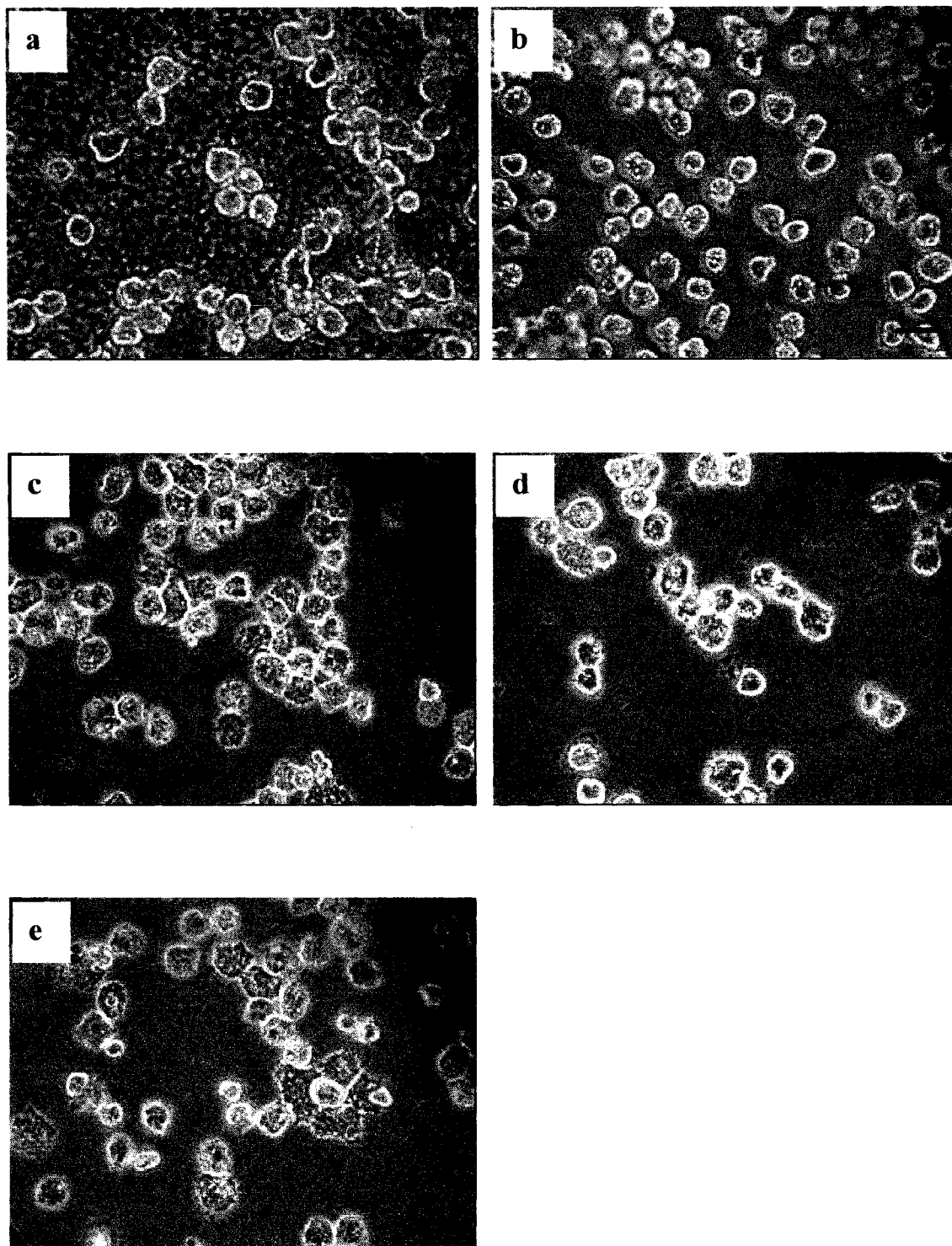
Figure 7.4 Morphology of rat hepatocytes after 24 h in the absence of L-Glutamine on (a) Control (TCP) (b) ITO (c) ITO-APTES (d) ITO-MPS and (e) ITO-ODT (Bar represents 40 μm).
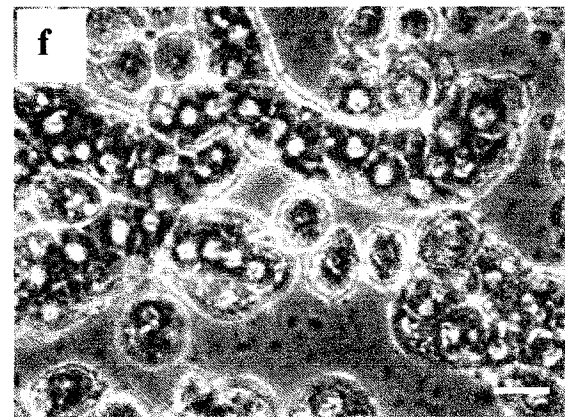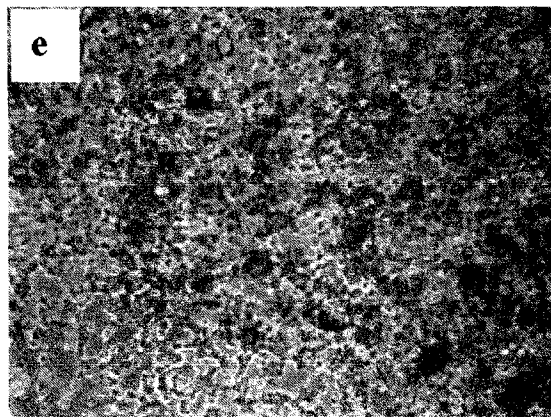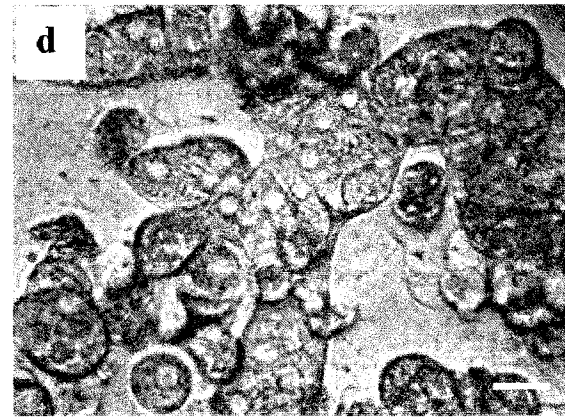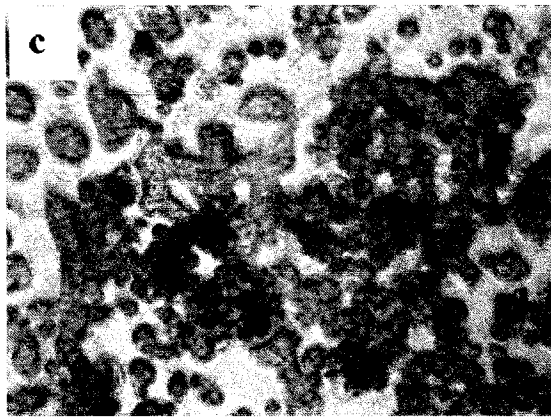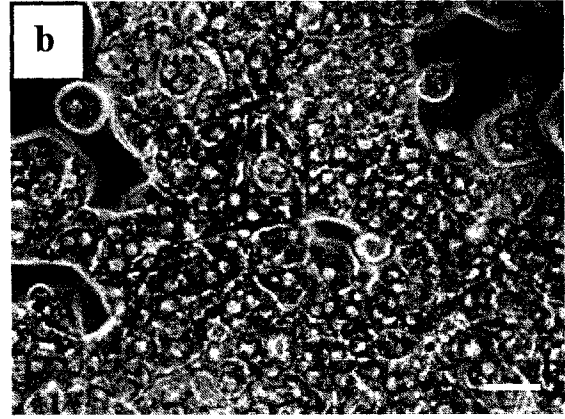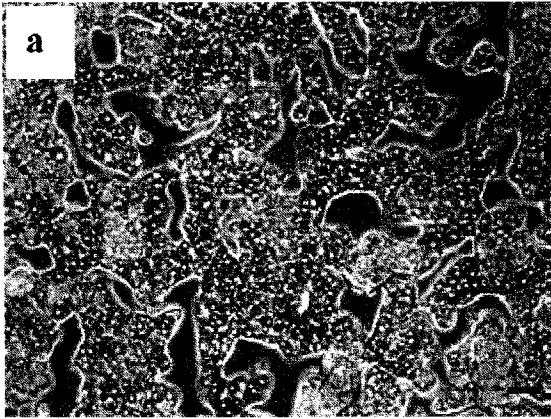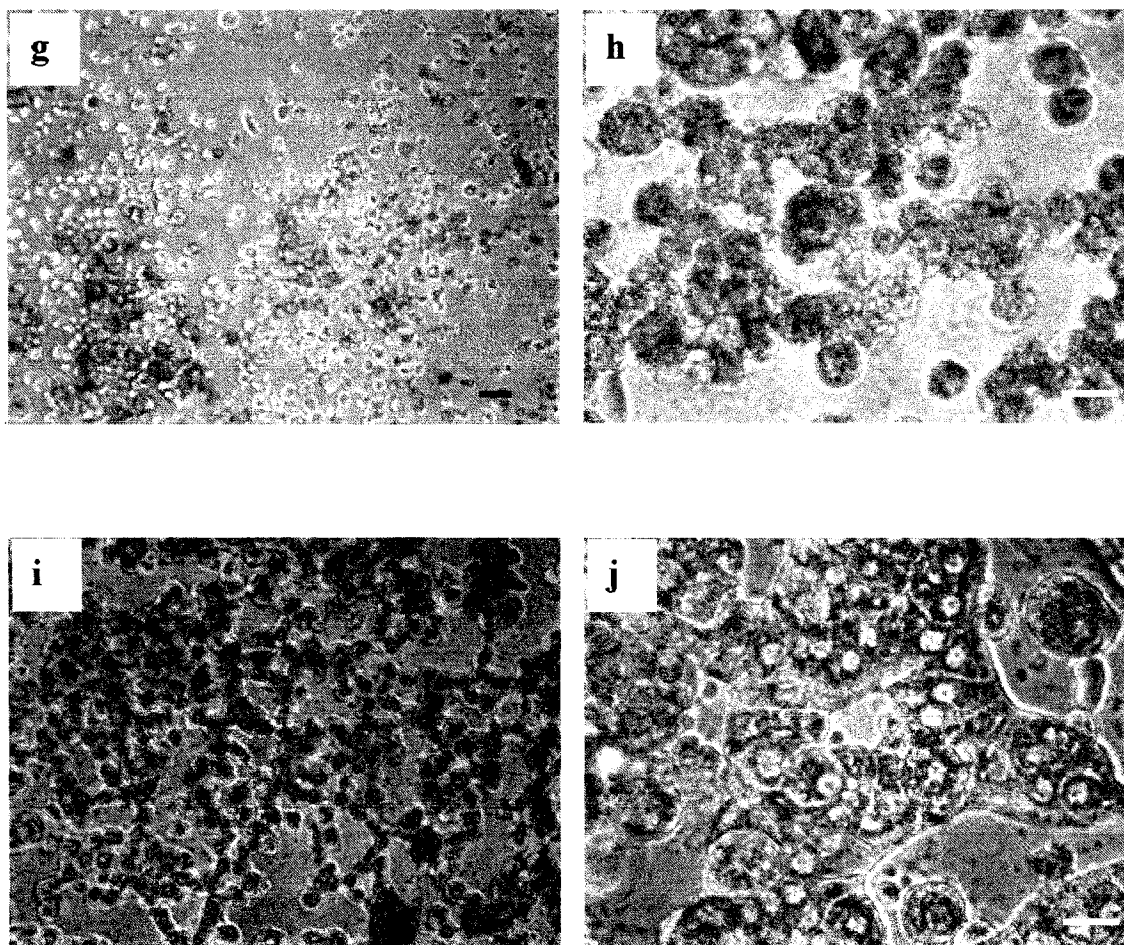
Figure 7.5 Morphology of rat hepatocytes after 24 h in the presesnce of L-Glutamine on (a,b) Control (TCP) (c,d) ITO (e,f) ITO-APTES (g,h) ITO-MPS and (i,j) ITO-ODT (Black bar represents 10 μm and white bar represesnts 40 μm).

7.5 Cell Viability

Figure 7.6 shows the LIVE/DEAD® response of hepatocytes cultured on different SAM-modified ITO substrates. The cells exhibited clustering with the presence of binucleate cells on all the SAM-modified ITO surfaces. The LIVE/DEAD® response of hepatocytes seeded on ITO-APTES substrates indicated a higher degree of viability with a lower number of dead cells. Cell attachment was uniform and clustering was observed. The LIVE/DEAD® response on ITO-MPS showed decreased hepatocyte viability on these substrates. This result is evident from the increased red fluorescence due to

ethidium dibromide activity. Cell clustering is observed on these substrates also. A limited number of viable cells were observed on ITO modified with ODT as seen in Figure 7.6. Random cell clustering was observed and there were a limited number of binucleate cells.
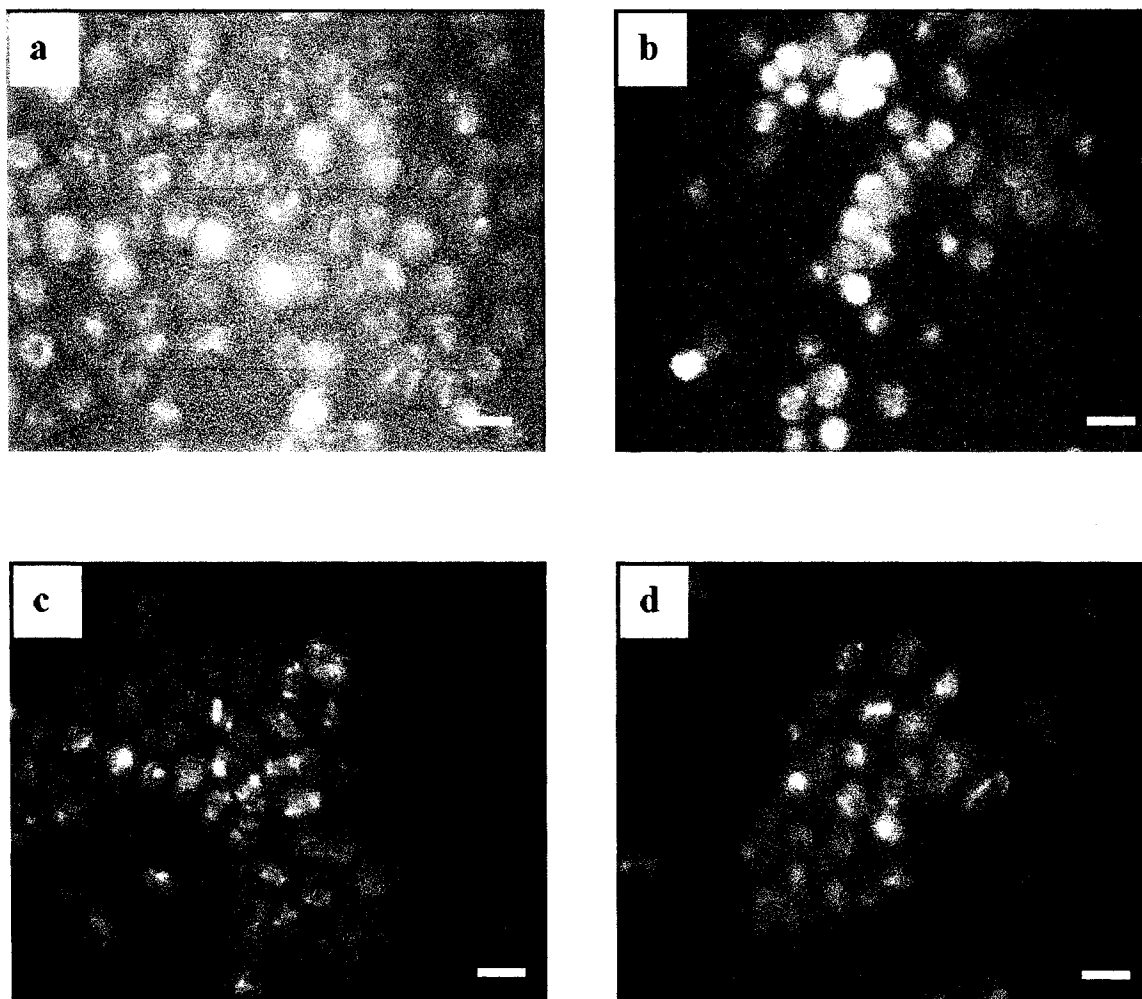
Figure 7.6 Cell viability of hepatocytes assessed using LIVE/DEAD® assay on (a) ITO (b) ITO-APTES (c) ITO-MPS and (d) ITO-ODT after 48 h (Bar represents 40 μm).

The LIVE/DEAD® assay qualitatively assessed hepatocyte viability on SAM-modified ITO substrates. Common hepatocyte characteristics like cell clustering and binucleate cells were observed. The increased cell density enabled the visualization of

live and dead cells at the same wavelengths. Cell viability was visibly higher on ITO and ITO modified with APTES when compared with ITO-ODT and ITO-MPS.

7.6 Cell Proliferation

Hepatocyte viability was quantitatively evaluated using the MTT assay. The principle of the MTT assay is the conversion of (3-(4,5-Dimethylthiazol-2-yl)-2,5-diphenyltetrazolium bromide) to form purple formazan in the presence of active mitochondrial reductase enzymes in viable cells. The amount of formazan produced is thus directly proportional to cell viability and can be measured spectrophotometrically using a spectrophotometer.

Hepatocytes were seeded with densities varying from 100,000-750,000 cells/ substrate. The cells were treated with the MTT reagent and incubated for four hours. The purple formazan crystals formed were dissolved using the MTT solvent and the absorbance was measured at 595 nm. MTT activity was measured after 24 and 48 h of seeding. The resultant absorbance was calculated and expressed as a function of time of culture. A standard curve was established measuring MTT activity as a function of cell density. Results were expressed as a mean of triplicate experiments ($\pm$ error).

A calibration curve of variation in absorbance as a function of cell density was first obtained. Figure 7.7 shows the plot of optical density versus hepatocyte density. The optical density increased with increase in cell density. The results were normalized using linear regression and a standard curve was obtained.
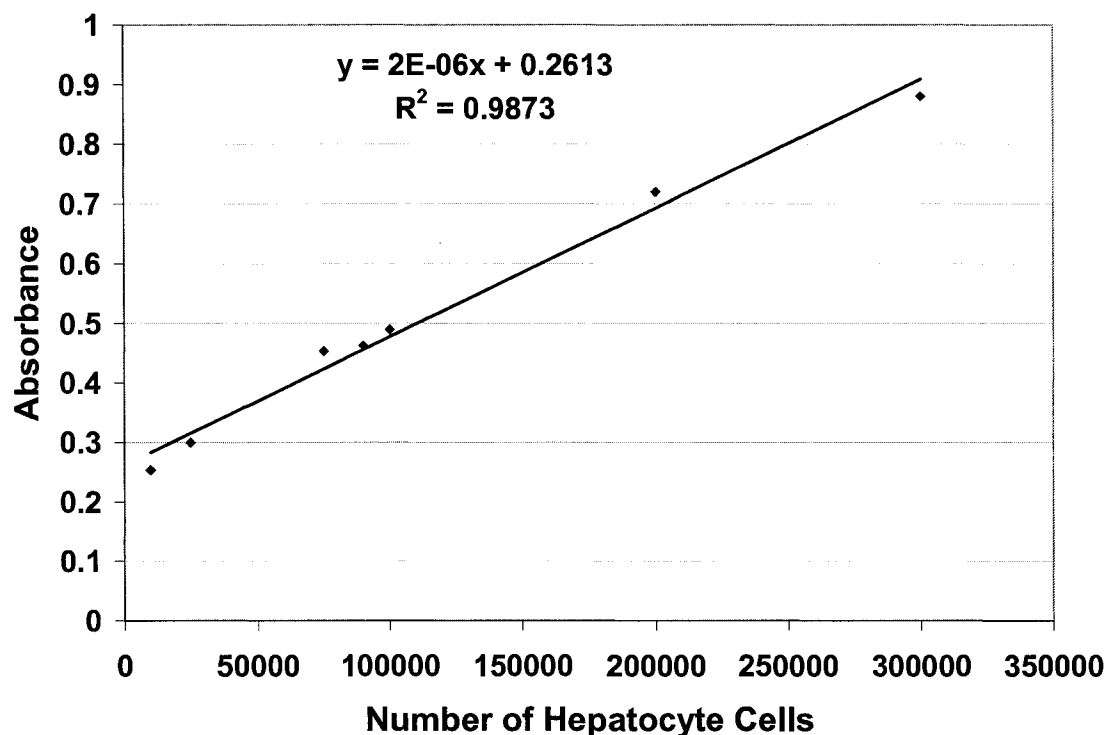
Figure 7.7 Variation of optical density as a function of hepatocyte density.

Hepatocyte viability was then evaluated by performing the MTT assay on cells seeded on different SAM-modified ITO substrates and control surfaces. Initially, a cell density of 100,000 cells/substrate was seeded on the substrates. The cells were maintained under normal humidified conditions for a period of 48 h and the viability was assessed after 24 and 48 h of culture. Figure 7.8 shows a plot of cell density on SAM-modified ITO substrates as a function of time in culture.

These cell densities were obtained by comparing the corresponding optical densities (mean of 3 values) with the standard curve (Figure 7.7). After 24 h higher cell density was observed on ITO and ITO-APTES substrates compared to ITO-MPS and ITO-ODT. After 48 h, the cell density increased rapidly with increase in culture time with higher cell densities observed on ITO-APTES. Since the initial cell density was 100,000

and after 24 and 48 h we observed cell densities > 100,000 we concluded that the cells proliferated on these substrates. This finding was in contradiction to the hypothesis that isolated hepatocytes do not proliferate. In general, the common trend observed in these experiments was that higher cell viability was seen on SAM-modified ITO compared to bare ITO surface.
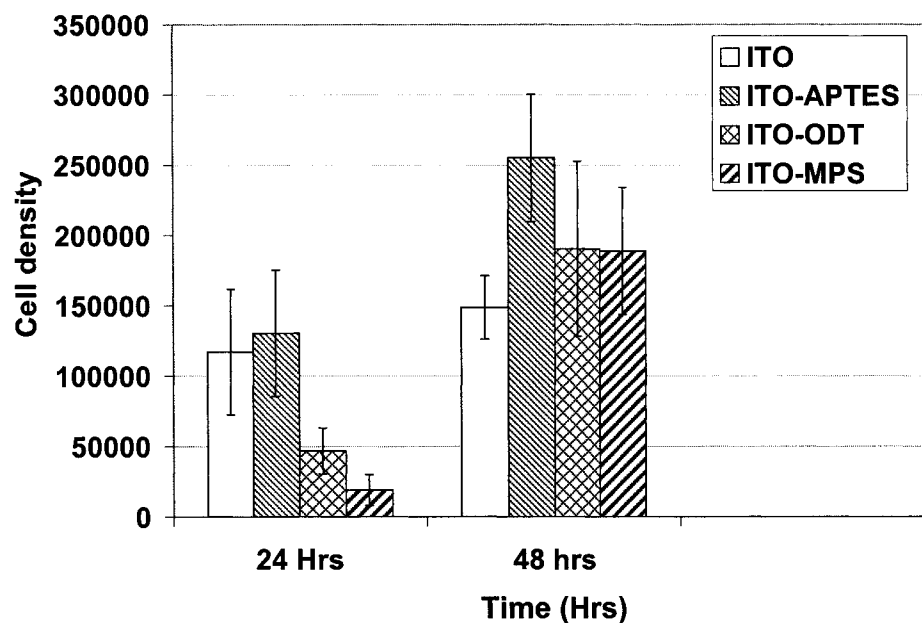
Figure 7.8 Hepatocyte cell proliferation on different SAM-modified ITO surfaces at 24 and 48 h. Data represent the mean±S.D, n=3.

7.7 Immunohistochemical Detection of Collagen

Type I collagen is a predominant component of bone and skin and is present as structural scaffolds in organs like the liver and tissue. Functional cells secrete Type I collagen in their cytoplasm, which can be immunohistochemically detected by employing suitable antibodies raised against it. The production of Type I collagen serves as a marker of phenotypic maintanence of hepatocytes cultured on SAM-modified surfaces.

In our studies, hepatocyte functionality and phenotypic maintanence were qualitatively evaluated by using immunohistochemical techniques. The cells were incubated using a suitable primary antibody raised against Type I collagen. Immunolocalization of the primary antibody was performed using the peroxidase-antiperoxidase technique (VECTASTAIN Elite ABC kit mouse, Vector Laboratories, Burlingame, CA).

Hepatocytes at densities of 2000 cells/substrate were seeded on ITO and SAM-modifed ITO substrates. The lower cell density was chosen to permit proper visualization of the cellular response. The presence of Type I collagen in the cytoplasm is indicated by the formation of a brown color. The intensity of the brown reaction is directly proportional to the amount of collagen produced by the cell. Minimal cell attachment was observed on ITO substrates (Figure 7.9). Visualization of IHC response showed the formation of a brown color. Cell aggregation was minimal.

The IHC response of hepatocytes cultured on ITO-APTES is shown in Figure 7.9 (b). Microscopic observations showed an increased cell attachment on ITO-APTES. Visualization of cell response using DAB substrates showed the formation of an intense brown reaction. The cells also showed signs of clustering. Figure 7.9 (c) shows the visualization of Type I collagen produced by hepatocytes cultured on ITO-MPS surfaces. A light brown reaction is observed. Cellular damage was observed on these surfaces. Figure 7.9 (d) shows Type I collagen response of hepatocytes cultured on ITO-ODT. Cellular attachment was observed to be minimal on these substrates and cellular disintegration was observed. The brown reaction observed was less intense comparatively.
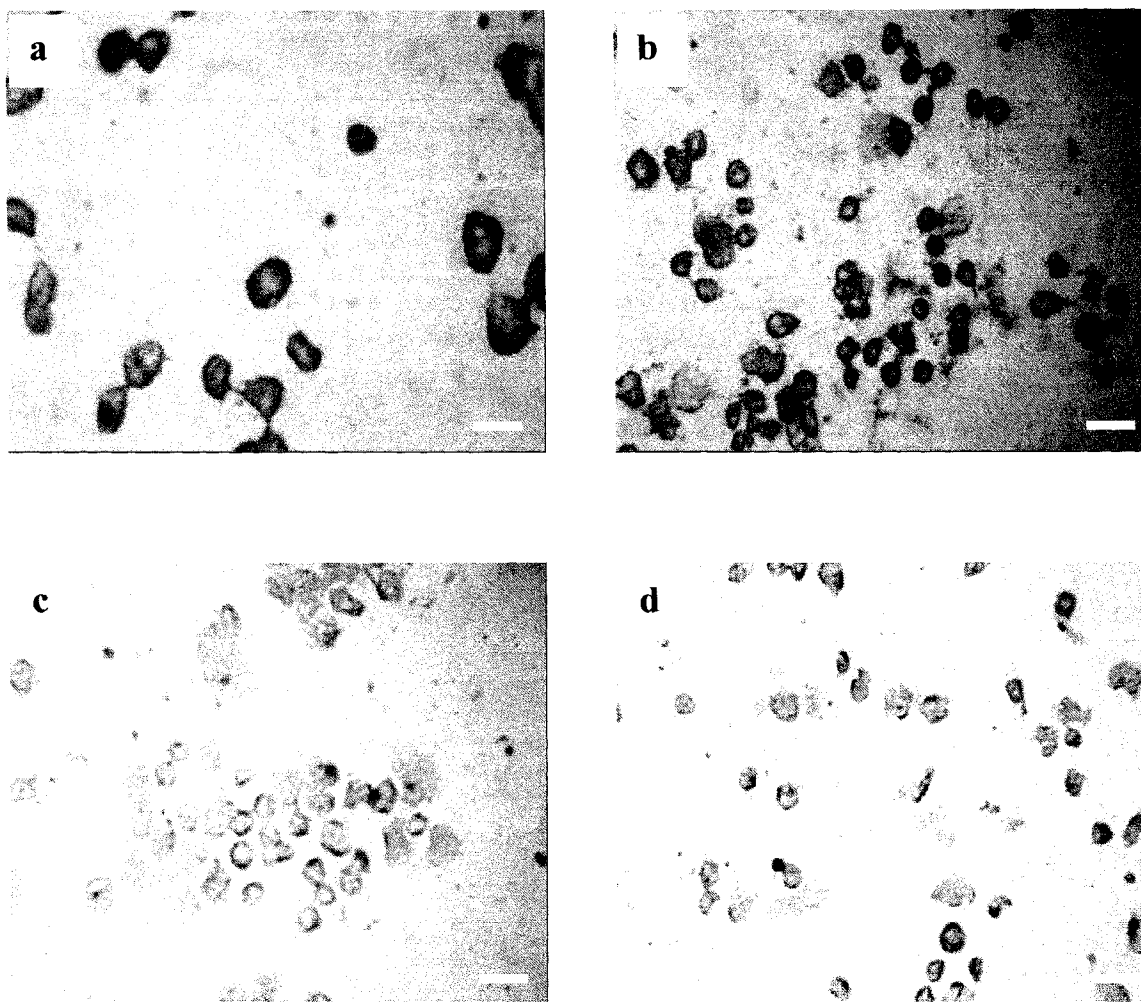
Figure 7.9 Immunohistochemical detection of Type I collagen observed on (a) ITO (b) ITO-APTES (c) ITO-MPS and (c) ITO-ODT (Bar represents 40 μm).

Type I collagen is a marker of cell phenotype and functionality. Functional hepatocytes produce Type I collagen in their cytoplasm. IHC techniques were used to measure the collagen content in the cellular cytoplasm. The collagen produced was visualized as a brown reaction. The intensity of the brown color produced in the cytoplasm of hepatocytes seeded on ITO-APTES was higher when compared to the other substrates. Cellular disintegration was observed on ITO-ODT and ITO-MPS. The most important observation made in these studies was the production of collagen by

hepatocytes on all the substrates which served as an indicator of maintanence of the hepatocyte phenotype.

7.8 Lactate Dehydrogenase Leakage

The substrates influence on cellular cytotoxicity is assessed by measuring the LDH release by dead or damaged cells. LDH is a stable cytoplasmic enzyme present in the cytoplasm of viable cells. When cell death occurs or when the cytoplasm is damaged , there is LDH leakage into the cell culture media. Thus a measure of LDH release is an indicator of cellular cytotoxicity. Although the activity of LDH can be measured utilizing pyruvate or lactate as a substrate, the LDH-L Reagent used in our studies uses lactate and is based on the recommendation of the IFCC. LDH catalyses the oxidation of lactate to pyruvate reducing NAD to NADH. The activity of LDH is determined by observing the absorbance at 340 nm.

Hepatocytes at densities of 100,000 cells/substrate were seeded on ITO and SAM-modifed ITO substrates. The substrates were maintained at 95% O_2 and 5% CO_2 under normal humidified conditions. The media was removed after specific intervals of time over a 48 h period and the LDH reagent was added to it. The LDH activity was measured using the spectrophotometer. LDH release (U/L) was measured as a function of duration in culture. The results obtained were expressed as mean of three independent trials ($\pm$ standard deviation). Control cultures were established on tissue culture dishes and bare ITO surfaces. From the absorbance measurements, the LDH concentration was calculated using the Equation 3.5 given in Chapter 3.

Figure 7.10 shows LDH activity plots of hepatocytes cultured on SAM-modified surfaces versus time in culture. The general trend observed was the decrease in LDH

activity with increase in time in culture. Initial LDH activity from hepatocytes was observed to be high on bare ITO (93.05 U/L) and control (150.7 U/L) when compared to hepatocytes cultured on ITO-APTES, ITO-MPS and ITO-ODT. Among the SAM-modified surfaces, LDH release was higher on ITO-ODT (90.1 U/L) followed by ITO-MPS and minimal on ITO-APTES.
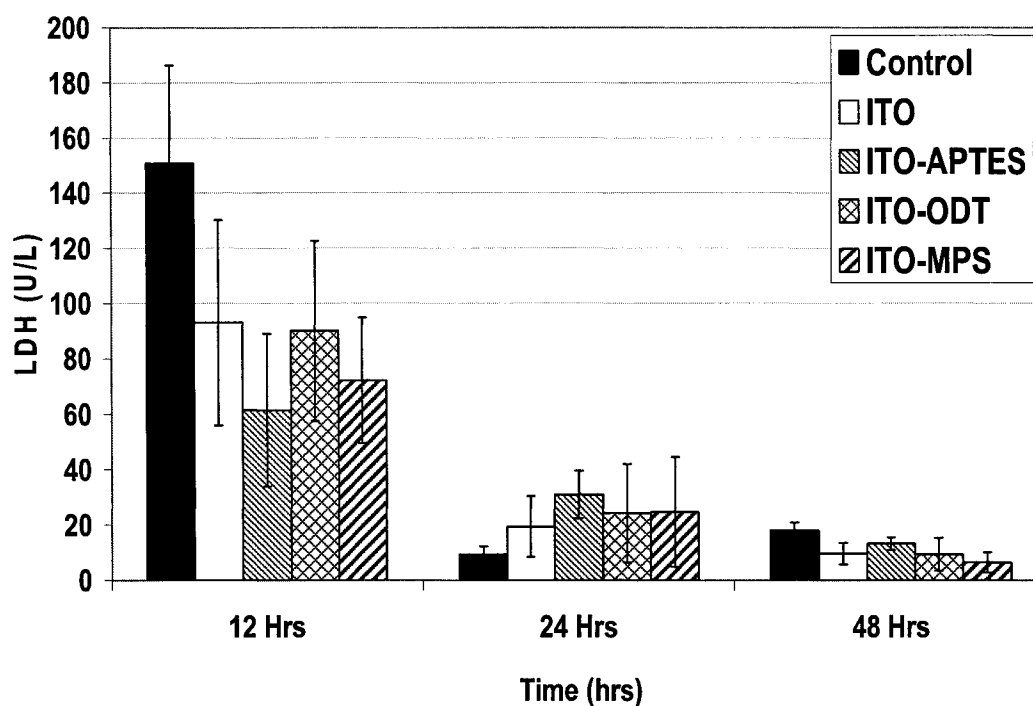
Figure 7.10 LDH release by hepatocytes from different SAM-modified substrates following 12, 24 and 48 h after seeding. Data represent the mean±S.D, n=3.

LDH activity showed a rapid decline following 24 h of culture on all the substrates. ITO showed a lower LDH release (19.366 U/L) compared to the other SAM-modified surfaces. LDH release from hepatocytes cultured on SAM-modified surfaces showed similar trends, with a large decrease in LDH activity with increase in culture time. After 48 h in culture, hepatocyte cultures showed further decrease in LDH activity

on all the surfaces except on the control cultures which showed a slight increase in LDH release.

An increased concentration of LDH in the cell culture supernatant, released by cell damage or death would increase its activity upon reaction with the LDH reagent. The above study of LDH activity (Figure 7.10) indicated a decrease in LDH activity with increase in time in culture. LDH activity was higher initially due to cytotoxicity caused by placing cells in a foreign environment. Subsequent adaptation to the new environment resulted in decreased cytotoxicity and LDH activity.

7.9 Total Protein Synthesis

The total concentration of accumulated protein in culture media was determined using Bradford assay. Viable cells are metabolically active and tend to discharge protein into the media. Maintanence of protein production is a key indicator of hepatocyte health and functionality. The serum free cell culture media was replaced after 12, 24 and 48 h of culture, stored at 4 $^{\circ}$C and analyzed.

The amount of protein released by hepatocytes cultured on SAM-modified surfaces was determined by the addition of the protein assay to the culture media and measuring the absorbance. A standard curve for the protein samples was established using bovine serum albiumin (BSA) as a standard. Protein concentrations were reported in micrograms.

Figure 7.11 shows the standard curve obtained by measuring the absorbance for varying concentrations of protein in solution. The results were normalized and linearly fitted. The absorbance increases with increase in protein concentration. The results are expressed as mean of three separate experimental trials (±S.D)(n=3).
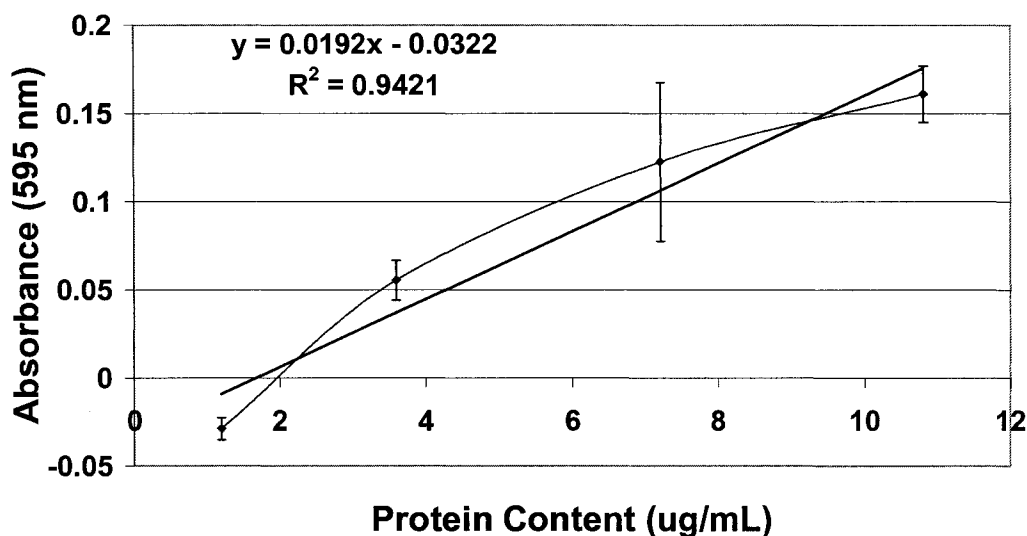
Figure 7.11 Typical standard curve for bovine serum albumin. O.D.595 corrected for blank. 1.25-25 µg/mL x 0.8 mL = 1-20 µg protein.

Figure 7.12 shows the total protein produced by hepatocytes cultured on ITO and SAM-modified ITO surfaces measured at intervals of 12, 24 and 48 h. The concentrations were determined by relating the measured absorbance to the corresponding protein concentration from the standard curve (Figure 7.11). The general trend observed is increased protein production by hepatocytes cultured on all the substrates with increase in time in culture. After 12 h, protein production by hepatocytes on SAM-modified ITO surfaces and bare ITO control was ~ 3 µg (n=3) with an increase in protein production following 24 h in culture. Hepatocytes cultured on ITO-APTES and ITO-ODT (~ 8 µg) produced identical amounts of protein. After 48 h in culture, ITO-APTES showed an increased protein production (18.75 µg) compared to ITO-ODT (13.4 µg) and ITO-MPS (11.42 µg).
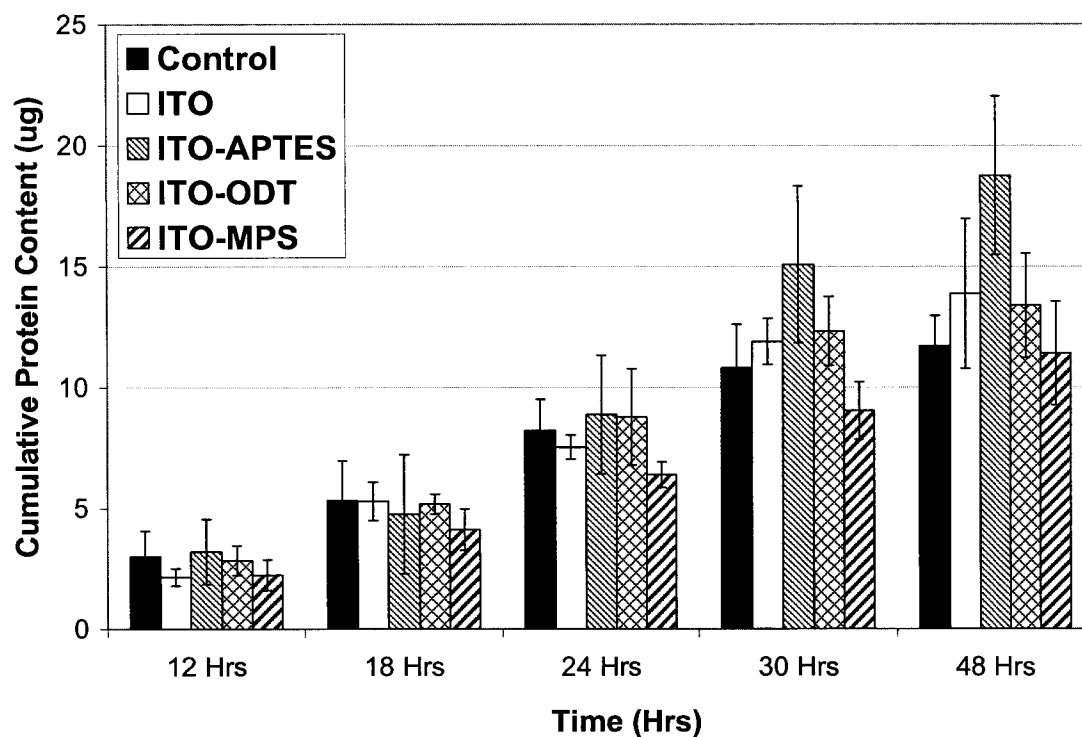
Figure 7.12 Total protein synthesized by hepatocytes on SAM-modified ITO surfaces measured at intervals of 12, 24 and 48 h. Data represent the mean±S.D, n=3.

The total protein production by hepatocytes seeded on SAM-modified surfaces provides a quantitative indication of cell viability and functionality since functional cells would only be able to carry out normal metabolic functions. The establishment of a standard curve (Figure 7.11) and determining the absorbance for various protein concentration serves as a standard for comparing measured absorbance to determine the protein content produed by cultured hepatocytes. Protein production is characteristic of normal hepatocyte functionality and the results obtained from the total protein measurements provides a validation of the same.

7.10 Discussions

Hepatocytes were isolated from adult male Sprague-Dawley rats (3-5 months old, 150 g) using the collagen perfusion technique. High viability (90-95%) of isolated hepatocytes is obtained from these methods. Hepatocyte viability has been studied on various substrates like ECM components, hydrogels and PEMs but the culture of hepatocytes on SAM-modified surfaces have not been investigated before.

In most cases, the presence of serum in media causes protein adsorption onto SAM-modified surfaces regulating cellular adhesion.[20,30,128] In our studies, we have used Williams E medium (Gibco® cell culture systems, Carlsbad, CA), a serum free medium supporting long-term culture of isolated liver cells. Williams E medium contains additional amino acids including asparagine, cysteine, proline and glutamate which appears to be an essential component for DNA synthesis in rat hepatocytes.[245] Isolated rat hepatocytes have been observed to express cell adhesion molecules like cadherins and integrins, which mediate cell-cell and cell-matrix interactions respectively. Molecular expression of cadherins and integrins increased upon culture on poly-N-p-vinylbenzyl-D-lactonamide (PVLA) surfaces in the presence of serum free media.[246]

In our case we assume that the charge and the hydrophobic nature associated with the SAM had an influence on the initial hepatocyte adhesion. Hepatocytes, like many other cell types possess a negative surface charge. At a neutral pH, the $-NH_2$ end group of APTES SAM is positively charged. The presence of opposite charges on the hepatocytes and the SAM surface leads to the formation of strong electrostatic forces of attraction, which along with the expression of adhesion molecules causes increased cellular attachment on ITO-APTES. ITO-ODT and ITO-MPS remain neutrally charged at

pH 7; hence, there is an absence of electrostatic forces between the SAMs and the cells and therefore exhibit comparatively weaker adhesion. In case of ITO-ODT and ITO-MPS initial attachment of hepatocytes is attributed to the tethering of the hydrophobic groups (–CH$_3$ and –SH) to the hydrophobic groups present on the hepatocyte surface with the release of several water molecules.

A study of cellular morphology on SAM-modified surfaces showed initial cellular attachment on ITO-APTES followed by cellular clustering. Cells showed limited signs of stress, and there was a limited decrease in cell density. Hepatocyte cultures on ITO-ODT and ITO-MPS showed initial cell clustering but exhibited a rapid decrease in cell density with increase in culture period. There was good attachment of hepatocytes on ITO substrates because of the initial negative charge present on the surface.

Phase contrast images of hepatocytes on ITO and SAM-modified ITO showed signs of proliferation after 24 and 48 h. The proliferation was quantitatively validated by using MTT-based assay. The MTT assay measured the formazan activity produced by the conversion of MTT by viable cells. Cell proliferation was observed on all these substrates. This finding is in contradiction to the hypothesis that isolated hepatocytes do not proliferate in vitro.[247,248] However, Gu et al.[225] have been able to create a hepatocyte/ colloid interface upon which cultured porcine hepatocytes showed increased cell number following 12 to 24 h in culture.

In our case, the proliferation of hepatocytes is attributed to the presence of L-Glutamine in the media. It can be seen from Figure 7.4 that in the absence of L-Glutamine there is no proliferation. It is reported that L-Glutamine causes proliferation in many cells including intestinal epithelial cell lines,[249] porcine jejunal cell line (IPEC-

J2),[250] human histiocytic lymphoma cells,[251] Caco-2 cell[252] etc due to production of extracellular signal-regulated kinases (ERKs). *In vivo* studies done on rats with ligated common bile duct (CBD) suggested that incorporation of glutamine attenuated or abolished hepatocyte apoptosis.[253] Also glutamine incorporated in malnourished rats promoted growth of the remnant liver, maintained cellular proliferation and hepatic morphology.[254] The exact mechanism of *in vitro* proliferation of hepatocytes due to glutamine is not understood and needs to be investigated.

Hepatocyte functionality and phenotypic preservation was studied by measuring the ability of hepatocytes to produce Type I collagen. Functional cells retain the ability to produce functional proteins like Type I collagen. The presence of Type I collagen was detected using primary antibodies raised specifically against it. Antigen-antibody conjugates were visualized using suitable markers. Hepatocytes cultured on all the surfaces produced the brown color response, indicative of their functionality. Cell spreading was observed on some of the surfaces. Cell damage was seen, which could have occurred during the process of fixing and staining.

Initial responses indicated increased cytotoxicity with increase in culture period on all the substrates. LDH release is higher because the hepatocytes take a longer time to adapt themselves to the substrates. After 24 and 48 h, the LDH release is minimal, which indicates much less cytotoxic damage to the cells. Protein production by functional hepatocytes is a key indicator of cellular viability and health. They provide valuable information about the effects of surface properties on the cellular response and vice-versa. The total protein content in solution released by cultured hepatocytes was

measured using the method of Bradford. This method was independent of interference from serum proteins since the serum free media was employed for cell culture.

In summary, these results provide experimental validation that cellular response is influenced by a number of properties like nature of the substrate and culture conditions. Since there is no previously established work studying hepatocyte culture on SAM-modified surfaces, further studies to study specific protein production, long term viability and biocompatibility could be performed to understand the cell-substrate interactions better. These results are extremely useful in the development of biomedical devices like CCPs and bioreactors, which permit researchers to understand cell-biomaterial interactions better.

CHAPTER 8

THREE-DIMENSIONAL CELL-BASED

BIOREACTORS

8.1 Cell-Based Bioreactors

In order to achieve physiologically meaningful functions in tissue engineering, it is necessary to culture cells at higher density and larger numbers.[255,256] This objective can not be fully realized using 2D surfaces presented in previous chapters. Also continuous nutrition and oxygen supply and waste removal through the culture medium have to be ensured for proper growth.[257] In conventional cell culture formats such as dishes and macroscale bioreactors, it is quite difficult to realize the delivery of a sufficient amount of those substances throughout the cultured tissue. This is due to the difficulty in designing and fabricating large complex bioreactors in which the cells are fed by a spatially homogeneous distribution of the fluid flow.[258] Microsystems technology enables us to realize microfluidic channels suitable for such oxygen and nutrition supply.[259,260] In this regards, new approaches to microfabricated bioreactors are more and more investigated.[261] Two-and/or three-dimensional structures have been fabricated to cultivate various types of mammalian cells with various materials, such as silicon, silicone elastomer, and biocompatible and biodegradable polymers.[262-266] In particular, silicon-

116

and silicone elastomer-based bioreactors have been developed for liver cell cultures in perfusion circuits.[237,267]

Cell-based bioreactors have also been used as biosensors to monitor physiological changes induced by exposure to toxicants, pathogens, or other agents.[268-270] Recent advancement in cell culture methods and microfabrication technologies have contributed to the development of cell-based biosensors for the functional characterization and detection of drugs, pathogens, toxicants, odorants, and other chemicals. Electrically excitable cells such as neurons and cardiomyocytes are particularly useful in this regard as the activity of the cells can be monitored using microelectrodes.[271] Many other non-excitable cells such as hepatocytes[237,235] and fibroblasts[272] have also been used to assess and predict the effect of toxicants.

In this research, we have tried to design and develop a SAM-based 3D system based on microfluidic channels for *in vitro* culture of mammalian cells. HDFs were used as the model cells. These devices find helpful in assessing different cell functions and can also be used for toxicological and pharmacological testing of chemicals and pharmaceuticals. Our goal is to develop an *in vitro* model that can inexpensively and realistically test the response of humans and animals to various chemicals. The design of the system is based on a physiologically based pharmacokinetic (PBPK) model. A PBPK model is a mathematical representation of the body as interconnected organ compartments.[273-275] The requirements of the PBPK model are: (1) The ratio of the chamber sizes and the liquid residence times in each compartment should be physiologically realistic,[275] (2) Each chamber should have a minimum of 10^4 cells to facilitate analysis of chemicals,[275] (3) The hydrodynamic shear stress on the cells should

be within physiological values ($<$ 2 dyn/cm^2),[237] (4) The liquid-to-cell ratio should be close to the physiological value (1:2).[275]

8.2 Simulation of Microfluidic Channels in the Bioreactor Using CoventorWare™

A single chamber/device containing microfluidic channels was simulated using CoventorWare™ software. Residence time of 25 sec, used for hepatocytes, and shear stress were the two parameters that were considered for the simulation:

$$\text{Re}quired\ simulation\ time = 25\sec, \tag{8.1}$$

$$Hydrodynamic\ stress = (2-14)dyns/cm^2 = (2-14)x10^{-7}MPa, \tag{8.2}$$

$$\text{Re}sidence\ time = \frac{Volume\ of\ the\ reactor\ (channels)}{Flow\ rate}, \tag{8.3}$$

$$25 = \frac{V}{Q}\sec \tag{8.4}$$

The steps involved in the simulation are as follows:

8.2.1 Design of Process File

Silicon was chosen as the substrate for the bioreactor. Etch depth based on shear stress, after repeated simulations, was fixed at 100 μm. The residence time and stress are calculated for the flow of water. This process file is for a etch depth of 20 μm (Figure 8.1). The next step was the design of the mask.

Figure 8.1 Design file of CoventorWare™ software containing parameters for material, etch depth, and flow in the bioreactor.

8.2.2 Design of Mask

The mask for patterning microfluidic channels with inlet and outlet ports was designed in the software itself (Figure 8.2). The dimensions of the reactor are 1.25 cm x 2 cm. The reactor has 120 channels with 50 μm width and 100 μm depths. The flow rate was calculated using the volume of the reactor and the fixed residence time of 25 sec. The mask was designed based on iterative simulations. After the end of the simulation, the mask was redrawn using L-Edit software. This mask was then generated using the pattern generator on a chrome mask.
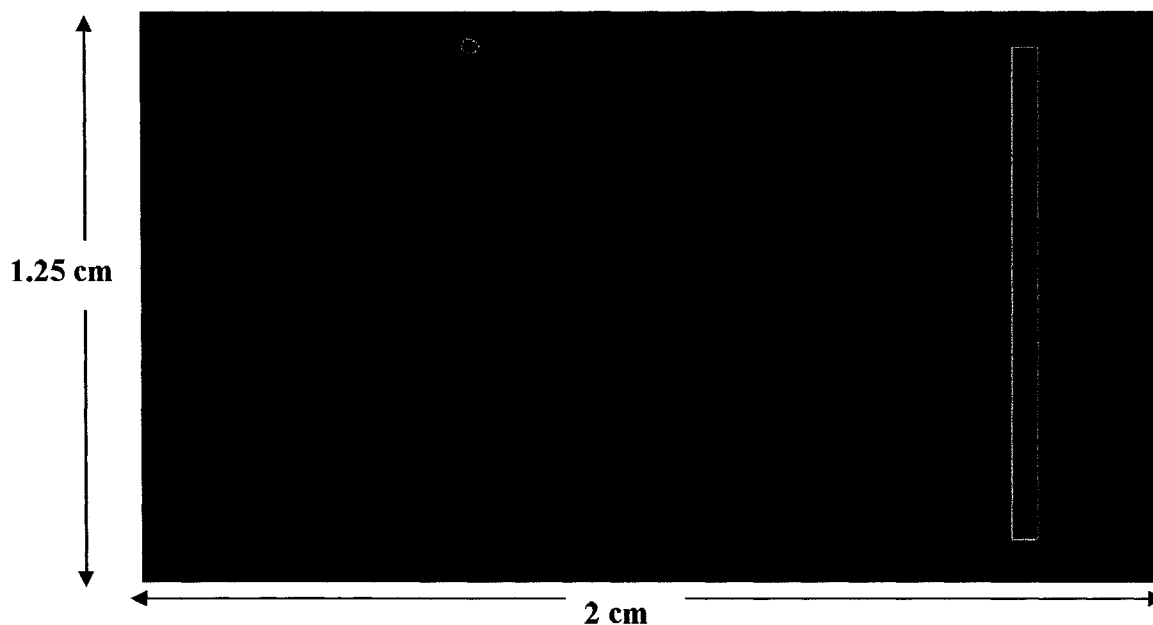
Figure 8.2 Design of the mask for a bioreactor containing channels with inlet and outlet ports (not to scale)

The dimensions of the mask are as follows:

Length of the channels = 10000 μm,

Width of the channels = 50 μm,

Depth of the channels = 100 μm,

Number of channels = 120

Volume of the reactor $= 10000 \times 50 \times 100 \times 120 = 60 \times 10^8 \, (\mu m)^3 = 6 \, \mu L$ (8.5)

Using Equation 8.4, Volumetric flow rate $Q = 24 \times 10^7 \, (\mu m)^3 \, sec^{-1} = 14.4 \, \mu L/min$.

The next step after mask design was to create a mesh model for the reactor where the stress analysis can be done.

8.2.3 Mesh Model

Figure 8.3 shows the mesh model (Manhattan Bricks. X=50. Y=50. Z=5) generated from the mask. After the mesh was created, it was then analysed for fluid flow.
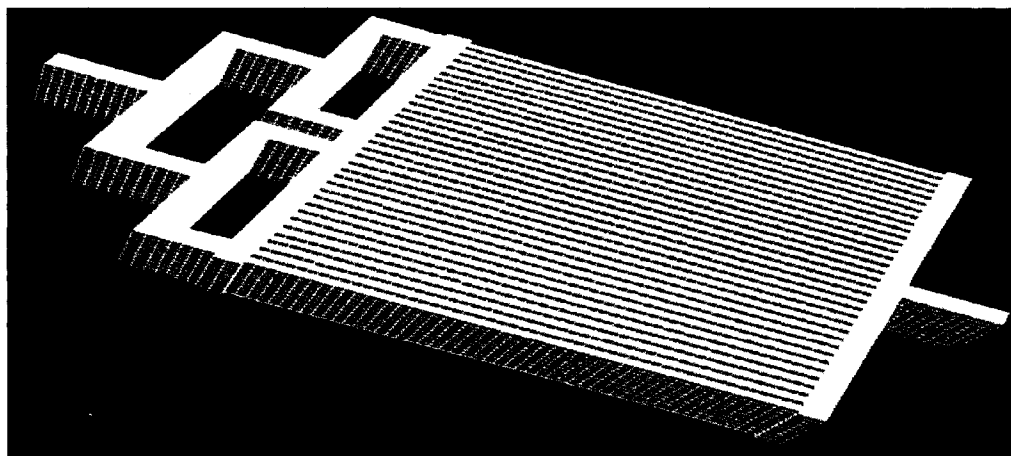
Figure 8.3 Mesh model generated from the mask (not to scale) for the bioreactor.

8.2.4 Analyzer

All the surfaces are defined as wall, except the input and output ports. The density model used was incompressible model with finite volume discretization and steady state time dependence. The flow rate used for the analysis was calculated using the volume of the reactor and the fixed residence time as presented before. Figure 8.4 shows the pressure drop of water at different points on the surface of the reactor. Within the

channel, a pressure drop of ~10^{-6} MPa is achieved, which is close to the hydrodynamic stress required.
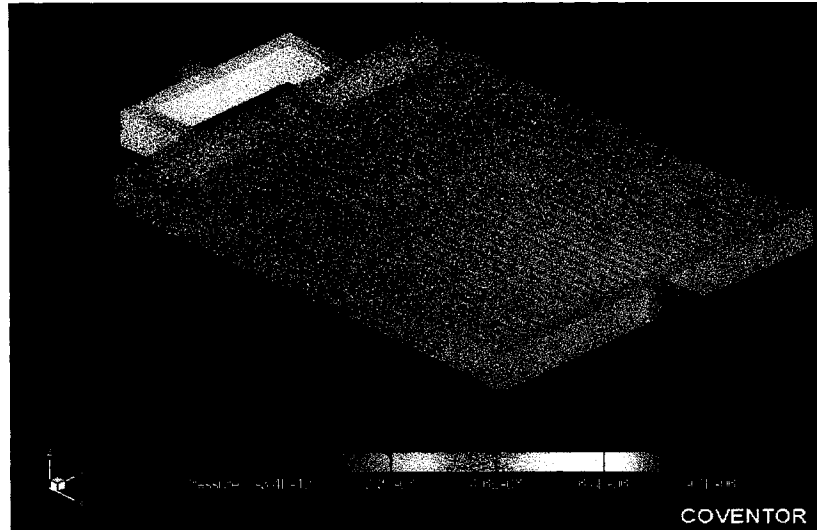
Figure 8.4 Analyzer showing different pressure drops on the surface of the microchannels of the bioreactor.

Based on these modeling results, the next step was to fabricate these reactors using photolithography.

8.3 Fabrication of the Proposed Bioreactor
Using Photolithography

The mask was designed in L-Edit and reporduced on a chrome mask using a mask generator. The fabrication steps are illustrated in Figure 8.5 and are as follows:

(1) Photoresist AZ9260 is spin coated at: 500 rpm for 10 sec and 900 rpm for 20 sec and the wafer is allowed to sit for five minutes

(2) The wafer is softbaked at 110 °C for five minutes and dried in vacuum oven for 10 sec.

(3) A second layer of AZ9260 is spun at: 500 rpm for 10 sec and 900 rpm for 20 sec

and the wafer is allowed to sit for five minutes.

(4) The wafer is softbaked at 110 °C for 5 min, and dried in vacuum oven for 10 sec.

(5) Exposed to UV for 175 sec.

(6) Developed in AZ400K (1:4 ratio with water) for 1-4 min with proper agitation.

Control over developing time is important for small feature size devices.

(7) The wafer is then hard baked for 30-60 min at 160 °C. This step guarantees that

the photoresist is free of bubbles during the dry etching process.
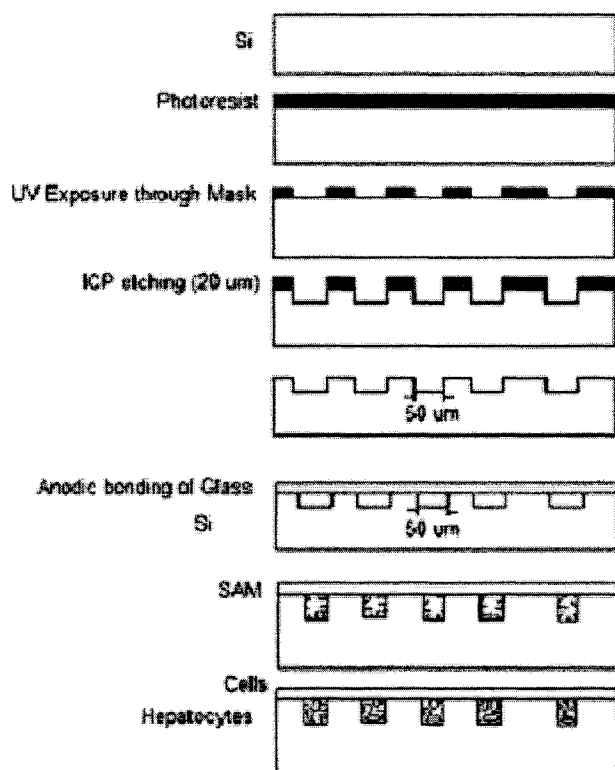
Figure 8.5 Fabrication and process steps involved in the construction of the bioreactor.

The bioreactor fabrication involves three chrome photomasks for pattern transfer:

microchannels, inlets and outlets, and for go-through vias. A front side alignment and a

backside alignment were performed with the mask aligner tool. Two etching steps were performed using Inductively Coupled Plasma (ICP) etching. The front side alignment assured that the channels are well aligned with the inlets and outlets, and the backside alignment method assured that the go-through vias, which lead the fluids in and out, were etched completely (go-through) to make the connections with the inlets and outlets of the microreactor. The frontside and backside misalignment is within 1~2 microns. The reactor is then immersed in a Nanostrip solution for 15 min at 90 °C to remove all the organic contaminants and provide uniform hydroxyl bonds on the walls of the reactor. The open channels are then enclosed by anodic bonding of pyrex glass. Figure 8.6 shows the optical image of the reactor and the SEM image of the cross section of the channels.
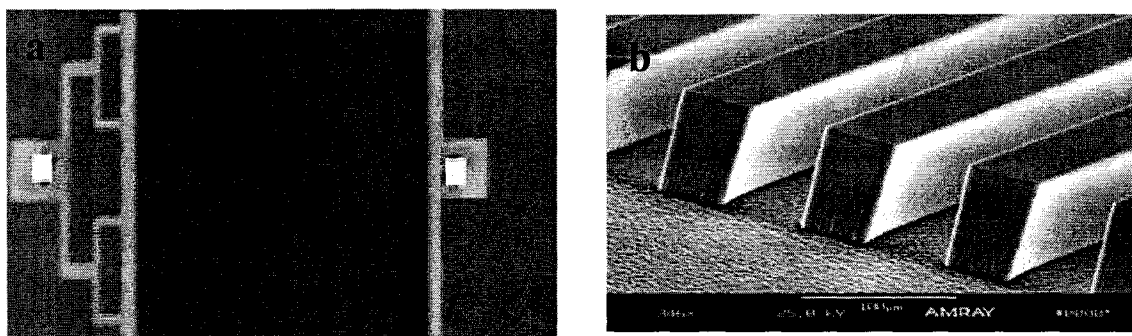
Figure 8.6 (a) Optical image of the reactor and (b) SEM image of 50 μm (W) and 100 μm (L) straight channels inside the reactor.

The housing for the reactor was made using plexiglass (PMMA sheets). Two PMMA sheets were cut, slightly bigger than the dimensions of the reactor to accommodate space for connecting tubes to the inlet/outlet ports. Recess is made on both the sheets to accommodate the reactor. Two more sheets of the same dimensions are cut. One of the sheet is glued to the other two (with recess) sheets forming the bottom of the housing. Holes were drilled on the other sheet for inlet/outlet ports, and also on four

corners of all the four sheets for tightening the housing using screws and nuts. A gasket with the same dimension of the reactor is cut and placed in the recess. The reactor was then temporarily placed on the gasket and the sheet containing inlet/outlet ports is tightened with screws. Figure 8.7 shows the optical image of the housing with the the gasket and the reactor. A syringe pump was used for circulation of the fluid with a flow rate calculated from the simulation of the reactor. After the device was assembled, deionized water (DI) was pumped through the device for 10-20 min to make sure there is no leak. Then, oil was passed through the inlet port and the movement of oil-water interface through the channels was observed using a microscope and timed using a stopwatch to calculate residence time. The measurement was repeated atleast three times to obtain a residence time of ~30±3 s.
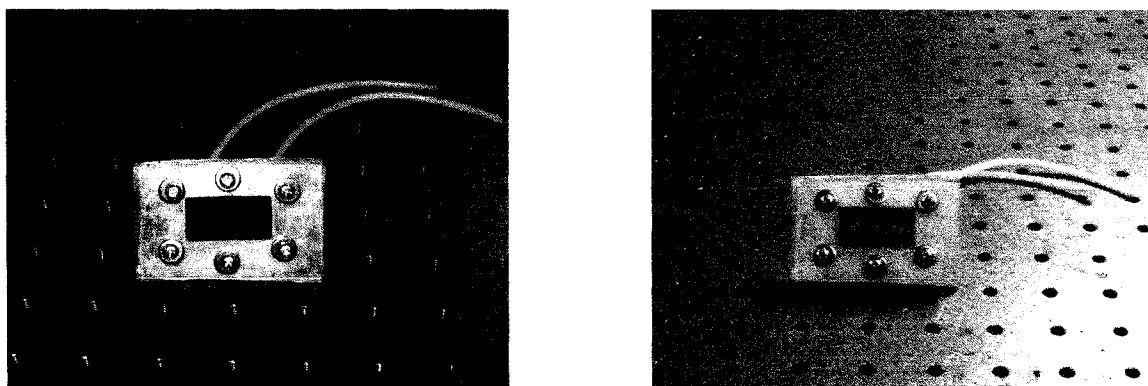
Figure 8.7 Housing for the bioreactor with (a) gasket and (b) gasket and the reactor.

APTES SAMs (with amino (–NH₂) end groups) were formed on the microchannels by circulating the organic solution containing SAM (5 mM) via the inlet port to the channels at a slow flow rate (2 µL/min) for 8 h. Then, ethanol was circulated at a flow rate of 200 µL/min for 45 min to remove any physisorbed species present on the

channels. The reactor inside the housing was sterilized for 2 h with 70% alcohol. Figure 8.8 shows the entire set-up used for the SAM deposition in the experiment.

Figure 8.8 Setup used for the SAM deposition inside the microchannels.

8.4 HDF Cell Culture Studies

All the components used for cell culture studies were sterilized with 70% ethanol including the syringe pump before placing them in the hood. HBSS buffer was passed through the inlet port to remove any ethanol present in the microchannels at a flow rate of 100 μL/min for 30 min. Then complete media is passed through the inlet at the same flow rate for 20 min. The media present in the connecting tubes including the channels was flushed out with air.

HDF cells were trypsinized from the TCP dish and counted using hemacytometer. They were then plated by circulating a cell suspension of 610 μL (1.56 x 10^6 cells/mL) through the syringe pump in such a way that most of the suspension was in the microchannels. The 610 μL media used for circulating was based on the following calculations:

Length of the tubing = 15 cm,

Diameter of the tubing = 0.157 cm,

Therefore, Volume of the tubing = $\Pi r^2 h$ = 0.2968 cm^3 = 296.8 µL,

Considering the two tubes used, Total volume = 593.6 µL.

Based on Equation 8.5, Volume of the channels = 6 µL

Considering the volume of the inlet and outlet subchannel as ~ 4 µL

Total volume required to plate the channels = 603.6 µL.

This volume gives us an approximate cell density of 9400 cells in the channels. The chip was removed from the housing and placed in the incubator at 37 °C for the cells to attach to the channels. After 6 h, the chip was assembled back in the housing and the inlet/outlet ports are connected to the syringe pump containing 10 mL DMEM media. Figure 8.9 shows the reactor setup used for the culture of HDFs inside the incubator.
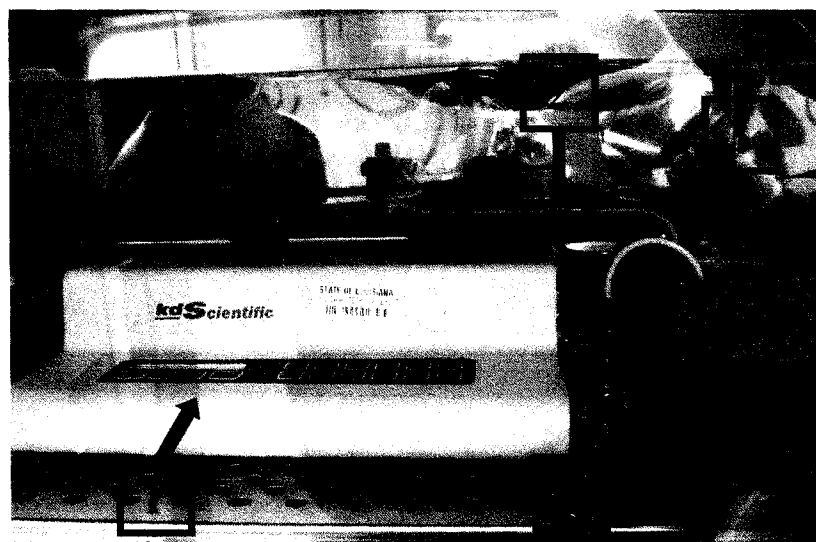
Figure 8.9 Setup used for the HDF culture inside the incubator. (1) Syringe pump (2) Syringe tube containing media (3) Reactor with inlet/outlet ports connected to tubing and (4) Vial for collecting media from outlet.

The media was circulated at a slow flow rate of ~14 μL/min. A vial was connected to the outlet to collect the media. The entire setup was placed in the incubator with 95% O_2 and 5% CO_2 and maintained overnight. The same procedure was followed for the bioreactor without SAM-modified micorchannels. Basic cell functionality such as LDH leakage was analyzed after 12, 24 and 48 h.

8.5 Cell Response Based on LDH Leakage

Figure 8.10 shows a plot of LDH leakage from HDFs (calculated using Equation 3.5) after 12, 24 and 48 h culture duration in SAM-modified reactor and unmodified reactor. It can be observed that the LDH leakage decreased with culture time for both the reactors. But it was prominent in the case of SAM modified reactor. For unmodified reactor, LDH quantity is >100 U/L indicating high cell death. These are preliminary results however, they indicate that modification of surfaces with SAM does enhance the material's properties even in the case of 3D microstructures.
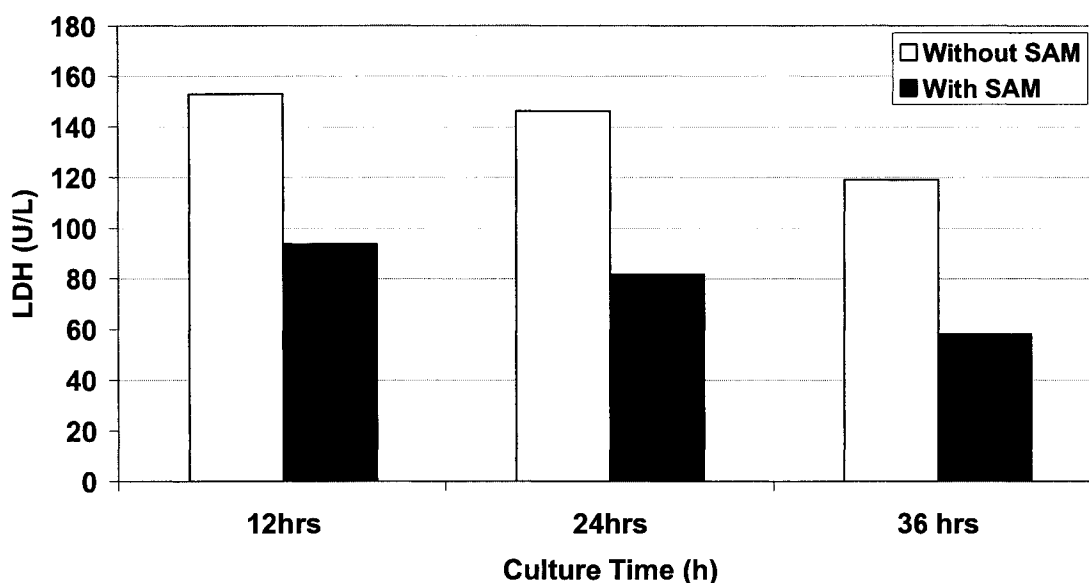
Figure 8.10 LDH release by HDFs from SAM-modified and unmodified 3D bioreactor following 12, 24 and 48 h after seeding.

CHAPTER 9

SUMMARY AND RECOMMENDATIONS

9.1 Summary

In this work, SAMs were used to modify different conducting and semi-conducting substrates to realize stable CCPs. These platforms were used to culture and maintain different cell types such as HDFs, MSCs, RBNs and rat hepatocytes.

This work initially presents the results on HDF culture on amino ($-NH_2$) end group modified Si and methyl ($-CH_3$) modified GaAs and ITO substrates. Morphology of the cells from the phase contrast images indicated that the HDFs presented their characteristic spindle shape with no visible signs of stress or cytoplasmic vacuolation on these surfaces. Cytotoxicity data from LIVE/DEAD® assay and proliferation from MTT assay indicated the preference of HDFs towards different surfaces following the order: ITO-CH_3 > Si-NH_2 > ITO> Si > GaAs-CH_3. Immunohistochemical study of HDFs indicated that the cells maintained their phenotype on all the surfaces except on GaAs, by producing Type-I collagen.

The attachment of HDFs and their subsequent proliferation on these surfaces is due to the formation of a protein layer from the media on the surface of the SAMs. Enhanced proliferation on ITO-CH_3 is due to adsorption of high amounts of protein on $-CH_3$ end group compared to other surfaces. The hydrophobic end group ($-CH_3$) couples with the hydrophobic part of the unfolding protein releasing many hydrophobically

128

structured water molecules and also leading to the large entropy gain for the system.[135,136] In the case of $-NH_2$ modified substrates, the attachment of HDFs is due to the translocation and organization of β_1 integrin subunits to fibronectin deposited on NH_2 end group.[30,137,138] This initial attachment then helps in the proliferation of these cells. It should be observed that SAM-modified GaAs surface supported HDF cell growth for a period of seven days compared to bare GaAs, where cell death occurred within 6 h. This is a great achievement, as a nanometer thin layer (~2 nm) can prevent arsenic leakage into the media and the subsequent cell death.

This work has helped to determine the right kind of substrate and the SAM for HDF attachment, growth and preservation of cell phenotype. Based on these findings, SAM-modified ITO was chosen as the best substrate for studying behavior of different cell types. Furthermore, the properties of ITO such as transparency and stability under physiological conditions enhance its significance. The behavior of stem cells, neurons and hepatocytes were studied to understand how different end group SAMs affect different cell types.

The MSCs grew well on all four different SAM-modified substrates along with unmodified ITO. LIVE/DEAD® analysis showed no cell death even after 3 DIV. Little cell death was observed after 5 and 7 DIV. Morphology images showed that the cell spreading started within 24 h of culture and continued till the end of the culture period (7 DIV). Quantification of proliferation data by MTT assay revealed surprising results. High proliferation was observed on MPS (–SH) modified ITO substrates. There was no significant difference in the proliferation rate among other surfaces. The reason for this high proliferation is not understood and need to be investigated.

The results from our study performed on neuronal culture on amino, methyl and thiol modified ITO substrates suggested that in the absence of serum, cell adhesion was rare. To further confirm these results, the cell density was increased by two-fold and the medium changed every other day as compared to every third day in earlier experiment. No cells were observed till 5 DIV on substrates. After 5 DIV, neuronal attachment was observed predominantly on substrates modified with amino and methyl groups compared to thiol group and control substrates. The experimental protocol was further changed by adding 1% FBS to the cell suspension containing Neurobasal medium. This step was done to neutralize the DMSO present in the cell freezing medium. Following this protocol, a dramatic increase in cell adhesion was observed with cell viability maintained until one week in culture. Better cell adhesion was observed on SAM-modified ITO surface in comparison to the untreated ITO and PLL surfaces.

LIVE/DEAD® analysis performed on these substrates confirmed that the neuronal cells interacted specifically to the amino modified ITO substrate. The results also suggest that the cells preferred the substrates in the order: $ITO-NH_2 > ITO-CH_3 > CS-PLL > ITO$ when cultured over a period of one week. Adsorption of protein layer from the media on the SAM-modified ITO substrates facilitates the initial adhesion of neurons. Further, the addition of B27 supplement in the media helps in maintaining the cells over long periods of time. Nerve cell phenotype studied by performing IHC using the NSE antibody indicated that a significant amount of immunopositive staining was observed on all SAM-coated ITO substrates followed by ITO and PLL.

Most differences in cell-surface interactions on different substrates were observed in the first 3-5 days of cell culture. While adhesion was greatest on $ITO-CH_3$, viability

was found to be more prominent on both SAM-coated substrates. The differences in cell phenotype, between the experimental and the positive control surfaces diminished over time (seven days) in culture as the cell density decreased due to the cell death on all the substrates. The SAM-modified ITO substrates undeniably enhanced the viability of neuron cells compared to their counterparts. They also helped in maintaining better neuron phenotype. And lastly, a decrease in cell density was noticed on all substrates as the culture time progressed (from day one to day seven).

Studies on hepatocyte cell behavior has been carried out on various substrates like ECM components, hydrogels and PEMs but SAM-modified surfaces have not been explored before. Rat hepatocytes were cultured on three ($-NH_2$, $-CH_3$, $-SH$) different SAM-modified ITO surfaces. Isolated hepatocytes were used because they have been used as models in various culture systems for studying the toxicological response of drugs and also closely resemble the liver and provide a metabolic profile of a drug *in vitro*, closest to that found *in vivo*. Serum-free Williams E medium with the presence of 2 mM L-Glutamine was used as the culture media.

The charge and the hydrophobic nature associated with the SAM influenced the initial hepatocyte adhesion. Enhanced adhesion of hepatocytes on ITO-NH_2 is most likely due to the strong electrostatic attraction between oppositely charged hepatocytes (-ve) and $-NH_3^+$ end group (+ve) at physiological conditions (~pH 7). On surfaces such as ITO-CH_3 and ITO-SH, the initial attachment of hepatocytes is attributed to the tethering of these hydrophobic endgroups to the hydrophobic groups present on the hepatocyte surface with the release of several water molecules.

Phase contrast images of hepatocytes on ITO and SAM-modified ITO clearly indicated the cell clustering, which is the characteristic of hepatocytes. Cells showed limited signs of stress and limited decrease in cell density. Cell viability, when quantitated using MTT-based assay, presented the proof of cell proliferation on all these substrates. This result is quite remarkable because proliferation of isolated rat hepatocytes is very difficult to realize. Considering all the possible cases and the importance of all the components used in the experiments the proliferation of hepatocytes was attributed to the presence of L-Glutamine in the media. It has been reported that L-Glutamine causes proliferation in many types of cells due to production of extracellular signal-regulated kinases (ERKs). The exact mechanism for this *in vitro* proliferation of hepatocytes due to glutamine is not yet understood and needs to be investigated further.

IHC studies done by using primary antibodies raised specifically against Type-I collagen indicated the capability of hepatocytes to synthesize collagen, an essential functional protein and preserve their phenotype. Higher LDH leakage was observed initially due to the cytotoxic response offered by the hepatocytes towards the surfaces. After 24 and 48 h, the LDH release reached minimal indicating the adaptation of hepatocytes on these surfaces. The total protein content in solution released by cultured hepatocytes on different substrates followed the order as shown: $ITO-NH_2$ > ITO > $ITO-CH_3$ > Control > ITO-SH. The HDF culture on 3D bioreactors showed that LDH release was low in the case of SAM-modified reactor compared to the unmodified one indicating the effect of surface modification by SAMs on material's properties.

In summary, these results provide experimental validation that cellular response is influenced by a number of properties like nature of the substrate and culture conditions.

These results are extremely useful in the development of CCPs and biomedical devices such as bioreactors and biosensors, which permit researchers to understand cell-biomaterial interactions better.

9.2 Recommendations for Future Work

The self-assembled monolayers formed on ITO are limited and there is much scope in using different kinds SAMs. The SAMs can be used as such or in combination with other end group SAMs (also called mixed SAMs). The characterization techniques used in this work such as contact angle, IR spectroscopy and AFM are good but are not enough to understand the chemisorption mechanism occurring at the SAM-ITO interface. Other characterization techniques such as XPS and NEXAFS should be used to determine whether the thiol molecules adsorb as thiolates or as unbound thiols. Also the thickness of the monolayer films could not be calculated due to the limitations imposed by ellipsometry wherein transparent substrates cannot be used. XPS can be used in this regard to determine the thickness of the monolayer films.

Mixed SAMs containing two or more constituent molecules provide a practical experimental system with which model systems can be generated to study fundamental aspects of the interactions of surfaces with bio-organic nanostructures, such as proteins, carbohydrates, and antibodies. One widely used system comprises an alkanethiol terminated with PEG groups and an alkanethiol terminated with either a biological ligand or a reactive site for linking to a biological ligand. PEG groups are known to resist nonspecific adsorption of biomolecules and cells and are commonly called "inert surfaces". These mixed SAMs can present ligands of interest in a structurally well-defined manner against a background that is inert (Figure 9.1). It would be beneficial to

develop such systems on ITO surface as it not only enhances the versatility of the substrate but also helps in understanding the interactions taking place at the surface.
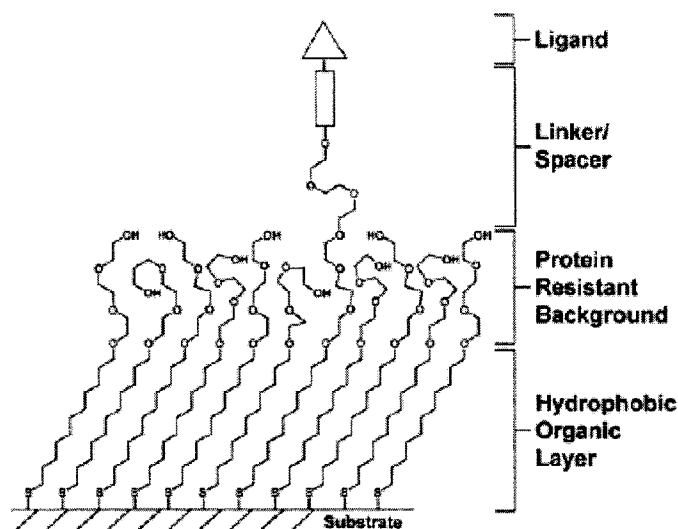
Figure 9.1 Schematic illustration of a mixed SAM consisting of PEG (inert) and ligand containing alkanethiol.[12]

The other important aspect of these studies is to understand the role of adsorbed protein on cell growth. It is difficult to elucidate the role of a single protein from the group of proteins that get adsorbed from the media on the SAMs that has a profound effect on the cell growth (HDFs, stem cells, neurons). Furthermore, the interaction of the protein with the end group of the SAMs and with the cells is not easy to interpret. In order to explore this phenomenon, it would be beneficial to understand the effect of single proteins (fibronectin, vitronectin, fibrinogen) on the cell growth. This effect can be realized by adsorbing the known protein before the cell culture in a serum-free media. Some work has already been done in our group by adsorbing fibonectin on different end group SAMs ($-NH_2$, $-COOH$, $-CH_3$, $-SH$) and culturing 3T3 fibroblasts on them. Contact angle measurements were made to detect the presence of fibronectin, while

impedance measurements were done on both the SAMs and fibronecin adsorbed SAMs to understand the properties and interactions with the cells (not yet analyzed). The cells grown on fibronecin adsorbed SAMs did not survive predominantly due to improper sterilization method used. Analyzing the impedance data and culturing of cells on protein surfaces would be very helpful for developing better CCPs.

The cell culture experiments using HDFs in this work comprised of determining viability, functionality (Type-I collagen synthesis) and proliferation of cells. It would also be helpful to determine the relative rate of collagen synthesis compared to its total synthesis. This rate could be estimated by counting the radioactivity found in the supernatant fraction containing collagenase sensitive material, and the radioactivity precipitated by collagenase resistant proteins. The effect of serum on the cell behavior could also be carried out to understand the interactions between cells and the extracellular matrix. Cells can be seeded on SAM substrates in the presence of DMEM containing reduced serum (1% FBS), normal serum (10% FBS) or enhanced serum (20% FBS). Presence and distribution of proteins secreted onto or adsorbed by SAM substrates can then be assessed using a suite of antibodies to ECM proteins, cytoskeletal and membrane proteins, and immunocytochemistry can be used to map the character and composition of SAM-modified surfaces. Also, the cytoskeletal, focal adhesion and integrin expression play an important role in signal transduction and integrin-mediated cell attachment. These can be determined by using fluorescent-labeled phalloidin, vinculin and integrin antibodies with a secondary antibody conjugated to fluorescein.

The other part of this dissertation is comprised of neuronal culture on SAMs modified platforms. Even though the viability of cells was maintained for a period of

seven days, the full potential of neurons was not realized using the set of SAMs used in this work. This work could be accomplished by incorporating a promising technique of covalently attaching protein-derived peptides such as the YIGSR and IKVAV sequences onto chemically modified ITO substrates because they have shown to promote better neural cell adhesion. Also, surfaces modified with the extended amino acid sequences such as CDPGYIGSR and CQAASIKVAV have been shown to have an improved cellular response, relative to shorter sequences of YIGSR and IKVAV. It would be of great importance to try some of these peptides and also that modified with additional amino acid sequences.

Hepatocyte culture has not been studied on SAM-modified substrates previously; therefore, these studies could establish a foundation for further analyses of cellular response. This work primarily concentrated on the short-term cell response studies of hepatocyte culture on these substrates. Long-term responses of hepatocyte biocompatibility, viability and phenotypic maintenance would provide further evidence of the substrate influence on cellular response. Variation of the monolayer chain length has an influence of SAM properties and hence cellular attachment. Study of hepatocyte response on molecules having identical end groups but varying chain lengths would permit us to reach a consensus on the choice of an ideal monolayer having an end group and chain length which would facilitate optimal cellular response. Also the use of peptides which can specifically recognize the cell binding sites on the hepatocyte surface will greatly enhance the SAM technique. These peptides can be coupled to the SAM end group using basic chemistry. Some of the peptides that could be considered include RGD (Arg-Gly-Asp), YIGSR (Tyr-Ile-Gly-Ser-Arg), PHSRN (Pro-His-Ser-Arg-Asn). The

tripeptide RGD, is present in all major extracellular matrix (ECM) proteins (fibronectin, collagen, laminin) and has been shown to enhance adhesion and spreading of fibroblasts, endothelial cells and smooth muscle cells. PHSRN, a cell binding sequence found only in fibronectin, has been known to act synergistically with RGD for cell adhesion. YIGSR, a peptide derived from the laminin B1 chain, interacts with the 67 k Da laminin binding protein and was found to promote adhesion and spreading of large number of cell types including endothelial cells, fibroblasts and smooth muscle cells. Another aspect which should be considered is the use of co-cultures. Co-cultures of hepatocytes with other cell types like fibroblasts, epithelial cells, nonparenchymal cells and also stem cells have been found to enhance the hepatocyte functionality. This could be established on SAM-modified surfaces to study cell-cell and cell-substrate interactions in detail at the molecular level.

The fabrication of a 3D bioreactor was used to analyze the LDH leakage from the HDF cells. The same system can be used for other cell types, most importantly, hepatocytes, for drug toxicity screening, by analyzing the metabolites using high performance liquid chromatography (HPLC). Neurons can also be grown on these SAM-modified microchannels and the neurite outgrowth can be directed within the channels. Thus, there is much scope towards this research, which needs to be explored.

BIBLIOGRAPHY

[1]K. R. Aithal, D. P. Kumaraswamy, D. K. Mills, and D. Kuila, "Proliferation, viability and functionality of hepatocytes cultured on self assembled monolayers (SAMs) modified indium tin oxide (ITO)," Submitted to *Biomaterials*, 2006.

[2]M. Mrkisch, "Directing cell adhesion with micropatterned substrates," *Biochemist*, Vol. 10, pp. 21-24, 2000.

[3]M. Mrkisch, "A surface chemistry approach to study cell adhesion," *Chemical Society Reviews*, Vol. 29, pp. 267-273, 2000.

[4]O. Jauregui, "Cell adhesion to biomaterials: The role of several extracellular matrix components in the attachment of non-transformed fibroblasts and parenchymal cells," *Transactions of American Society For Artificial Organs*, Vol. 10, pp. 66-74, 1987.

[5]L. Richert, Ph. Ravalle, D. Vautier, B. Senger, J. F. Stoltz, P. Schaaf, J. C. Voeget, and C. Picart, "Cell interactions with polyelectrolyte multilayer films," *Biomacromolecules*, Vol. 3, pp. 1170-1178, 2002.

[6]G. Whitesides, J. P. Mathias, and C. T. Seto, "Molecular self-assembly and nanochemistry: A new strategy for the synthesis of nanostructures," *Science*, Vol. 254, pp. 1312-1319, 1991.

[7]L. Leoni, D. Attiah, and T.A. Desai, "Nanoporous platforms for cellular sensing and delivery," *Sensors*, Vol. 2, pp. 111-120. 2001.

[8]J. Pancrazio, P. Whelan, and D. A. Borkholder, "Development and application of cell-based biosensors," *Annals of Biomedical Engineering*, Vol. 27, pp. 697-711, 1999.

[9]S. Ber, G. Torun Kose, and V. Hasici, "Bone tissue engineering on patterned collagen films: A comparative study," *Biomaterials*, Vol. 26, pp. 1977-1986, 2005.

[10]W. G. Koh, A. Reyzin, M. V. Pishko, "Poly (ethylene glycol) hydrogel microstructures encapsulating living cells," *Langmuir*, Vol. 18, pp. 2459-2462, 2002.

[11]D. S. Kommireddy, A. A. Patel, T. G. Shutava, D. K. Mills, and Y. M. Lvov, "Layer-by-layer assembly of TiO_2 nanoparticles for stable hydrophillic biocompatible coatings," *Journal of Nanoscience and Nanotechnology*, Vol. 5, pp. 1081-1087, 2005.

[12]J. C. Love, L. A. Estroff, J. K. Kriebel, R. G. Nuzzo, and G. M. Whitesides, "Self-assembled monolayers of thiolates on metals as a form of nanotechnology. *Chemical Reviews*, Vol. 105, pp. 1103-1169, 2005.

[13]M. Mrksich, C. Chen, Y. Xia, L. Dike, D. Ingber, and G. Whitesides, "Controlling cell attachment on contoured surfaces with self-assembled monolayers of alkanethiolates on gold," *Proceedings of the National Academy of Sciences* USA, Vol. 93, pp. 10775-10778, 1996.

[14]M. Mrksich, and G. Whitesides, "Using self-assembled monolayers to understand the interactions of man-made surfaces with proteins and cells," *Annual Review of Biophysics and Biomolecular Structure*, Vol. 25, pp. 55-78, 1996.

[15]M. Mrksich, L. Dike, J. Tien, D. Ingber, and G. Whitesides, "Using microcontact printing to pattern the attachment of mammalian cells to self-assembled monolayers of alkanethiolates on transparent films of gold and silver," *Experimental Cell Research*, Vol. 235, pp. 305-313, 1997.

[16]C. A. Scotchford, E. Cooper, G. J. Leggett, and S. Downes, "Growth of human osteoblast-like cells on alkanethiol on gold self-assembled monolayers: The effect of surface chemistry," *Journal of Biomedical Materials Research*, Vol. 41, pp. 431-442, 1998.

[17]E. Cooper, L. Parker, C. A. Scotchford, S. Downes, G. J. Leggett, and T. L. Parker, "The effect of alkyl chain length and terminal group chemistry on the attachment and growth of murine 3T3 fibroblasts and primary human osteoblasts on self-assembled monolayers of alkanethiols on gold," *Journal of Materials Chemistry*, Vol. 10, pp. 133-139, 2000.

[18]B. Zhu, T. Eurell, R. Gunawan, and D. Leckband, "Chain-length dependence of the protein and cell resistance of oligo(ethylene glycol)-terminated self assembled monolayers on gold," *Journal of Biomedical Material Research*, Vol. 56, pp. 406-416, 2001.

[19]C. Roberts, C. S. Chen, M. Mrksich, V. Martichonok, D. E. Ingber, G. M. Whitesides, "Using mixed self-assembled monolayers presenting RGD and (EG)$_3$OH groups to characterize long-term attachment of bovine capillary endothelial cells to surfaces," *Journal of the American Chemical Society*, Vol. 120, pp. 6548-6555, 1998

[20]M. Kato and M. Mrksich, "Rewiring cell adhesion," *Journal of the American Chemical Society*, Vol. 126, pp. 6504-6505, 2004

[21]E. Ostuni, L. Yan, and G. M. Whitesides, "The interaction of proteins and cells with self-assembled monolayers of alkanethiolates on gold and silver," Colloids and Surfaces B: Biointerfaces, Vol. 15, pp. 3-30, 1999.

[22]C. S. Chen, M. Mrksich, S. Huang, G. M. Whitesides, and D. E. Ingber, "Micropatterned surfaces for control of cell shape, position, and function," *Biotechnology Progress*, Vol. 14, pp. 356-363, 1998.

[23]K. K. Parker, A. L. Brock, C. Brangwynne, R. J. Mannix, N. Wang, E. Ostuni, N. A. Geisse, J. C. Adams, G. M. Whitesides, and D. E. Ingber, "Directional control of lamellipodia extension by constraining cell shape and orienting cell tractional forces," *Federation of American Societies for Experimental Biology Journal*, Vol. 16, pp. 1195-1204, 2002.

[24]X. Jiang, R. Ferrigno, M. Mrksich, and G. M. Whitesides, "Electrochemical desorption of self-assembled monolayers noninvasively releases patterned cells from geometrical confinements," *Journal of the American Chemical Society*, Vol. 125, pp. 2366-2367, 2003.

[25]C. K. Bertha, F. M. Hawkridge and B. M. Hoffman, "Electrochemical studies of cyanometmyoglobin and metmyoglobin: implications for long-range electron transfer in proteins," *Journal of the American Chemical Society*, Vol. 114, pp. 10603-10608, 1996.

[26]S.-Y. Oh, Y.-J. Yun, D.-Y. Kim, and S.-H. Han, "Formation of a self-assembled monolayer of diaminododecane and a heteropolyacid monolayer on the ITO surface," *Langmuir*, Vol. 15, pp. 4690-4692, 1999.

[27]A. Fang, H. T. Ng, X. Su, and S. F. Y. Li, "Soft-lithography-mediated submicrometer patterning of self-assembled monolayer of hemoglobin on ITO surfaces," *Langmuir*, Vol. 16, pp. 5221-5226, 2000.

[28]E. Bieberich, A. Guiseppi-Elie, "Neuronal differentiation and synapse formation of PC12 and embryonic stem cells on interdigitated microelectrode arrays: Contact structures for neuron-to-electrode signal transmission (NEST)," *Biosensors and Bioelectronics*, Vol. 19, pp. 923–931, 2004.

[29]R. Kapur and A. S. Rudolph."Cellular and cytoskeleton morphology and strength of adhesion of cells on self-assembled monolayer model surfaces," *Experimental Cell Research*, Vol. 244, pp. 275–285, 1998.

[30]N. Faucheux, R. Schweiss, K. L.utzow, C. Werner, and T. Groth, "Self-assembled monolayers with different terminating groups as model substrates for cell adhesion studies," *Biomaterials*, Vol. 25, pp. 2721–2730, 2004.

[31]M. H. Brodsky, "Progress in gallium arsenide semiconductors," *Scientific American*, Vol. 262, pp. 68-75, 1990.

[32]C. Kirchner, M. George, B. Stein, W. J. Parak, H. E. Gaub, and M. Seitz, "Corrosion protection and long-term chemical functionalization of gallium arsenide in an aqueous environment," *Advanced Functional Materials*, Vol. 12, pp. 266-276, 2002.

[33]B. Liebl, H. Mueckter, P. T. Nguyen, E. Doklea, S. Islambouli, B. Fichtl, and W. Forth, "Differential effects of various trivalent and pentavalent organic and inorganic arsenic species on glucose metabolism in isolated kidney cells, *Applied Organometallic Chemistry*, Vol. 9, pp. 531-540, 1995

[34]W. Deng Guo, A. Gonen, S. Dmitry, U. V. Rachel, N. Ron, S. Abraham, and C. David, "Novel NO biosensor based on the surface derivatization of GaAs by "hinged" iron porphyrins," *Angewandte Chemie International Edition*, Vol. 39, pp. 4496-4500, 2000.

[35]A. Ulman, "Formation and structure of self-assembled monolayers," *Chemical Reviews*, Vol. 96, pp. 1533-1554, 1996.

[36]W. C. Bigelow, D. L. Pickett, and W. A. Zisman, "Oleophobic monolayers. 1. Films adsorbed from solution in nonpolar liquids," *Journal of Colloid and Interface Science*, Vol. , pp. 513-538, 1946.

[37]R. G. Nuzzo and D. L. Allara, "Adsorption of bifunctional organic disulfides on gold surfaces, *Journal of the American Chemical Society*, Vol. 105, pp. 4481-4483, 1983.

[38]http://www.ifm.liu.se/applphys/ftir/sams.html

[39]J. Sagiv, "Organized monolayers by adsorption. 1. Formation and structure of oleophobic mixed monolayers on solid surfaces, *Journal of the American Chemical Society*, Vol. 102, pp. 92-98, 1980.

[40]J. D. Le Grange, J. L. Markham, and C. R. Kurjian, "Effects of surface hydration on the deposition of silane monolayers on silica, *Langmuir*, Vol. 9, pp. 1749-1753, 1993.

[41]C. Cao, A. Y. Fadeev, and T. J. McCarthy, "Reactions of organosilanes with silica surfaces in carbon dioxide," *Langmuir*, Vol. 17, pp. 757-761, 2001.

[42]R. Boukherroub, S. Morin, P. Sharpe, and D. M. Wayner, "Insights into the formation mechanisms of Si-OR monolayers from the thermal reactions of alcohols and aldehydes with Si(111)-H," *Langmuir*, Vol. 16, pp. 7429-7434, 2000.

[43]P. Harder, K. Bierbaum, Ch. Woell, and M. Grunze,"Induced orientational order in long alkyl chain aminosilane molecules by preadsorbed octadecyltrichlorosilane on hydroxylated Si(100)," *Langmuir*, Vol. 13, pp. 445-454, 1997.

[44]N. Tillman, A. Ulman, J. S. Schildkraut, and T. L. Penner, "Incorporation of phenoxy groups in self-assembled monolayers of trichlorosilane derivatives. Effects on film thickness, wettability, and molecular orientation," *Journal of the American Chemical Society*, Vol. 110, pp. 6136-6144, 1988.

[45]N. S. Tambe and B. Bhushan, "Nanotribological characterization of self-assembled monolayers deposited on silicon and aluminium substrates," *Nanotechnology*, Vol.16, pp. 1549–1558, 2005.

[46]H. Hillebrandt and M. Tanaka, "Electrochemical characterization of self-assembled alkylsiloxane monolayers on indium-tin oxide (ITO) semiconductor electrodes," *Journal of Physical Chemistry B*, Vol. 105, pp. 4270-4276, 2001.

[47]C. Yan, M. Zharnikov, A. Golzhauser, and M. Grunze, "Preparation and characterization of self-assembled monolayers on indium tin oxide," *Langmuir*, Vol. 16, pp. 6208-6215, 2000.

[48]C. R. Kessel and S. Granick, "Formation and characterization of a highly ordered and aell- anchored alkylsilane monolayer on mica by self –assembly," *Langmuir*, Vol. 7, pp. 532-538, 1991.

[49]K. Mathauser and C. W. Frank, "Binary self-assembled monolayers as prepared by successive adsorption of alkyltrichlorosilanes, *Langmuir*, Vol. 9, pp. 3446-3451, 1993.

[50]J. Gun and J. Sagiv, "On the formation and structure of self-assembling monolayers. III. Time of formation, solvent retention, and release, *Journal of Colloid and Interface Science*, Vol. 112, pp. 457-472, 1986.

[51]S. Brandriss and S. Margel, "Synthesis and characterization of self-assembled hydrophobic monolayer coatings on silica colloids," *Langmuir*, Vol. 9, pp. 1232-1240, 1993.

[52]P. Silberzan, L. Leger, D. Ausserre, and J. J. Benattar, "Silanation of silica surfaces. A new method of constructing pure or mixed monolayers," *Langmuir*, Vol. 7, pp. 1647-1651, 1991.

[53]S. R. Wassweman, Y.–T. Tao, and G. M. Whitesides, "Structure and reactivity of alkylsiloxane monolayers formed by reaction of alkyltrichlorosilanes on silicon substrates," *Langmuir*, Vol. 5, pp. 1074-1087, 1989.

[54]K. Bierbaum, M. Kinzler, C. Woll, M. Grunze, G. Hahner, S. Heid, and F. Effecberger, "A near edge X-ray absorption fine structure spectroscopy and X-ray photoelectron spectroscopy study of the film properties of self-assembled monolayers of organosilanes on oxidized Si(100)," *Langmuir*, Vol. 11, pp. 512-518, 1995.

[55]C. D. Bain and G. M. Whitesides, "Modelling organic surfaces with self-assembled monolayers," *Angewandte Chemie International Edition England*, Vol. 28, pp. 506-516, 1989.

[56]T. R. Lee, P. E. Laibinis, J. P. Folkers, and G. M. Whitesides, "Heterogeneous catalysis on platinum and self-Assembled monolayers on metal and metal oxide surfaces", *Pure and Applied Chemistry*, Vol. 63, pp. 821-828, 1991.

[57]H. Sellers, A.Ulman, Y. Shnidman, and J. E. Eilers, "Structure and binding of alkanethiolates on gold and silver surfaces: Implications for self-assembled monolayers," *Journal of the American Chemical Society*, Vol. 115, pp. 9389-9401, 1993.

[58]E. B. Troughton, C. D. Bain, G. M. Whitesides, D. L. Allara, and M. D. Porter, "Monolayer films prepared by the spontaneous self-assembly of symmetrical and unsymmetrical dialkyl sulfides from solution onto gold substrates: Structure, properties, and reactivity of constituent functional groups," *Langmuir*, Vol. 4, pp. 365-385, 1988.

[59]E. Sabatani, J. Cohen-Boulakia, M. Bruening, I. Rubinstein, "Thioaromatic monolayers on gold: a new family of self-assembling monolayers," *Langmuir*, Vol. 9, pp. 2974-2981, 1993.

[60]K. Uvdal, P. Bodo, and B. Liedberg, "L-cysteine adsorbed on gold and copper: An X-ray photoelectron spectroscopy study," *Journal of Colloid and Interface Science*, Vol. 149, pp. 162-173, 1992.

[61]A. J. Arduengo, J. R. Moran, J. Rodriguez-Paradu, and M. D. Ward, "Molecular control of self-assembled monolayer films of imidazole-2-thiones: adsorption and reactivity," *Journal of the American Chemical Society*, Vol. 112, pp. 6153-6154, 1990.

[62]C. D. Bain, E. B. Troughton, Y.-T. Tao, J. Evall, G. M. Whitesides, and R. G. Nuzzo, "Formation of monolayer films by the spontaneous assembly of organic thiols from solution onto gold, *Journal of the American Chemical Society*, Vol. 111, pp. 321-335, 1989.

[63]Buck, M.; Eisert, F.; Fischer, J.; Grunze, M.; Tra¨ger, F. *Appl.Phys.* **1991**, *A53*, 552.

[64]G. Haehner, Ch. Woell, M. Buck, and M. Grunze,"Investigation of intermediate steps in the self-assembly of n-alkanethiols on gold surfaces by soft x-ray spectroscopy," *Langmuir*, Vol. 9, pp. 1955-1958, 1993..

[65]M. D. Porter, T. B. Bright, D. L. Allara, C. E. D. Chidsey, "Spontaneously organized molecular assemblies. 4. Structural characterization of n-alkyl thiol monolayers on gold by optical ellipsometry, infrared spectroscopy, and electrochemistry," *Journal of the American Chemical Society*, Vol. 109, pp. 3559-3568, 1987.

[66]R. G. Nuzzo, B. R. Zegarski, and L. H. Dubois, "Fundamental studies of the chemisorption of organosulfur compounds on gold(111). Implications for molecular self-assembly on gold surfaces," *Journal of the American Chemical Society*, Vol. 109, pp. 733-740, 1987.

[67]Y. Li, J. Huang, R. T. McIver, J. C. Hemminger, "Characterization of thiol self-assembled films by laser desorption Fourier transform mass spectrometry," *Journal of the American Chemical Society*, Vol. 114, pp. 2428-2432, 1992.

[68]M. A. Bryant and J. E. Pemberton, "Surface Raman scattering of self-assembled monolayers formed from 1-alkanethiols: behavior of films at gold and comparison to films at silver," *Journal of the American Chemical Society*, Vol. 113, pp. 8284-8293, 1991.

[69]L. Strong and G. M. Whitesides, "Structures of self-assembled monolayer films of organosulfur compounds adsorbed on gold single crystals: electron diffraction studies," *Langmuir*, Vol. 4, pp. 546-558, 1988.

[70]C. E. D. Chidsey and D. N. Loiacono, D. N, "Chemical functionality in self-assembled monolayers: structural and electrochemical properties," *Langmuir*, Vol. 6, pp. 682-691, 1990.

[71]C. E. D. Chidsey, G.-Y. Liu, Y. P. Rowntree, and G. Scoles, "Molecular order at the surface of an organic monolayer studied by low energy helium diffraction," *Journal of Chemical Physics*, Vol. 91, pp. 4421, 1989.

[72]C. A. Alves, E. L. Smith, and M. D. Porter, "Atomic scale imaging of alkanethiolate monolayers at gold surfaces with atomic force microscopy," *Journal of the American Chemical Society*, Vol. 114, pp. 1222-1227, 1992.

[73]W. E. Spicer, P. W. Chye, P. R. Skeath, C. Y. Su, and I. Lindau, "New and unified model for Schottky barrier and III–V insulator interface states formation," *Journal of Vacuum Science and Technology*, Vol. 16, pp. 1422-1433, 1979.

[74]C. W. Sheen, J. X. Shi, J. Martensson, A. N. Parikh, and D. L. Allara, "A new class of organized self-assembled monolayers: alkane thiols on gallium arsenide(100)," *Journal of the American Chemical Society*, Vol. 114, pp. 1514-1515, 1992.

[75]H. Ohno, M. Motomatsu, W. Mizutani, and H. Tokumoto, "AFM Observation of Self-Assembled Monolayer Films on GaAs (110)," *Japanese Journal of Applied Physics*, Vol. 34, pp. 1381-1386, 1995.

[76]T. Baum, S. Ye, and K. Uosaki, "Formation of self-assembled monolayers of alkanethiols on GaAs surface with in situ surface activation by ammonium hydroxide," *Langmuir*, Vol. 15, pp. 8577-8579, 1999.

[77]S. Ye, G. Li, H. Noda, K. Uosaki, and M. Osawa, "Characterization of self-assembled monolayers of alkanethiol on GaAs surface by contact angle and angle-resolved XPS measurements," *Surface Science*, Vol. 529, pp. 163-170, 2003..

[78]T. Kondo, M. Yanagida, K. Shimazu, and K. Uosaki, "Determination of thickness of a self-assembled monolayer of dodecanethiol on Au(111) by Angle-Resolved X-ray Photoelectron Spectroscopy," *Langmuir*, Vol. 14, pp. 5656-5658, 1998.

[79]M. R. Linford and C. E. D. Chidsey, "Alkyl monolayers covalently bonded to silicon surfaces," *Journal of the American Chemical Society*, Vol. 115, pp. 12631-12632, 1993.

[80]D. P. Dowling, K. Donnelly, M. L. McConnell, R. Eloy, and M. N. Arnaud, "Deposition of anti-bacterial silver coatings on polymeric substrates," *Thin Solid Films*, Vol. 398-399, pp. 602-606, 2001.

[81]P. E. Laibinis, P. E, G. M. Whitesides, D. L. Allara, Y. T. Tao, A. N. Parikh, and R. G. Nuzzo, Comparison of the structures and wetting properties of self-assembled monolayers of n-alkanethiols on the coinage metal surfaces, copper, silver, and gold," *Journal of the American Chemical Society*, Vol. 113, pp. 7152-7167, 1991.

[82]J. C. Love, D. B. Wolfe, M. L. Chabinyc, K. E. Paul, and G. M. Whitesides, "Self-assembled monolayers of alkanethiolates on palladium are good etch resists," *Journal of the American Chemical Society*, Vol. 124, pp. 1576-1577, 2002..

[83]S. Wolf, *Silicon Processing for the VLSI Era*. Lattice Press: Sunset Beach, 1990.

[84]X. Jiang, D. A. Bruzewicz, M. M. Thant, and G. M. Whitesides, "Palladium as a substrate for self-assembled monolayers used in biotechnology," *Analytical Chemistry*, Vol. 76, pp. 6116-6121, 2004.

[85]J. Yang and J. M. Kleijn, "Order in phospholipid langmuir-blodgett layers and the effect of electric potential on the substrate," *Biophysics Journal*, Vol. 76, pp. 323-332, 1999.

[86]R. Margalit and R. P. Vasquez, "Determination of protein orientation on surfaces with X-ray photoelectron spectroscopy," *Journal of Protein Chemistry*, Vol. 9, pp. 105-108, 1990.

[87]C. K. Bertha, F. M. Hawkridge, and B. M. Hoffman, "Electrochemical studies of cyanometmyoglobin and metmyoglobin: implications for long-range electron transfer in proteins", *Journal of the American Chemical Society*, Vol. 114, pp. 10603-10608, 1996.

[88]S.-Y. Oh, Y.-J. Yun, D.-Y. Kim, and S.-H. Han, "Formation of a self-assembled monolayer of diaminododecane and a heteropolyacid monolayer on the ITO surface," *Langmuir*, Vol. 15, pp. 4690-4692, 1999.

[89]C. Williams and T. M. Wick, "Endothelial cell-smooth muscle cell co-culture in a perfusion bioreactor system," *Annals of Biomedical Engineering*, Vol. 33, pp. 920-928, 2005.

[90]S. Zheng, L. Yan, M. Altman. M. Lassle, H. Nugent, F. Frankel, A. Luffenberger, G.M. Whitesides, and A. Rich, "Biological surface engineering: A simple system for cell pattern formation," *Biomaterials*, Vol. 20, pp. 1212-1220, 1999.

[91]M. Lampkin, R. Clerout, M. Degrange, C. Legris, and M. F. Luizard, "Correlation between substratum roughness and wettability, cell Adhesion and cell Migration," *Journal of Biomedical Materials Research*, Vol. 36, pp. 99-108, 1997.

[92]J. Pancrazio, P. Whelan, and D. A. Borkholder, "Development and application of cell-based biosensors," *Annals of Biomedical Engineering*, Vol. 27, pp. 697-711, 1999.

[93]R. G. LeBaron and K. A. Athaniasiou, "Extracellular matrix cell adhesion peptides: Functional applications in orthopaedic materials," *Tissue Engineering*, Vol. 6, pp. 85-103, 2000.

[94]S. Yashiki, R. Umegaki, M. Kino-Oka, and M. Taya, "Evaluation of attachment and growth of anchorage-dependent cells on culture surfaces with type I collagen coating. *Journal of Bioscience and Bioengineering*, Vol. 92, pp. 385-388, 2001.

[95]B. Zavan, P. Brun, V. Vindigni, A. Amadori, W. Hebeler, P. Pontisso, D. Montumurro, G. Abatangelo, and R. Cortivo, "Extracellular matrix-enriched polymeric scaffolds as a substrate for hepatocyte cultures: *In vitro* and *in vivo* studies," *Biomaterials*, Vol. 26, pp. 7038-7035, 2005.

[96]J. Fukuda, Y. Sakai, and K. Nakazawa, "Novel hepatocyte system developed using microfabrication and collagen/ polyethylene glycol microcontact printing," *Biomaterials*, Vol. 27, pp. 1061-1070, 2006.

[97]C. A. Scotchford, M. G. Cascone, S. Downes, and P. Guisti, "Osteoblast responses to collagen-PVA bioartificial polymers *in-vitro*: The effect of cross-linking method and collagen content," *Biomaterials*, Vol. 19, pp. 1-11, 1998.

[98]X. Wang, D. Li, W. Wang, Q. Feng, F. Cui, Y. Xu, X. Song, and M. Van der Weff, " Cross linked collagen/chitosan matrix for artificial livers," *Biomaterials*, Vol. 24, pp. 3213-3220, 2003.

[99]Y. Lvov, F. Essler, and G. Decher, "Combining of polycation/polyanion self-assembling and Langmuir-Blodgett techniques in production of film superlattices," *Journal of Physical Chemistry*, Vol. 97, pp. 13773-13776, 1993.

[100]Y. Ito, "Surface micropatterning to regulate cell functions," *Biomaterials*, Vol. 20, pp. 2333-2342, 1999.

[101]D. Vautier, V. Karsten, C. Egles, J. Chluba, P. Schaaf, J-C Voegel, and J. Ogier, " Polyelectrolyte multilayer films modulate cytoskeletal organization in chondrosarcoma cells," *Journal of Biomaterials Science Polymer Edition*, Vol. 13, pp. 712-731, 2002.

[102]S. Kidambi, I.Lee, and C. Chan, "Controlling primary hepatocyte adhesion and spreading on protein free polyelectrolyte multi-layer films," *Journal of the American Chemical Society*, Vol 126, pp.16286-16287, 2004.

[103]M. Fujimoto, M. Isobe, S. Yamaguchi, T. Amagasa, A.Watanabe, T. Ooya, and Yui, "Poly(ethylene glycol) hydrogels cross-linked by hydrolyzable polyrotaxane containing hydroxyapatite particles as scaffolds for bone regeneration," *Journal of Biomaterial Science Polymer Edition*, Vol. 16, pp. 1611-1621, 2005.

[104]J. E. Barralet, L. Wang , M. Lawson, J. T. Triffitt, P. R. Cooper, and R. M. Shelton, "Comparison of bone marrow cell growth on 2D and 3D alginate hydrogels," *Journal of Materials Science: Materials in Medicine*, Vol. 16, pp. 515-519, 2005.

[105]S. Hou, Q. Xu, W. Tian, F. Cui, Q. Cai, J. Ma, and I. S. Lee, "The repair of brain lesion by implantation of hyaluronic acid hydrogels modified with laminin," *Journal of Neuroscience Methods*, Vol. 148, pp. 60-70, 2005.

[106]L. J. Itle, W. G. Koh, and M. V. Pishko, "Hepatocyte viability and protein expression within hydrogel microstructures," *Biotechnology Progress*, Vol. 32, pp. 926-932, 2005.

[107]D. S. Benoit and K. S. Anseth, "The effect on osteoblast function of colocalized RGD and PHSRN epitopes on PEG surfaces," *Biomaterials*, Vol. 26, pp. 5609-5620, 2005.

[108]H. Shin, J. S. Temenoff , G. C. Bowden, K. Zygourakis, M. C. Farach-Carson , M. J. Yaszemski, and A. G. Mikos, "Osteogenic differentiation of rat bone marrow stromal cells cultured on Arg-Gly-Asp modified hydrogels without dexamethasone and beta-glycerol phosphate," *Biomaterials*, Vol. 26, pp. 3645-3654, 2005.

[109]M. Mrksich, G. B. Sigal, and G. M. Whitesides, "Surface plasmon resonance permits in situ measurement of protein adsorption on self-assembled monolayers of alkanethiolates on gold," *Langmuir*, Vol. 11, pp. 4383-4385, 1995.

[110]J. M. Brockman, B. P. Nelson, and R. M. Corn, "Surface plasmon resonance imaging measurements of ultrathin organic films," *AnnualReview of Physical Chemistry*, Vol. 51, pp. 41-63, 2000.

[111]M. Lestelius, B. Liedberg, and P. Tengvall, *In vitro* plasma protein adsorption on ω-functionalized alkanethiolate self-assembled monolayers," *Langmuir*, Vol. 13, pp. 5900-5908, 1997.

[112]P. Tengvall, I. Lundstrom, and B. Liedberg, "Protein adsorption studies on model organic surfaces: an ellipsometric and infrared spectroscopic approach," *Biomaterials*, Vol. 19, pp. 407-422, 1998.

[113]Marx, K. A., "Quartz crystal microbalance: a useful tool for studying thin polymer films and complex biomolecular systems at the solution-surface interface," *Biomacromolecules*, Vol. 4, pp. 1099-1120, 2003.

[114]D.-H. Min, W.-J. Tang, and M. Mrksich, "Chemical screening by mass spectrometry to identify inhibitors of anthrax lethal factor," *Nature Biotechnology*, Vol. 22, pp. 717-720, 2004.

[115]A. Bhaumik, M. Ramakanth, L. K. Brar, A. L. Raychaudhuri, F. Rondelez, and D. Chatterji, "Formation of a DNA layer on Langmuir-Blodgett films and its enzymatic digestion," *Langmuir*, Vol. 20, pp. 5891-5896, 2004.

[116]M. P. Srinivasan, T. V. Ratto, P. Stroeve, and M. L. Longo, "Patterned supported bilayers on self-assembled monolayers: Confinement of adjacent mobile bilayers," *Langmuir*, Vol. 17, pp. 7951-7954, 2001.

[117]K. A. Burridge, M. A. Figa, and J. Y. Wong, "Patterning adjacent supported lipid bilayers of desired composition to investigate receptor-ligand binding under shear flow," *Langmuir*, Vol. 20, pp. 10252-10259, 2004.

[118]C. Roberts, C. S. Chen, M. Mrksich, V. Martichonok, D. E. Ingber, and G. M. Whitesides, Using mixed self-assembled monolayers presenting RGD and $(EG)_3OH$ groups to characterize long-term attachment of bovine capillary endothelial cells to surfaces," *Journal of the American Chemical Society*, Vol. 120, pp. 6548-6555, 1998.

[119]K. K. Parker, A. L. Brock, C. Brangwynne, R. J. Mannix, N. Wang, E. Ostuni, N. A. Geisse, J. C. Adams, G. M. Whitesides, and D. E. Ingber, "Directional control of lamellipodia extension by constraining cell shape and orienting cell tractional forces," *Federation of American Societies for Experimental Biology Journal*, Vol. 16, pp. 1195-1204, 2002.

[120]J. Fick, R. Steitz, V. Leiner, S. Tokumitsu, M. Himmelhaus, and M. Grunze, Swelling behavior of self-assembled monolayers of alkanethiol-terminated Poly(ethylene glycol): A neutron reflectometry study," *Langmuir*, Vol. 20, pp. 3848-3853, 2004.

[121]N. T. Flynn, T. N. T. Tran, M. J. Cima, and R. Langer, "Long-term stability of self-assembled monolayers in biological media," *Langmuir*, Vol. 19, pp. 10909-10915, 2003.

[122]http://www.p2pays.org/ref/13/12920.htm.

[123]MSDS, Catalog No: 500-0002 and 500-0006, Bio-Rad protein assay. Bio-Rad Laboratories, USA.

[124]C. Asbill, N. Kim, A. El-Kattan, K. Creek, P. Wertz, and B. Michniak, "Evaluation of a human bio-engineered skin equivalent for drug permeation studies," *Pharmaceutical Research*, Vol. 17, pp. 1092-1097, 2000.

[125]M. Blaha, W. Jr. Bowers, J. Kohl, D. DuBose, J. Walker, A. Alkhyyat, and G. Wong, "Effects of CEES on inflammatory mediators, heat shock protein 70A, histology and ultrastructure in two skin models," *Journal of Applied Toxicology*, Vol. 20, pp. 101-108, 2000.

[126]D. J. K. Lee, D. B. Kim, J. I. Kim, and P. Y. Kim, "In vitro cytotoxicity tests on cultured human skin fibroblasts to predict skin irritation potential of surfactants," *Toxicology In Vitro*, Vol. 14, pp. 345-349, 2000.

[127]M. Nakamura, N. Sato, T. Chikama, Y. Hasegawa, and T. Nishida, "Fibronectin facilitates corneal epithelial wound healing in diabetic rats," *Exprimental Eye Research*, Vol. 64, pp. 355–359, 1997.

[128] K. McClary, T. Ugarova, and D. Grainger, "Modulating fibroblast adhesion, spreading and proliferation using self-assembled monolayer films of alkythiols on gold," *Journal of Biomedical Materials Research*, Vol. 50, pp. 428-439, 2000.

[129]M. Mrksich, "What can surface chemistry do for cell biology?," *Current Opinion in Chemical Biology*, Vol. 6, pp. 794-797, 2002.

[130]T. G. van Kooten, J. M. Schakenraad, H. C. Van der Mei and H. J. Busscher, "Influence of substratum wettability on the strength of adhesion of human fibroblasts," *Biomaterials*, Vol. 13, pp. 897-904, 1992.

[131]D. R. Absolom, L. A. Hawthorn, and G. Chang, "Endothelialization of polymer surfaces," *Journal of Biomedical Material Research*, Vol. 22, pp. 271-285, 1988.

[132]T. A. Hobertt and M .B. Schway, "Correlations between mouse 3T3 cell spreading and serum fibronectin adsorption on glass and hydroxyethylmethacrylate-ethylmethacrylate copolymers," *Journal of Biomedical Material Research*, Vol. 22, pp. 763-793, 1988.

[133]E. Cooper, R. Wiggs, D. A. Hutt, L. Parker, G. J. Leggett, and T. L. Parker, "Rates of attachment of fibroblasts to self-assembled monolayers formed by the adsorption of alkylthiols onto gold surfaces," *Journal of Material Chemistry*, Vol. 7, pp. 435-441, 1997.

[134]R. Daw, I. M. Brook, A. J. Delvin, R. D. Short, E. Cooper, and G. J. Leggett, "A comparative study of cell attachment to self-assembled monolayers and plasma polymers," *Journal of Material Chemistry*, Vol. 8, pp. 2583-2585, 1998.

[135]A. S. J. Hoffman, "A general classification scheme for hydrophilic and hydrophobic biomaterial surfaces," *Journal of Biomedical Material Research*, Vol. 20, pp. 9-11, 1986.

[136]A. S. J. Hoffman, "Non-fouling surface technologies," *Journal of Biomedical Material Research Polymer Edition*, Vol. 10, pp. 1011-1014, 1999.

[137]G. Altankov, T. Groth, N. Krasteva, W. Albrecht, and D. Paul, "Morphological evidence for a different fibronectin receptor organization and function during fibroblast adhesion on hydrophilic and hydrophobic glass substrate," *Journal of Biomaterial Science Polymer Edition*, Vol. 8, pp. 721-740, 1997.

[138]J. Sottile, D. C. Hocking, and P. Swiatek. "Fibronectin matrix assembly enhances adhesion-dependent cell growth," *Journal of Cell Science*, Vol. 111, pp. 2933-2943, 1998.

[139]Department of Health and Human Services. Stem cells: scientific progress and future research directions (DHHS, Washington, DC, 2001). http://www.nih.gov/news/stemcell/scireport.htm.

[140]I. L. Weissman, "Translating stem and progenitor cell biology to the clinic: barriers and opportunities," *Science*, Vol. 287, pp. 1442-1446, 2000.

[141]K. Hubner, G. Fuhrmann, L. K. Christenson, J. Kehler, R. Reinbold, R. De La Fuente, J. Wood, J. F. Strauss III, M. Boiani, H. R. Scholer, "Derivation of oocytes from mouse embryonic stem cells," *Science*, Vol. 300, pp. 1251-1256, 2003.

[142]Y. Toyooka, N. Tsunekawa, R. Akasu, and T. Noce, "Embryonic stem cells can form germ cells *in vitro*," *Proceedings of the National Academy of Science USA*, Vol. 100, pp. 11457-11462, 2003.

[143]N. Geijsen, M. Horoschak, K. Kim, J. Gribnau, K. Eggan, and G. Q. Daley, "Derivation of embryonic germ cells and male gametes from embryonic stem cells," *Nature*, Vol. 427, pp. 148-154, 2004.

[144]F. M. Watt, "Epidermal stem cells: markers, patterning and the control of stem cell fate," *Philosphical Transactions of the Royal Society of London B, Biological Sciences*, Vol. 353, pp. 831-837, 1998.

[145]F. H. Gage, J. Ray, L. J. Fisher, "Isolation, characterization, and use of stem cells from the CNS," *Annual Review of Neuroscience*, Vol. 18, pp.159-192, 1995.

[146]E. Schultz and K. M. McCormick, "Skeletal muscle satellite cells," *Reviews of Physiology Biochemistry and Pharmacology*, Vol. 123, pp. 213-257, 1994.

[147]I. L. Weissman, "Stem cells: units of development, units of regeneration, and units in evolution," *Cell*, Vol. 100, pp. 157-168, 2000.

[148]M. Alison and C. Sarraf, "Hepatic stem cells," *Journal Hepatology*, Vol. 29, pp. 676-682, 1998.

[149]B. E. Welm, S. B. Tepera, T. Venezia, T. A. Graubert, J. M. Rosen, M. A. Goodell, "Sca-1(pos) cells in the mouse mammary gland represent an enriched progenitor cell population," *DeviceBiology*, Vol. 245, pp. 42-56, 2002.

[150]L. G. Smith, I. L. Weissman, and S. Heimfeld, "Clonal analysis of hematopoietic stem-cell differentiation *in vivo*," *Proceedings of the National Academy of Science USA*, Vol. 88, pp. 2788-2792, 1991.

[151]C. Holden and G. Vogel, "Stem cells. Plasticity: time for a reappraisal?," *Science*, Vol. 296, pp. 2126-2129, 2002.

[152]F. H. Gage, "Neurogenesis in the adult brain," *Journal of Neuroscience*, Vol. 22, pp. 612-613, 2002.

[153]L. Gabay, S. Lowell, L. L. Rubin, and D. J. Anderson, "Deregulation of dorsoventral patterning by FGF confers trilineage differentiation capacity on CNS stem cells *in vitro*," *Neuron*, Vol. 40, pp. 485-499, 2003.

[154]S. Ding and Peter G Schultz, "A role of chemistry in stem cell biology," *Nature Biotechnology*, Vol. 22, pp. 833-840, 2004.

[155]N. Jaiswal, S. E. Haynesworth, A. I. Caplan, and S. P. Bruder, "Osteogenic differentiation of purified, culture-expanded human mesenchymal stem cells *in vitro*," *Journal of Cellular Biochemistry*, Vol. 64, pp. 295-312, 1997.

[156]A. E. Grigoriadis, J. N. Heersche, and J. E. Aubin, "Differentiation of muscle, fat, cartilage, and bone from progenitor cells present in a bone-derived clonal cell population: effect of dexamethasone," *Journal of Cell Biology*, Vol. 106, pp. 2139-2151, 1988.

[157]N. Terada, T. Hamazaki, M. Oka, M. Hoki, D. M. Mastalerz, Y. Nakano, E. M. Meyer, L. Morel, B. E. Petersen, and E. W. Scott, "Bone marrow cells adopt the phenotype of other cells by spontaneous cell fusion," *Nature*, Vol. 416, pp. 542-545, 2002.

[158]Q.-L. Ying, J. Nichols, E. P. Evans, and A. G. Smith, "Changing potency by spontaneous fusion," *Nature*, Vol. 416, pp. 545-548, 2002.

[159]G. Vassilopoulos, P. R. Wang, and D. W. Russell, "Transplanted bone marrow regenerates liver by cell fusion," *Nature*, Vol. 422, pp. 901-904, 2003.

[160]X. Wang, H. Willenbring, Y. Akkari, Y. Torimaru, M. Foster, M. Al-Dhalimy, E. Lagasse, M. Finegold , S. Olson, and M. Grompe, "Cell fusion is the principle source of bone-marrow-derived hepatocytes" *Nature*, Vol. 422, pp. 897-901, 2003.

[161]H. Xie, M. Ye, R. Feng, and T. Graf, "Stepwise reprogramming of B cells into macrophages," *Cell*, Vol. 117, pp. 663-676, 2004.

[162]Y.-Y. Jang, M. I. Collector, S. B. Baylin, A. Mae Diehl, and S. J. Sharkis, "Hematopoietic stem cells convert into liver cells within days without fusion," *Nature Cell Biology,*" Vol. 6, pp. 532-539, 2004.

[163]Q. L. Ying, J. Nichols, E. P. Evans, and A. G. Smith, "Changing potency by spontaneous fusion," *Nature*, Vol. 416, pp. 545–548, 2002.

[164]T. H. Young and C. H. Hung, "Behavior of embryonic rat cerebral cortical stem cells on the PVA and EVAL substrates," *Biomaterials*, Vol. 26, pp. 4291-4299, 2005.

[165]M. Horiuchi and Y. Tomooka, "An attempt to generate neurons from an astrocyte progenitor cell line FBD-104," *Journal of Neuroscience Research*, Vol. 53, pp. 104-115, 2005.

[166]L. Meinel, V. K. Georgiou, R. Fajardo, B. Snyder, V. S. Patil, L. Zichner, D. Kaplan, R. Langer, and G. Vunjak-Novakovic, "Bone tissue engineering using human mesenchymal stem cells: Effects of scaffold material and medium flow," *Annals of Biomedical Engineering*, Vol. 32, pp.112–122, 2004.

[167]A.A. Sawyer, K.M. Hennessy, and S.L. Bellis, "Regulation of mesenchymal stem cell attachment and spreading on hydroxyapatite by RGD peptides and adsorbed serum proteins," *Biomaterials,* Vol. 26, pp. 1467–1475, 2005.

[168]W. J. Li, R. Tuli, C. Okafor, and A. Derfoul, "A three-dimensional nanofibrous scaffold for cartilage tissue engineering using humanmesenchymalstem cells," *Biomaterials,* Vol. 26, pp. 599-609, 2005.

[169]S. A. Catledge, Y. K. Vohra, S. L. Bellis, and A. A. Sawyer, "Mesenchymal stem cell adhesion and spreading on nanostructured biomaterials," *Journal of Nanoscience and Nanotechnology*, Vol. 4, pp. 986-989, 2004.

[170]L. Meinel, S. Hofmann, O. Betz, R. Fajardo, H. P. Merkle, G. Vunjak-Novakovic, R. Langer, and D. Kaplan, "Osteogenesis of human mesenchymal stem cells cultured on silk biomaterials: Comparison of adenoviral gene and protein delivery of Bmp2," *European Cells and Materials*, Vol. 7, pp. 5, 2004.

[171]M. Weber, A. Steinert, A. Jork, A. Dimmler, N. Schütze, F. Thürmer, C. Hendrich, and U. Zimmermann, "Cartilage formation by encapsulated cells. Formation of cartilage matrix proteins by BMP-transfected murine mesenchymal stem cells encapsulated in a novel class of alginates," *Biomaterials*, Vol. 23, pp. 2003-2013, 2002.

[172]A. Perrin, A. Elassari, A. Theretz, and A. Chapot, "Atomic force microscopy as a quantitative technique: correlation between network model approach and experimental study," Colloids and Surfaces B: Biointerfaces, Vol. 11, pp.103–112, 1998.

[173]N. M. Elaine, Essentials of human anatomy & physiology. Benjamin-Cummings Publishing Company, 2002

[174]E. S. Christine and B. L. Jennie, "Neural tissue engineering, strategies for repair and regeneration," *Annual Review of Biomedical Engineering*, Vol 5, pp. 293-347, 2003.

[175]G. S. H. Wong, Y. Goldshmit, and A. M. Turnley, "IFNg but not TNFa promotes neuronal differentiation of neural stem cells," *Experimental Neurology*, Vol. 187, pp. 171-177, 2004.

[176]J. Mokry, J. Karbanova, J. Pazour, and D. Cizkova, "Capacity of neural stem cells to repair CNS myelin deficits," *Charles University Medical Faculty, Hradec Kralove*, pp. 82, 2004.

[177]T. L Svetlana, A. W. John, P. Jerome, and D. Timothy, "Silicon-micromachined neurochips for *in vitro* studies of cultured neural networks," in *International Conference on Solid-State Sensors and Actuators: Tranducers*, pp. 943-946, 1993.

[178]M. S. C. Scholl, M. Denyer, M. Krause, K. Nakajima, A. Maelicke, W. Knoll, and A. Offenhausser, "Ordered networks of rat hippocampal neurons attached to silicon oxide surfaces," *Journal of Neuroscience Methods*, Vol. 104, pp. 65-75, 2000.

[179]L. G. D. Cyster, K. G. Parker, and T. Parker, "The effect of surface chemistry and structure of titanium nitride (TiN) films on primary hippocampal cells," *Biomolecular Engineering*, Vol 19, pp. 171-175, 2002.

[180]Y. W. Fan, F. Z. Cui, S. P. Hou, Q. Y. Xu, L. N. Chen, and I. S. Lee, "Culture of neural cells on silicon wafers with nano-scale surface topograph," *Journal of Neuroscience Methods*, Vol 120, pp. 17-23, 2002.

[181]W. Russell, H. Jennifer, G. Donna, G. Andres, and C. Robert, "Surface treatment to enhance neuronal adhesion to a silicon-based elastic substrate," in *ASME Bioengineering Conference*, 2001.

[182]D. Kleinfeld, K. Kahler, and P. Hockberger, "Controlled outgrowth of dissociated neurons on patterned substrates," *Journal of Neuroscience*, Vol 8, pp. 4098-4120, 1988.

[183]M. S. Ravenscroft, K. E. Bateman, K. M. Shaffer, H. M. Schessler, D. R. Jung, T. W. Schneider, C. B. Montgomery, T. L. Custer, A. E. Schaffner, Q. Y. Liu, Y. X. Li, J. L. Barker, and J. J. Hickman. "Developmental neurobiology implications from fabrication and analysis of hippocampal neuronal networks on patterned silane-modified surfaces," *Journal of the American Chemical Society*, Vol. 120, pp. 12169-12177, 1998.

[184]H. Sorribas, C. Padeste, and L. Tiefenauer, "Photolithographic generation of protein micropatterns for neuron culture applications," *Biomaterials*, Vol 23, pp. 893–900, 2002.

[185]D. A. Stenger, J. J. Hickman, K. E. Bateman, M. S. Ravenscroft, W. Ma, J. J. Pancrazio, K. Shaffer, A. E. Schaffner, D. H. Cribbs, and C. W. Cotman, "Microlithographic determination of axonal/dendritic polarity in cultured hippocampal neurons," *Journal of Neuroscience Methods*, Vol. 82, pp. 167-173, 1998.

[186]J. C. Chang, G. J. Brewer, and B. C. Wheeler, "A modified microstamping technique enhances polylysine transfer and neuronal cell patterning," *Biomaterials*, Vol 24, pp. 2863-2870, 2003.

[187]D. W. Branch, J. M. Corey, J. A. Weyhenmeyer, G. J. Brewer, and B. C. Wheeler, "Microstamp patterns of biomolecules for high-resolution neuronal networks," *Medical and Biological Engineering and Computing*, Vol 36, pp. 135-141, 1998.

[188]J. K. Kang, M. Poeta, L. Riedel, M. Das, C. Gregory, P. Molnar, and J. J. Hickman, "Patterned neuronal networks for robotics, neurocomputing, toxin detection and rehabilitation," in *Proceeding of 24th Army Science Conference*, 2004.

[189]D. A. Stenger, C. J. Pike, J. J. Hickman, and C. W. Cotman, "Surface Determinants of neuronal survival and growth on self-assembled monolayers in culture," *Brain Research*, Vol. 630, pp. 136-147, 1993.

[190]K. Lewandowska, E. Pergament, C. N. Sukenik, and L. A. Culp, "Cell-type-specific adhesion mechanisms mediated by fibronectin adsorbed to chemically derivatized substrata," *Journal of Biomedical Materials Research*, Vol 26, pp. 1343-1363, 1992.

[191]D. A. Stenger, J. H. Georger, C. S. Dulcey, J. J. Hickman, A. S. Rudolph, T. B. Nielsen, S. M. McCort, and J. M. Calvert, "Coplanar molecular assemblies of amino- and perfluorinated alkylsilanes: Characterization and geometric definition of mammalian cell adhesion and growth," *Journal of the American Chemical Society*, Vol. 114, pp. 8435-8442, 1992.

[192]P. L. Abriel, W. A. Mark, L. S. Stuart, C. Reed, P. Ernest, and M. W. George, "Convenient methods for pattering the adhesion of mammalian cells to surfaces using self-assembled monolayers of alkanethiolates on gold," *Journal of the American Chemical Society*, Vol. 115, pp. 5877-5878, 1993.

[193]S. I. Ertel, A. Chilkoti, T. A. Horbett, and B. D. Ratner, "Endothelial cell growth on oxygen-containing films deposited by ratio-frequency plasmas: the role of surface carbonyl groups," *Journal of Biomaterial Science Polymer Edition*, Vol 3, pp. 163-183 1991.

[194]A. S. David, J. H. James, E. B. Karen, S. R. Melissa, M. Wu, J. P. Joseph, S. Kara, E. S. Anne, H. C. David, W. C. Carl, "Microlithographic determination of axonal: Dendritic polarity in cultured hippocampal neurons," *Journal of Neuroscience Methods*, Vol. 82, pp. 167-173, 1998.

[195]N. Yukie, E. Akiko, T. Hiroyuki, and S. Norio, "Neurite outgrowths of neurons on patterned self-assembled monolayers," *Journal of Bioscience and Bioengineering*, Vol 94, pp. 434-439, 2002.

[196]R. S. Potember, M. Matsuzawa, and P. Liesi, "Conducting networks from cultured cells on self-assembled monolayers," *Synthetic Metals*, Vol. 71, pp. 1997-1999, 1994.

[197]V. Kunjukrishna and A. Mohammed, "Applications of self-assembled monolayers for biomolecular electronics," *Applied Biochemistry and Biotechnology*, Vol 96, pp. 25-40, 2001.

[198]B. Kiran and S. C. Christopher, "Engineering cellular microenvironments to improve cell-based drug testing," *Drug Discovery Today*, Vol 7, pp. 612-620, 2002.

[199]Y. Nam, J. C. Chang, B. C. Wheeler, G. J. Brewer, "Gold-coated microelectrode array with thiol linked self-assembled monolayers for engineering neuronal cultures," *IEEE Transactions on Biomedical Engineering, ,* Vol 51, pp. 158-165, 2004.

[200]V. Shanigaram, "An *in vitro* study of cell response to different self assembled monolayered (SAMs) substrates," M. S. Thesis, Louisiana Tech University, Ruston, Louisiana, USA, 2005.

[201]A. E. Schaffner, J. L. Barker, D. A. Stenger, and J. J. Hickman, "Investigation of the factors necessary for growth of hippocampal neurons in a defined system," *Journal of Neuroscience Methods*, Vol. 62, pp. 111-119, 1995.

[202]M. Mrksich and G. M. Whitesides, "Using self-assembled monolayers to understand the interactions of man-made surfaces with proteins and cells," *Annual Review of Biophysics and Biomolecular Structure*, Vol 25, pp. 55-78, 1996.

[203]S. N. Bhatia, U. J. Balis, M. L. Yarmush, and D M. Toner, "Effect of cell– cell interactions in preservation of cellular phenotype: cocultivation of hepatocytes and nonparenchymal cells," *Federation of American Societies for Experimental Biology Journal*, Vol.13, pp. 1883–1900, 1999.

[204]N. Kaplowitz, "Structure and function of the liver," in *Liver and Biliary Diseases*, N. Kaplowitz, N. Ed, pp. 5, Williams & Wilkins, Baltimore, Maryland, 1992.

[205]P. M. Eckl and N. Bresgen, "The cultured primary hepatocyte and its application in toxicology," *Journal of Applied Biomedicine*, Vol. 1, pp. 117-126, 2003.

[206]M. J. Gomez-Lechon, M. T. Donato, J. V. Castell, and R. Jover, " Human hepatocytes as a tool for studying toxicity and drug metabolism," *Current Drug metabolism*, Vol. 4, pp. 292-312, 2003.

[207]E. L. LeCluyse, P. Bullock, and A. Parkinson, "Strategies for restoration and maintenance of normal hepatic structure and function in long term cultures of rat hepatocytes," *Advanced Drug Delivery Review*, Vol. 22, pp. 133-186, 1996.

[208]J. W. Allen and S. N. Bhatia, "Improving the next generation of bioartificial liver devices," *Seminars in Cell and Development Biology*, Vol. 13, pp. 447-454. 2002

[209]A. K. Nussler, A. Wang, P. Neuhaus, J. Fischer, J. Yuan, L. Liu, K. Zeilinger, J. Gerlach, P. Arnold and W. Albrecht, "The suitability of hepatocyte culture models to study various aspects of drug metabolism," *Altex*, Vol. 18, pp. 91-101, 2001.

[210]Y. J. Wang, H. L. Liu, H. W. Wen, and J. Liu, "Primary hepatocyte cultures in collagen gel mixture and collagen sandwich," *World Journal on Gastroenterology*, Vol. 10, pp. 699-702, 2004.

[211]M. J. Gomez-Lechon, X. Ponsoda, R. Bort, and J. V. Castell, "The use of cultured hepatocytes to investigate the metabolism of drugs and mechanisms of drug hepatotoxicity," *Alternatives to Lab Animals*, Vol. 29, pp. 225-231, 2001.

[212]D. M. Bissell, D. M. Arenson, J. J. Maher, and F. J. Roll, "Support of cultured hepatocytes by a laminin-rich gel," *Journal of Clinical Investigation*, Vol. 79, pp. 801-812, 1987.

[213]E. G. Schuetz, D. Li, C. J. Omiccinski, U. Mueller-Eberhard, H. K. Kleinman, B. Elswick, and P. S. Guzelian, „Regulation of gene expression in adult rat hepatocytes cultures on a basement membrane matrix," *Journal of Cell Physics*, Vol. 134, pp. 309-323, 1988.

[214]S. R. Khetani, G. Szulgit, J. A. Del Rio, C. Barlow, and S. N. Bhatia, "Exploring interactions between rat hepatocytes and nonparenchymal cells using gene expression profiling," *Hepatology*, Vol. 40, pp. 545-554, 2004.

[215]S. N. Bhatia, M. L. Yarmush, and M. Toner, "Controlling cell interaction by micropatterning in co-cultures: hepatocytes and 3T3 fibroblasts," *Journal of Biomedical Material Research*, Vol. 34, pp. 189-199, 1997.

[216]J. C. Y. Dunn, R. G. Tompkins, and M. L. Yarmush, "Long-term *in vitro* function of adult hepatocytes in collagen sandwich configuration," *Biotechnology Progress*, Vol. 7, pp. 237-245, 1991.

[217]I.-K. Park, J. Yang, H.-J. Jeong, H.-S. Bom, I. Harad, T. Akaike, S. Kima, C.-S. Cho, "Galactosylated chitosan as a synthetic extracellular matrix for hepatocytes attachment," *Biomaterials*, Vol. 24, pp. 2331–2337, 2003.

[218]J. E. Babensee, U. De Boni, and M. V. Sefton, "Morphological assessment of hepatomacells (HepG2) microencapsulated in a HEMA-MMA copolymer with and without Matrigel," *Journal of Biomedical Material Research*, Vol. 26, pp. 1401–1418, 1992.

[219]K. H. Park, K. Na, S. W. Kim, S. Y. Jung, K. H. Park, and H. M. Chung, "Phenotype of hepatocyte spheroids behavior within thermo-sensitive poly(NiPAAm-co-PEG-g-GRGDS) hydrogel as a cell delivery vehicle," *Biotechnology Letters*, Vol. 27, pp. 1081-1086, 2005.

[220]J. J. Yoon, Y. S. Nam, J. H. Kim, and T. G. Park, "Surface immobilization of galactose onto aliphatic biodegradable polymers for hepatocyte culture," *Biotechnology Bioengineering*, Vol. 5, pp. 1-10, 2002.

[221]H. C. Fiegel, J. Havers, U. Kneser, M. K. Smith, T. Moeller, D. Kluth, D. J. Mooney, X. Rogiers, and P. M. Kaufmann, "Influence of flow conditions and matrix coatings on growth and differentiation of three-dimensionally cultured rat hepatocytes," *Tissue Engineering*, Vol. 10, pp. 165-174, 2004.

[222]E. S. Carlisle, M. R. Mariappan, K. D. Nelson, B. E. Thomes, R. B. Timmons, A. Constantinescu, R. C. Eberhart, and P. E. Bankey," Enhancing hepatocyte adhesion by pulsed plasma deposition and polyethylene glycol coupling," *Tissue Engineering*, Vol. 6, pp. 45-52, 2000.

[223]S. S. Kim, H. Utsonomiya, J. A. Koski, B. M. Wu, M. J. Cima, J. Sohn, K. Mukai, L. G. Griffith, and J. P. Vacanti, "Survival and function of hepatocytes on a novel three dimensional synthetic biodegradable polymeric scaffold with an intrinsic network of channels," *Annals of Surgery*, Vol. 8, pp. 8-13, 1998.

[224]S. Kidambi, I. Lee, C. Chan, "Controlling primary hepatocyte adhesion and spreading on protein free polyelectrolyte multi-layer films," *Journal of the American Chemical Society*, Vol. 126, pp.16286-16287, 2004.

[225]H.-Y Gu, Z. Chen, R.–X. Sa, S.-S. Yuan, H.-Y. Chen, Y.-T. Ding, A.-M. Yu, "The immobilization of hepatocytes on 24 nm-sized gold colloid for enhanced hepatocytes proliferation," *Biomaterials*, Vol. 25, pp. 3445-3451, 2004.

[226]C. Dilworth, G. A. Hamilton, E. George and J. A. Timbrell "The use of liver spheroids as an *in vitro* model for studying induction of the stress response as a marker of chemical toxicity, *Toxicology in Vitro*, Vol. 14, pp. 169-176, 2000.

[227]G. K. Michalopoulos and Z. Zarnegar, "Hepatocyte growth-factor," *Hepatology*, Vol.15, pp. 440-451, 1992.

[228]T. Mitaka, M. Mikami, G. Sattler, H. C. Pitot, and Y. Mochizuki, "Small-cell colonies appear in the primary culture of adult-rat hepatocytes in the presence of nicotinamide and epidermal growth-factor," *Hepatology*, Vol. 16, pp. 440-450, 1992.

[229]G. D. Block, J. Locker, W. C. Bowen, B. E. Peterson, S. Khatyal, S. C. Strom, T. Riley, T. A. Howard, and G. K. Michalopolous, "Population explosion, clonal growth and apecific differentiation patterns in primary cultures of hepatocytes induced by HGF\SF,EGF and TGF alpha in a chemically defined (HGM) medium," *Journal of Cell Biology*, Vol. 132, pp. 1133-1145, 1996.

[230]T. Nakamura, Y. Yomita, R. Hirai, K. Yamaoka, K. Kaji, and A. Ichihara, "Inhibitory effect of transforming growth factor-beta on DNA synthesis of adult rat hepatocytes in primary culture," *Biochemistry Biophysics Research Community*, Vol. 133, pp. 1042-1051, 1985.

[231]G. J. Cruise and G. Michalopoulos, "Norephinephrine and epidermal growth factor-dynamics of their interaction in the stimulation of hepatocyte DNA synthesis," *Journal of Cell Physiology*, Vol. 125, pp. 45-58, 1985.

[232]F. Goulet, C. Normand, and O. Morin, "Cellular interactions promote tissue-specific function, biomatrix deposition and junctional communication of primary cultured hepatocytes," *Hepatology*, Vol. 8, pp.1010-1018, 1986.

[233]C. Guguen-Guillouzo, B. Clement, G. Baffet, C. Beaumont, E. Morel-Chany, D. Glaise, and A. Guillouzo, "Maintenance and reversibility of active albumin secretion by adult rat hepatocytes co-cultured with another liver epithelial cell type," *Experimental Cell Research*. Vol. 143, pp. 47-54, 1983.

[234]J. Washizu, F. Berthiaume, Y. Mokuno, R.G. Tomkins, and M. Toner, "Long term maintanence of cytochrome p450 activities by rat hepatocyte\3T3 cell co-cultures in heparinized human plasma, " *Tissue Engineering*, Vol. 7, pp. 691-703, 2001.

[235]A. Bader, E. Knop, N. Frauhauf, O. Crome, K. Boker, U. Christians, K. Oldhafer, B. Ringe, R. Pichmayr, and K. F. Sewing, "Reconstruction of liver tissue *in-vitro*: Geometry of characteristic flat bed, hollow fiber, and sprouted bioreactors with reference to the *in vivo* liver," *Artificial Organs*, Vol. 19, pp. 941-950, 1996.

[236]A. Ghanem and M. L. Shuler "Characterization of a perfusion reactor utilizing mammalian cells on microcarrier beads, *Biotechnology Progress*, Vol. 16, pp. 471-479, 2000.

[237]K. Viravaidya, A. Sin, and M. L. Shuler, "Development of a microscale cell culture analog to probe naphthalene toxicity," *Biotechnology Progress*, Vol. 20, pp. 316-323, 2004.

[238]T. H. Park and M. L. Shuler. Integration of cell culture and microfabrication technology," *Biotechnology Progress*, Vol. 19, pp. 243-253, 2003.

[239]A. Sin, K. C. Chin, M. F. Jamil,Y. Kostov, G. Rao, and M. L. Shuler. The design and fabrication of three-chamber microscale cell culture analog devices with integrated dissolved oxygen sensors," *Biotechnology Progress*, Vol. 20, pp. 338-345, 2004.

[240]M. J. Powers, K. Domansky, M. R. Kaazempur- Mofrad, A. Kalezi, A. Capitano, A. Upadhyaya, P. Kurzawski, K. E. Wack, D. B. Stolz, R. Kamm, and L. G. Griffith, "A microfabricated array bioreactor for perfused 3D cell culture," *Biotechnology and Bioengineering*, Vol. 78, pp. 257- 269, 2002.

[241]M. Mrkisch, C. Chen, Y. Xia, L. E. Dike, and D. I. Ingber, "Controlling cell attachment on contoured surfaces with self-assembled monolayers of alkanethiolates on gold," *Proceedings Of The National Academy of Sciences*, Vol. 93, pp. 10775-10778, 1996.

[242]F. Schreiber, "Self-assembled monolayers: From simple "Model" systems to biofunctionalized interfaces," *Journal of Physics: Condensed Matter*, Vol. 16, pp. 881-900, 2004.

[243]S. H. Brewer, D. A. Brown, and S. Franzen, "Formation of thiolate and phosphonate adlayers on indium-tin oxide: Optical and electronic characterization," *Langmuir*, Vol. 18, pp. 6857-6865, 2002.

[244]P. B. Limaye, U. M. Apte, T. J. Bucci, A. Warbritton , H. M. Mehendale, "Calpain released from dying hepatocytes mediates progression of acute liver injury induced by model hepatotoxicants," *Toxicology and Applied Pharmacology*, Vol. 191, pp. 211-226, 2003.

[245]T. Battle and G. Stacey, "Cell culture models for hepatotoxicology", *Cell Biology and Toxicology*, Vol. 17, pp. 287–299, 2001.

[246]D. X. Hou, M. Arimura, M. Fukuda, T. Oka, and M. Fujii, "Expression of cell adhesion molecule and albumin genes in primary culture of hepatocytes," *Cell Biology International*, Vol. 25, pp. 239-244, 2001.

[247]R. N. B. Bhandari, L. A. Riccalton, A. L. Lewis, J. R. Fry, A. H. Hammond, S. J. B. Tendler, K. M. Shakessheff, "Liver tissue engineering: A role for co-culture systems in modifying hepatocyte function and viability," *Tissue Engineering*, Vol. 7, pp. 345-357, 2001.

[248]K. M. Kulig and J. M. Vacanti, "Hepatic tissue engineering," *Transplant Immunology*, Vol. 12, pp. 303-310, 2004.

[249]J. M. Rhoads, R. A. Argenzio, W. Chen, R. A. Rippe, J. K. Westwick, A. D. Cox, H. M. Berschneider, D. A. Brenner, "L-glutamine stimulates intestinal cell proliferation and activates mitogen-activated protein kinases," *American Journal of Physiology*, Vol. 272, pp.G943-G953, 1997.

[250]H. M. Kandil, R. A. Argenzio, W. Chen, H. M. Berschneider, A. D. Stiles, J. K. Westwick, R. A. Rippe, D. A. Brenner, and J. M. Rhoads. L-glutamine and L-asparagine stimulate ODC activity and proliferation in a porcine jejunal enterocyte line," *American Journal of Physiology: Gastrointestine Liver Physiology*, Vol. 269, pp. G591-G599, 1995.

[251]H. S. Haas, R. Pfragner, V. Siegl, E. Ingolic, E. Heintz, and K. Schauenstein," Glutamate receptor-mediated effects on growth and morphology of human histiocytic lymphoma cells, *International Journal of Oncology*, Vol. 27, pp. 867-874, 2005.

[252]K. Yamauchi , T. Komatsu, A. D. Kulkarni, Y. Ohmori, H. Minami, Y. Ushiyama, M. Nakayama, S. Yamamoto," Glutamine and arginine affect Caco-2 cell proliferation by promotion of nucleotide synthesis," *Nutrition*, Vol. 18, pp. 329-333, 2002.

[253]S. M. Sheen-Chen, K. S. Hung, H. T. Ho, W. J. Chen, and H. L. Eng," Effect of glutamine and bile acid on hepatocyte apoptosis after bile duct ligation in the rat," *World Journal of Surgery*, Vol. 5, pp. 457-460, 2004.

[254]R. Passos de Jesus Mazza, P. L. Bertevello, R. Matos de Miranda Torrinhas, S. Nonogaki, V. Avancini Ferreira Alves, J. Gama Rodrigues, and D. L. Waitzberg," Effect of glutamine dipeptide on hepatic regeneration in partially hepatectomized malnourished rats," *Nutrition,* Vol. 19, pp. 930-935, 2003.

[255]A. J. Strain and J. M. Neuberger, "A bioartificial liver-state of the art," *Science*, Vol. 295, pp. 1005-1009, 2002.

[256]L. Griffith and G. Naughton, "Tissue engineering-current challenges and expanding opportunities," *Science*, Vol. 295, pp. 1009-1014, 2002.

[257]R. Fuchs, "Design and development of a novel textile composite scaffold bioreactor for application as bioartificial liver support device," Thesis, Swiss Federal Institute of Technology, Zurich, 2002

[258]J. W. Allen, T. Hassanein, S. N. Bhatia, "Advances in bioartificial liver devices. *Hepatology,* Vol. 34, pp. 447-455, 2001.

[259]J. R. Anderson, D. T. Chiu, J. C. McDonald, R. J. Jackman, O. Cherniavskaya, H. Wu, S. Whitesides, G. M. Whitesides, G. M," Fabrication of topologically complex three-dimensional microfluidic systems in PDMS by rapid prototyping," *Analytical Chemistry*, Vol. 72, pp. 3158-3164, 2000.

[260]D. T. Chiu, N. L. Jeon, S. Huang, R. S. Kane, C. J. Wargo, I. S. Choi, D. E. Ingber, G. M. Whitesides, "Patterned deposition of cells and proteins onto surfaces by using threedimensional microfluidic systems," *Proceedings of National Acadamy of Science USA*, Vol. 12, pp. 2408-2413, 2000.

[261]J. P. Vacanti, "Translating technologies to build whole vital organs," *Tissue Engineering*, Vol. 8, pp. 1115, 2002.

[262]S. N. Bhatia, U. Balis, M. Yarmush, and M. Toner, "Microfabrication of hepatocyte and fibroblast coculture: role of homotypic cell interactions," *Biotechnology Progress*, Vol. 14, pp. 378-387, 1998.

[263]A. Folch and M. Toner, "Microengineering of cellular interactions," *Annual Review of Biomedical Engineering*, Vol. 2, pp. 227-256, 2000.

[264]G. Vozzi, C. Flaim, F. Bianchi, A. Ahluwalia, S. Bhatia, "Microfabricated PLGA scaffolds: a comparative study for application to tissue engineering," *Material Science Engineering C*, Vol. 20, pp. 43-47, 2002.

[265]G. Ciaravella, G. Vozzy, F. Bianchi, M. Rosi, C. Costanza, P. Madeddu, and A. Ahuwalia, "Microfabricated fractal trees as scaffolds for capillary morphogenesis: applications in therapeutic angiogenesis and vascular tissue engineering," in *IEEE-EMBS MCTE Conference*, Genova, Italy, pp. 46-47, 2002.

[266]E. Leclerc, K. S. Furukawa, F. Miyata, Y. Sakai, T. Ushida, and T. Fujii, "Fabrication of microstructures in photosensitive biodegradables polymers for tissue engineering applications," *Biomaterials*, Vol. 25, pp. 4683-4690, 2003.

[267]J. T. Borenstein, H. Terai, K. King, C. Weinberg, M. Kaazempur-Mofrad, and J. P. Vacanti, "Microfabrication technology for vascularized tissue engineering," *Biomedical Microdevices*, Vol. 4, pp. 167-175, 2002.

[268]A. M. Aravanis, B. D. DeBusschere, A. J. Chruscinski, K. H. Gilchrist, B. K. Kobilka, and Gregory T.A. Kovacs, "A genetically engineered cell-based biosensor for functional classification of agents," *Biosensors & Bioelectronics*, Vol. 16, pp. 571–577, 2001.

[269]D. A. Stenger, G. W. Gross, E. W. Keefer, K. M. Shaffer, J. D. Andreadis, W. Ma, and J. J. Pancrazio, "Detection of physiologically active compounds using cell-based biosensors," *TRENDS in Biotechnology*, Vol. 19, pp. 304-309, 2001.

[270]S. A. Gray, J. K. Kusel, K. M. Shaffer, Y. S. Shubin, D. A. Stenger, and J. J. Pancrazio, "Design and demonstration of an automated cell-based biosensor," *Biosensor and Bioelectronics*, Vol. 16, pp. 535-542, 2001.

[271]J. J. Pancrazio, J. P. Whelan, and D. A. Borkholder, "Development and application of cell-based biosensors," *Annals of Biomedical Engineering*, Vol. 27, pp. 697-711, 1999.

[272]K. Viravaidya and M. L. Shuler, "Incorporation of 3T3-L1 cells to mimic bioaccumulation in a microscale cell culture analog device for toxicity studies," *Biotechnology Progress*, Vol. 20, pp. 590-597, 2004.

[273]H.J. Clewell III, "The application of physiologically based pharmacokinetic modeling in human health risk assessment of hazardous substances," *Toxicology Letters*, Vol. 79, pp. 207-217, 1995.

[274]J. I. Delic, P. D. Lilly, A. J. MacDonald, and G. D. Loizou, "The utility of PBPK in the safety assessment of chloroform and carbon tetrachloride," *Regulatory Toxicology and Pharmacology*, Vol. 32, pp. 144–155, 2000.

[275]D. J. Quick and M. L. Shuler, "Use of *in vitro* data for construction of a physiologically based pharmacokinetics model for naphthalene in rats and mice to probe species differences," *Biotechnology Progress*, Vol. 14, pp. 540-555, 1999.